MESOTHELIAL AND MURAL CELL CONTRIBUTION TO VASCULAR DEVELOPMENT THROUGH PDGF SIGNALING

APPROVED BY SUPERVISORY COMMITTEE

Chairperson: Scott Cameron, M.D., Ph.D.

Michael White, Ph.D.

David Mangelsdorf, Ph.D.

Michelle Tallquist, Ph.D.

To my parents,
Alfredo and Eloisa French

For their unconditional
love, faith, encouragement, and support

ACKNOWLEDGEMENTS

I am very grateful to have had the opportunity to be a part of the scientific community at UT Southwestern. I found my experiences from core course to qualifiers to benchwork to be very challenging and educational. I would like to thank my committee for providing support and encouragement. I would like to acknowledge Dr. Michelle Tallquist for many lessons learned about science and life. I will never forget my time in the lab and everything I learned. A special thanks to my labmates and friends, especially Amy, Chase, Alicia, Alethia, Gabe, Courtney, Stephen, and Gilbert, for the science talks and great times.

Most of all I would like to thank my family for all of their support and understanding during my graduate school years. My parents, Alfredo and Eloisa French, for their unconditional love and complete faith in my abilities that keeps me going day after day. My sister, Ceci Erales, for constantly challenging me to do better both professionally and personally. She is truly an amazing person that I aspire to be like as a sister, a mother, and a friend. My brother in law, Alex Erales, for making me laugh, being a great cook, and always making it possible for the family to get together even though we live far apart. My nieces, Trinity and Sydney, for their loving phone calls and their curious questions including why am I still in school. The entire Jones family for their support and prayers. My husband, Raymond Jones, for everything from planning our wedding to patiently sitting by my side everyday hour upon hour waiting for me to finish my work.

MESOTHELIAL AND MURAL CELL CONTRIBUTION TO VASCULAR DEVELOPMENT THROUGH PDGF SIGNALING

by

WENDY JOY FRENCH

DISSERTATION

Presented to the Faculty of the Graduate School of Biomedical Sciences

The University of Texas Southwestern Medical Center at Dallas

In Partial Fulfillment of the Requirements

For the Degree of

DOCTOR OF PHILOSOPHY

The University of Texas Southwestern Medical Center at Dallas

Dallas, Texas

May, 2009

MESOTHELIAL AND MURAL CELL CONTRIBUTION TO VASCULAR DEVELOPMENT THROUGH PDGF SIGNALING

WENDY JOY FRENCH, Ph.D.

The University of Texas Southwestern Medical Center at Dallas, 2009

MICHELLE D. TALLQUIST, Ph.D.

Vascular development during embryogenesis and adulthood occurs through vasculogenesis and angiogenesis. Vasculogenesis is the de novo formation of blood vessels from mesoderm precursor cells. Angiogenesis is the formation of new vessels from existing vessels. Both processes involve hematopoietic, endothelial, and mural cells for the formation of mature, stable vasculature. While hematopoietic and endothelial cell contributions and function in vascular development have been extensively studied identifying the VEGF and TGF families as major contributors, the role of mural cells has not been clearly defined. The platelet derived growth factor beta (PDGFR beta) is

essential for mural cell recruitment and expansion. Deletion of PDGFR beta leads to perinatal lethality resulting from vascular defects attributed to severe decreases in mural cells. PDGFR beta is a receptor tyrosine kinase with high homology in signal activation to PDGFR alpha. Downstream signaling pathway activation includes PI3 kinase, Src, RasGAP, Grb2, Shp-2, and PLC gamma for the regulation of cellular functions.

The focus of this research was to determine the temporal and functional requirements of PDGFR signaling in mural cells. To address the temporal requirements for PDGFR beta, genetic manipulation was used to delete the receptor in precursor and differentiated mural cells. In addition, mutant mice were generated with the additional deletion of PDGFR alpha to address the potential for compensatory or cooperative function between the two receptors. These studies identified a cooperative role for PDGFR alpha and PDGFR beta in yolk sac mesothelial cells. Mutant mice were lethal around E10.5 with disrupted yolk sac vascular remodeling and extracellular matrix composition. The PDGFR regulate collagen matrix through regulation of matrix metalloproteinase activity and thus disrupt integrin activation. The functional role of PDGFR beta in mural cells was addressed by signaling point mutants targeting and disrupting specific downstream pathways. These studies resulted in a progressive decrease in mural cells that correlated to the number of disrupted PDGFR beta signaling pathways. Together these analyses demonstrate PDGFR and mural cells are essential for vascular development and maintenance.

TABLE OF CONTENTS

LIST OF PUBLICATIONS

Tallquist, MD, **French, WJ**, and Soriano, P. (2003) Additive Effects of PDGF Receptor b Signaling Pathways in Vascular Smooth Muscle Cell Development. *PLoS*, 1(2): 288-299.

French, WJ, Creemers, EE, and Tallquist, MD. (2008) PDGF receptors direct vascular development independent of vascular smooth muscle cell function. *Molecular and Cellular Biology*, 18: 5646-5657.

Zovein, AC, Hofmann, JJ, Lynch, M, **French, WJ**, Yang, Y, Turlo, KA, Zanetta, L, Dejana, E, Gasson, JC, Tallquist, MD, Iruela-Arispe, ML. (2008) Fate tracing reveals the endothelial origin of hematopoietic stem cells. *Cell Stem Cell*, 3(6): 625-636.

LIST OF FIGURES

LIST OF TABLES

LIST OF APPENDICES

LIST OF ABBREVIATIONS

αSMA = α smooth muscle actin
EC = endothelial cell
EPC = endothelial precursor cell
ECM = extracellular matrix
ee = extraembryonic endoderm
fl = floxed
mes = mesothelium
MKO = Myocardin^{Cre} knock out
PECAM = platelet/endothelial cell adhesion molecule
PDGF = platelet derived growth factor
PDGFR = platelet derived growth factor receptor
PI3K = phosphoinositol 3 kinase
SKO = SM22-Cre^{Tg} knock out
SM22 = smooth muscle
SMC = smooth muscle cell
Tg = transgenic
TGF = transforming growth factor
RTK = receptor tyrosine kinase
VEGF = vascular endothelial growth factor
VSMC = vascular smooth muscle cell
V/P = vascular smooth muscle/pericyte

CHAPTER ONE
Introduction to Vascular Development

One of the first developmental processes to take place during embryogenesis is the formation of the vasculature. This is an essential process for development of tissues and organs during embryogenesis and postnatally that if disrupted could lead to abnormal development and/or lethality. Vascular development can occur by two processes: vasculogenesis or angiogenesis. Vasculogenesis is the de novo formation of vasculature from differentiating progenitor cells that will migrate into a vascular plexus and remodel into large defined vessels. Initiation of vasculogenesis can be detected around E7.5 with the first detection of vascular cells. Angiogenesis is the process in which new vessels form by sprouting from existing vasculature. In both vasculogenesis and angiogenesis, the newly formed vessels undergo a capillary plexus and a maturation stage. Maturation of vasculature includes recruitment of support cells and establishment of extracellular matrix (ECM) to provide vessel stability.

Vascular development requires three main cell populations for proper function including hematopoietic, endothelial, and mural cells. Hematopoietic precursor cells are essential for the formation of all types of blood cells determined by the signaling molecules involved and by the site of terminal differentiation. Endothelial cells have been extensively studied to identify the molecules required for proper endothelial cells differentiation, proliferation, and migration necessary for tube formation and remodeling. Mural cells will be recruited as support cells for the vessel stability. The main molecules involved in vascular development include members of the VEGF, TGF, and PDGF families. Signaling for mural cell recruitment and proliferation has largely been attributed

to TGF and PDGFRβ. However the exact role of the mural cells has not been clearly defined and a better understanding could help in regulating neovascularization in injury and disease states.

Mechanisms of Vascular Development

Vascular development is an essential process for the development of tissues and organs during embryogenesis and adulthood. The different regions of vasculature are developed either by vasculogenesis or angiogenesis. During both, angiogenesis and vasculogenesis, specific cell populations are required for proper signaling and matrix deposition to prevent abnormal growth that could lead to vascular defects, developmental retardation, and lethality.

Vasculogenesis

Multiple organs undergo vasculogenesis during development including the heart, yolk sac, and the liver. The most primitive vasculature in the mouse embryo is first detected as early as E7.5 as the heart and the yolk sac begin to develop. The first stage of vasculogenesis is the formation of blood islands that consist of a hematopoietic center surrounded by endothelial cells along the periphery (Yoder et al. 1994). The tight signal regulation required for proper formation can be seen as early as the blood island stages through the contributions of FGF and BMP signaling pathways. Genetic deletion studies have demonstrated the role of BMP in the formation of mesoderm and the subsequent effects on proliferation and differentiation of essential cell populations (Winnier et al. 1995; Larsson and Karlsson 2005). In vitro studies have increased the understanding of

BMP signaling requirements by demonstrating that ES cells can only differentiate into hematopoietic precursors in the presence of active Bmp4 signaling (Johansson and Wiles 1995; Park et al. 2004). The complexity and balance of cell signaling in blood island formation was further demonstrated through the contribution of FGF signaling. It was demonstrated in Xenopus that misexpression of FGF led to inhibition of blood island formation while expression of dominant negative FGF resulted in increased blood island formation. Furthermore, FGF activity disrupted expression of downstream targets of the BMP pathway (Xu et al. 1999). Additional factors that play a role in blood island formation include regulators of hematopoiesis and endothelial cell differentiation such as VEGF (Carmeliet et al. 1996).

The next stage of vasculogenesis is the differentiation of blood islands into mature endothelial cells. This process has been attributed in large part to signaling by VEGF and its receptors, VEGFR1 (Flt1) and VEGFR2 (Flk1). Mice heterozygous for VEGF ligand are lethal at E11.5-12.5 and demonstrate severe vascular defects and an absence of endothelial cells (Carmeliet et al. 1996). *VEGFR1 (Flt-1)* and *VEGFR2 (Flk-1)* null mice result in lethality at E9.5 with abnormal blood island formation (Fong et al. 1995; Shalaby et al. 1995).

In addition to the activation required for initiation of endothelial cell differentiation, there also exists specific signaling requirements for the expansion and remodeling of vessels. As the endothelial cells mature they will proliferate and migrate to form endothelial tubes that organize into a vascular plexus. The vascular plexus is a signature structure of vascular development that resembles a honeycomb and will remodel to form the adult vascular network. While many molecules have been shown to

play a role in plexus formation and remodeling, some of the main pathways include TGF, Notch, and Hedgehog families (Dickson et al. 1995; Oshima et al. 1996; Krebs et al. 2000; Larsson et al. 2001; Byrd et al. 2002; Fischer et al. 2004; Nagase et al. 2006).

The final stages of vasculogenesis occur as the vasculature remodels. Endothelial cell signaling will lead to mesodermal differentiation and recruitment of mural cells and extracellular matrix (ECM) deposition (Holmgren et al. 1991; Hirschi et al. 1998; Hirschi et al. 1999; Jain 2003). ECM and mural cells will coat the vasculature providing vessel strength and stability. Disruptions in these processes can lead to hemorrahage and edema as observed in the *PDGFRβ* null embryos (Soriano 1994). Vascular disease models have been proposed of the *endoglin* and *Alk-1* null mice for hereditary hemorrhagic telangiectasia (HHT). These mutant embryos die at E9.5 and demonstrate vascular remodeling defects and defects in matrix composition of the yolk sac (McAllister et al. 1994; Johnson et al. 1996). This data suggests that proper vascular development does not end with vessel formation but rather there is a requirement for a complex environment consisting of specific cell populations, signaling molecules, and matrix components for proper vessel function.

Angiogenesis

Vasculogenesis and angiogenesis have many similarities in signaling components involved in the formation of new vessels, but they vary greatly in the origin of the new vessels. While the formation of new vessels from existing vasculature is more often associated with wound healing or disease, there are several developmental processes that undergo angiogenesis. In the adult, retinal and reproductive blood vessels are formed by

angiogenesis (Reynolds and Redmer 1992; Gariano and Gardner 2005). Analysis of angiogenesis has demonstrated specific protein signaling and activation required for sprouting and elongation of endothelial cells from pre-existing cells.

Blood vessels consist of tight endothelial cell associations with other endothelial cells and mural cells, as well as basement membrane providing vessel stability. Therefore the first stages of angiogenesis include the disruption of the cell to cell interactions and basement membrane surrounding existing vasculature to allow expansion of the endothelial cells. Angiopoietin-1 (Ang-1) and angiopoietin-2 (Ang-2) have been shown to regulate the ECM dissociation allowing ligand access to endothelial cells (Kim et al. 2000; Das et al. 2003; Zhu et al. 2005). Next, endothelial cells must receive proper signaling for migration away from the existing vasculature and towards the angiogenic stimulus. In addition to migration, endothelial cells must receive proliferative signals to generate enough endothelial cells to develop the new vessels. Similar to vasculogenesis, VEGF family members have been shown to regulate endothelial cells proliferation and migration in angiogenesis (Gerhardt et al. 2003). Finally new vessels undergo maturation through the recruitment of mural cells and deposition of basement membrane. At this stage, TGF signaling activates vessel-associated cells for increased differentiation into mural cells and PDGF is suggested to function in proliferation and migration of the mural cells (Jain 2003). In disease, angiogenesis is largely studied as a mechanism for regulating cancer, retinopathy, and arthritis. Studies attempt to understand and characterize angiogenesis in disease states by identifying and analyzing expression patterns of angiogenesis markers and comparing them to developmental processes (Shih et al. 2002).

Vascular Components

The three main cell types (hematopoietic, endothelial, and mural cells) of blood vessels are derived from the mesoderm. However there has been debate regarding the intermediates from which these cells are derived. Precursor cells that give rise to these are referred to as angioblasts. In recent times the close proximity, common marker expression, and timing of first appearance of hematopoietic and endothelial cells led to the hypothesis of a common precursor, a hemangioblast (Mikkola and Orkin 2002). Common markers found on hematopoietic and endothelial cells include Flk1, CD34, Scl/tal-1, Flt1, Gata-2, Runx1, and Pecam (Sugiyama and Tsuji 2006). Evidence of a common precursor is also suggested through genetic studies analyzing the deletion of Flk-1. As described above, mice null for *Flk-1* result in the complete absence of both hematopoietic and endothelial cells (Shalaby et al. 1997). However direct effects by cell specific function on differentiation must be separated from indirect effects from neighboring cell populations important for establishing the appropriate environment that will support vascular growth. In addition to hematopoietic and endothelial cells, mural cells are an important component of the vasculature. Mural cells include pericytes, VSMC, and fibroblasts derived from mesoderm surrounding the developing vasculature. Disruption of any of these cell types leads to absence of, disrupted or unstable vasculature.

Hematopoietic cells

The earliest and most primitive hematopoietic cells are first detected in the yolk sac at E7.5 and soon after in the embryo in the para-aortic splanchnopleura (PAS) and

aorta-gonad mesonephros (AGM) (Yoder et al. 1994; Medvinsky and Dzierzak 1996; Yoder 2001; Mikkola and Orkin 2002). Primitive hematopoietic cells consist of nucleated erythrocytes including erythroblasts, megakaryocytes and primitive macrophages. Around E10.5 hematopoiesis moves to the liver where differentiated hematopoietic cells are detected. Finally, just prior to birth and into adulthood the bone marrow becomes the prime source for hematopoietic cells. Important signaling components have been identified for both the differentiation and expansion of hematopoietic cells during embryogenesis as well as in the adult (Pearson et al. 2008).

Endothelial cells

Endothelial cells have been extensively studied to understand early stages of vascular development and how the mechanisms relate to disease or injury states. While endothelial cell markers are first detected in blood islands, it has been shown that these cells will continue to differentiate into mature endothelial cells during vasculogenesis. Therefore many studies have focused on the signaling requirements for mesoderm and endothelial progenitor cells to become differentiated endothelial cells. Furthermore it has been suggested that during angiogenesis endothelial cells undergo dedifferentiation to generate the cell signaling necessary for vessel growth (Jain 2003).

Endothelial progenitor and endothelial cells have been difficult to distinguish because they share many of the same markers such as VEGFR2, Tie2, Tie1, and VE Cadherin (Suri et al. 1996). However differences have been identified in expression and behavior. Endothelial progenitor cells express AC133 and expression is lost upon endothelial cell differentiation. Additionally endothelial progenitor cells are highly

proliferative in response to angiogenic factors whereas differentiated endothelial cells are more stable and do not readily proliferate (Gehling et al. 2000). During vascular development endothelial cells secrete basement membrane and participate in cell to cell interactions that will result in a stable vessel. For vascular expansion by angiogenesis, the basement membrane and cellular interactions must be disrupted. This disruption will allow access to ligands and stimulation of migration and proliferation.

Defects in vasculogenesis have typically been described by the disruption of endothelial cell function. Completely avascular phenotypes result from a failure of endothelial cells to form and can be seen in the *endoglin* and *alk-1* mutants (McAllister et al. 1994; Johnson et al. 1996). When vasculature forms but fails to remodel, it is described as a failure in maturation of endothelial cells and has been shown in the *TGFbRII* and *SMAD* mutants (Oshima et al. 1996; Yang et al. 1999). Furthermore, it as established by cell specific deletion of TGF that endothelial cells are responsible for the vascular defects observed in *TGF* null mice (Carvalho et al. 2007). It was suggested that these phenotypes result from defects in endothelial cell differentiation, expansion, and endothelial cell recruitment of other cell types as well as deposition of proper extracellular matrix.

Mural cells

Mural cells will migrate towards the forming vasculature and differentiate into pericytes, VSMC, or fibroblasts. While these cell types are support cells they are found in distinct regions of the vasculature. Pericytes are found along capillaries and at branch points. VSMC are found in multi-cell layers surrounding large vessels. Fibroblasts make

up the adventitial layer surrounding VSMC on larger vessels. Many studies have suggested an essential role for these cells in vascular development however their exact role is still not well defined. They are broadly described as the cell populations required for vessel stability by contributing to ECM and halting vessel growth. The TGF family signaling directs differentiation of these cell types (Orlidge and D'Amore 1987). Upon differentiation these vessel associated cells will express markers such as αSMA, SMMHC, desmin, caldesmin, calponin, and NG2. However expression of these markers is not absolute and variation of expression can be found based upon differentiation state, location, and function (Hughes and Chan-Ling 2004).

The function of mural cells in vascular development has been difficult to define because many of the genetic mutants exhibiting defects in mural cells are expressed in endothelial cells as well. For example, failure of recruitment of mural cells is suggested in some of the TGF mutants that lead to remodeling defects (Oshima et al. 1996). However these molecules are also expressed on endothelial cells. It is important to distinguish the direct role of mural cells in vascular development as opposed to secondary defects resulting from altered endothelial cells signaling. Overall, studies suggest that mural cells are essential for development but further studies through cell specific analysis would aid in understanding the variability in function for each cell type.

Major signaling pathways for vascular development

VEGF Family

Vascular endothelial growth factor (VEGF) family members can be described as the main signaling components for vasculogenesis because of the early and dramatic

phenotypes observed upon genetic deletion. As described above, VEGF, VEGFR1 (Flt1) and VEGFR2 (Flk1) result in lethality as early as E8.5 demonstrating avascular or defective vascular development (Fong et al. 1995; Shalaby et al. 1995; Carmeliet et al. 1996). While both receptors are expressed on endothelial cells, VEGFR2 is described as the main source of proangiogenic stimulus. VEGFR2 is mainly thought to function through the PLCγ pathway leading to proliferation and migration (Cross et al. 2003). In 2005, a study was published analyzing all the known genetic deletions that lead to vascular defects. In summary, the majority of the genes identified as critical for vasculogenesis were involved in the VEGF signaling pathway (Argraves and Drake 2005). Therefore it is easy to understand why endothelial signaling and growth through the VEGF family is targeted in anti-angiogenic therapy for tumor suppression by inhibition of vascular growth.

TGF family

The TGF family consists of TGFβ1, Alk-5, TβRII, TβRI (Alk-1), endoglin, Bmp, and downstream SMAD signaling. They are expressed in mesenchymal cells as well as differentiated cells such as endothelial cells. Genetic deletion analysis has demonstrated similar vascular development defects and requirements for the TGF family. Analysis of the detrimental effects upon deletion of the TGF family members in vascular development began with the deletion of the ligand TGFβI. *TGFβI* null embryos died around E8.5-9.5 and demonstrated avascular development (Dickson et al. 1995). Further analysis of receptor deletion demonstrated TβRII is required for endothelial cell organization but not differentiation (Dickson et al. 1995). Similarly endoglin and Alk-1

also demonstrated vascular defects and became a model for hereditary hemorrhagic telangiectasia (HHT) (McAllister et al. 1994; Johnson et al. 1996). Careful analysis has suggested that while the TGF family members all function in endothelial cells they vary in the exact mechanism affected. For example it is suggested that Alk-1 and SMAD 1/5 play a role in endothelial cell proliferation and Alk5 and SMAD 2/3 in endothelial cell differentiation (Goumans et al. 2002).

PDGF family

The PDGF family consists of four ligands, PDGFA, PDGFB, PDGFC and PDGFD, and two receptors, PDGFRα and PDGFRβ. *PDGFRα* null embryos die around E9.5 with hemorrhaging, cleft palate, and aortic arch defects suggesting an important role in neural crest cell function (Soriano 1997). PDGFRβ is expressed in vascular smooth muscle cells and genetic deletion results in perinatal lethality exhibiting severe hemorrhaging and edema (Soriano 1994). The vascular defects and expression patterns of PDGFRβ contribute to the hypothesis that vascular smooth muscle cells play an essential role in vascular development. Analysis of the ligands has demonstrated similar defects to those observed in the receptor mutants. PDGFB is expressed and secreted by endothelial cells to recruit mural cells to the developing vasculature. Similar to the receptor analysis, PDGFB deletion results in failure of pericyte and vascular smooth muscle cell, severe hemorrhaging, and perinatal lethality (Lindahl et al. 1997).

Upon ligand binding and dimmerization, PDGFRα and PDGFRβ autophosphorylate the tyrosine residues along their cytoplasmic tail. They can homodimerize and heterodimerize dependent upon ligand interaction and have high

homology in downstream signaling activation. Common signaling pathways include PI3 kinase, Src, Grb2, PLCγ, and Shp-2. Pathways unique to each receptor include Crk for PDGFRα and RasGAP for PDGFRβ. While ligand interaction and high homology would suggest redundant function, only recently has coexpression and cooperative function been suggested in neural crest cells and aortic arch formation (Richarte et al. 2007). Because deletion of both receptors leads to hemorrhaging and lethality, it would be interesting to explore cooperative function in vascular development as well.

ECM

While much emphasis has been placed on studying receptor tyrosine kinases for differentiation, proliferation, and migration, another aspect of vasculature essential for proper development is the deposition of ECM. Components of ECM are believed to provide stability to developing vasculature as well as dictate whether endothelial cells will proliferate or migrate. ECM has proven to be more difficult to understand during vasculogenesis because of potential functional redundancy between molecules that may be observed based on common ligand-receptor interactions. However, the varying composition/expression during different stages of development and disease does suggest some specificity in function (Risau and Lemmon 1988; Baldwin 1996). Traditional genetic analysis has demonstrated a role for key molecules including fibronectin (FN), collagens, and laminin as well as their receptors, mainly members of the integrin family. Fibronectin is expressed early during vasculogenesis then is reduced in quiescent vessels and will only be upregulated again with activation of vasculature in cases of wound healing and tumors. Fibronectin mutant embryos result in severe developmental and

vascular defects at E8.5 demonstrating essential roles for fibronectin in the embryo as well as extraembryonic tissues (George et al. 1997). Collagens play an important role in embryonic development as they are specifically expressed in the different regions of the embryo to provide matrix and signaling required for proper development. Collagen 1 is secreted by endothelial cells and is important for vessel stability. Mouse mutants lacking collagen 1 were embryonic lethal around E12 due to hemorrhaging (Lohler et al. 1984). Collagen 4 mutations lead to lethality at E10.5-E11.5 due to deficiencies in basement membrane integrity (Poschl et al. 2004). Laminins are also an important component of vascular basement membranes. Deletion of laminin a4 is not embryonic lethal but does result in unstable vasculature, hemorrhaging, and misexpression of other matrix molecules including other laminins and collagen 4 (Thyboll et al. 2002). These are just some examples of the different matrix molecules that are involved in vascular development and that have been implicated in genetic mutants exhibiting vascular defects.

The most common receptors for these matrix molecules are the integrins, heterodimeric proteins consisting of α and β subunit. Cells can express multiple combinations of integrins on their surface and one of the most commonly studied in vivo is the β1 integrins. β1 integrins interact with all three matrix molecules described above and specificity is obtained by the α subunit. Similar to FN, deletion of α5β1 integrin results in early embryonic lethality and vascular defects (Francis et al. 2002). Furthermore, β1 integrins have been shown to be upregulated in response to angiogenic growth factors as well as being essential in tumor angiogenesis. In addition, β1 has been

proposed to interact with PDGF receptors resulting in activation in the absence of PDGF ligands.

Summary

Vascular development is complex process requiring specific temporal and spatial regulation of cells, signaling molecules, and matrix composition. Although vasculature consists of only three main cell types, there are many signaling molecules involved and misexpression of a single molecule can lead to lethality. Therefore it is important to fully understand the role of each cell type and the mechanisms used for proper function. The goal of this study was to gain knowledge on the function of mural cells in vascular development and stability and the role of the PDGFR in this process.

CHAPTER TWO
PDGF Receptors Direct Vascular Development Independent of Vascular Smooth Muscle Cell Function

Wendy J. French[1], Esther E. Creemers[2], and Michelle D. Tallquist[1]

[1]Molecular Biology Department, University of Texas Southwestern Medical Center, Dallas, TX and [2]Heart Failure Research Center, University of Amsterdam, The Netherlands

ABSTRACT

Complete loss of platelet derived growth factor (PDGF) receptor signaling results in embryonic lethality around embryonic day E9.5, but the cause of this lethality has not been identified. Because cardiovascular failure often results in embryonic lethality at this time point, we hypothesized that a failure in cardiovascular development could be the cause. To assess the combined role of the PDGF receptors, PDGFRα and PDGFRβ, we generated embryos that lacked these receptors in cardiomyocytes and vascular smooth muscle cells (VSMC) using conditional gene ablation. Deletion of either PDGFRα or PDGFRβ caused no overt vascular defects, but loss of both receptors using an *SM22α-Cre* transgenic mouse line led to a disruption in yolk sac blood vessel development. The cell population responsible for this vascular defect was the yolk sac mesothelial cell not the cardiomyocyte or the VSMC. Coincident with loss of PDGF receptor signaling we found a reduction in collagen deposition and an increase in MMP-2 activity. Finally, *in vitro* allantois cultures demonstrated a requirement for PDGF signaling in vessel growth. Together, these data demonstrate that PDGF receptors cooperate in yolk sac mesothelium to direct blood vessel maturation and suggest that these effects are independent from their role in VSMC development.

INTRODUCTION

Vascular remodeling and maturation are complex processes that transform an endothelial plexus into vessels of various caliber and stability. Although angiogenesis has been studied extensively, the mesodermal signals directing these cellular processes are not well understood. One of the earliest tissues to undergo remodeling during development is the yolk sac, and the proper formation of yolk sac blood vessels is essential for embryonic development and hematopoiesis. Disruption of yolk sac vascular development, either directly or indirectly by aberrant cardiac function, often results in embryonic lethality between E9.5 and E11.5 (Copp 1995). In a majority of cases the primary cell type responsible for yolk sac vessel abnormalities is the endothelial cell (Argraves and Drake 2005). While endothelial cells are commonly implicated in yolk sac phenotypes, the contribution of other yolk sac cell populations should not be discounted. For example, BMP-4 and retinoic acid secretion by the visceral endoderm are required in a paracrine manner for hematopoietic and endothelial development (Yoder et al. 1994; Dickson et al. 1995; Bohnsack et al. 2004; Bohnsack et al. 2006), while fibronectin and laminin deposition by the yolk sac mesothelium is required for endothelial remodeling (Goumans et al. 1999).

Due to their close proximity to endothelial cells, VSMC are also believed to influence blood vessel integrity. In the absence of these support cells, some endothelial vessels are hyperplastic, tortuous, dilated, and leaky (Lindahl et al. 1997; Hellstrom et al. 2001). In the yolk sac vasculature, it has been difficult to ascertain the function of VSMC because many relevant regulatory molecules are expressed by both endothelial cells and VSMC. Mice that have mutations in TGFβ signaling exhibit defects in VSMC

formation and recruitment, but they also possess cardiovascular and endothelial cell defects (McAllister et al. 1994; Dickson et al. 1995; Johnson et al. 1996; Li et al. 1999; Yang et al. 1999). Therefore, the lack of VSMC in these mutants may be secondary to aberrant circulation and not the cause of yolk sac vascular demise.

PDGF receptors have been implicated in cardiovascular development by their functions in cardiac neural crest cells (Tallquist and Soriano 2003; Richarte et al. 2007), retinal astrocytes (Gerhardt et al. 2003), mesoderm precursors to endothelial cells (Rolny et al. 2006), VSMC (Soriano 1994), and tumor stroma (Pietras et al. 2008), but few investigations have looked at a role for these receptors in cardiac and yolk sac development. To address this topic, we used Cre/loxP technology to remove PDGF receptors from cardiomyocytes and VSMC. We learned that PDGF receptor expression in the yolk sac mesothelium is essential for yolk sac blood vessel development and that one function of these receptors may be to direct extracellular matrix deposition to promote vascular remodeling. These data demonstrate that PDGF receptor function in vascular development may be broader than once thought and potentially these receptors may play similar roles in vascular development in other tissues.

MATERIALS AND METHODS

Mouse Lines

The mouse lines used in these studies were *PDGFRα*$^{fl/fl}$ (Tallquist and Soriano 2003), *PDGFRβ*$^{fl/fl}$ (Richarte et al. 2007), *Tg(Tagln-cre)1Her/J (SM22α-Cre*^{Tg}*)* (Holtwick et al. 2002), *Meox2*$^{Cre/+}$ (Tallquist and Soriano 2000), *myocardin*$^{Cre/+}$ (Long et al. 2007), *Tie2Cre*^{Tg} (Kisanuki et al. 2001), ROSA26 Reporter LacZ (*R26R*) (Soriano 1999),

Tie2GFP^{Tg} (Schlaeger et al. 1997), and *PDGFRα*^{GFP} (Hamilton et al. 2003). *SM22α-Cre*^{Tg} mice were purchased from Jackson Laboratories. Transgene levels of *SM22α-Cre*^{Tg} animals were detected by Southern blot analysis using a probe for the *Cre* gene. These mice were maintained by inbreeding lines that were homozygous for the *SM22α-Cre*^{Tg}. Control embryos and yolk sacs were either *SM22α-Cre*^{Tg} littermate embryos bearing heterozygous floxed alleles or wild type embryos (somite stage matched). Detection of a vaginal plug was defined as embryonic day 0.5 (E0.5). *PDGFR*^{MKO} embryos were recovered up to E18.5 but we recovered fewer than expected after birth. Often we found P1 animals with spina bifida and a cleft palate. Previously, we have determined that the *PDGFRα* floxed allele is hypomorphic and is lethal in combination with a null allele. These data combined with the fact that *myocardin*^{Cre} can lead to germline deletion of floxed alleles, suggested that the lethality was not caused by the conditional deletion of the PDGF receptors but by loss of PDGFRα signaling regardless of the *myocardin*^{cre} status of the mice.

Histology and Immunohistochemistry

Samples stained for β-galactosidase were fixed in 2% formaldehyde/0.2% glutaraldehyde for 10 minutes, stained in x-gal overnight at room temperature, and postfixed in 10% buffered formalin for 20 minutes. Whole embryos were stained for PECAM and αSMA according to standard procedures and cleared using benzylalcohol:benzyl benzoate (1:2) for imaging (Hogan 1994). Yolk sacs were fixed for 1 hour in 4% paraformaldehyde (PFA) at 4°C and blocked for 30 minutes in 1.5% normal serum. For section analysis, samples were fixed for 1-3 hours in 4% PFA,

embedded in paraffin wax or OCT compound, and sectioned at 7-10 microns. Immunohistochemistry was performed by incubation in primary antibody for 2 hours to overnight at 4°C and visualized using Alexafluor secondary antibodies or Vectastain Elite ABC kit and DAB peroxidase substrate kit (Vector Laboratories, Burlingame, CA) according to manufacturer's instructions. Antigen retrieval for PECAM and αSMA paraffin sections was performed as previously described (Tallquist and Soriano 2003). Hematoxylin and eosin (H&E) staining and picrosirius red staining were performed according to standard methods.

Western blotting and immunoprecipitation

For immunoprecipitation, whole yolk sac lysates were incubated overnight at 4°C with 1μg of antibody then 1 hour with protein A sepharose beads. After washing, precipitated proteins were run on SDS-PAGE. For western blotting, yolk sac lysate was quantified using Bradford reagent and equal amounts of protein were run on SDS-PAGE and transferred onto nitrocellulose membranes following standard protocols. The membranes were incubated with 1% BSA/0.05% Tween-20 in TBS for 30 minutes, primary antibody overnight at 4°C, and secondary antibody for 1 hour. Results were visualized using ECL (Amersham Biosciences, Piscataway, NJ).

Antibodies

Primary antibodies used for immunohistochemistry and whole mount include PDGFRβ (eBioscience, San Diego, CA), 1:250; PECAM (clone MEC13.3, BD Bioscience, San Jose, CA), 1:250; αSMA-FITC (clone 1A4, Sigma, St. Louis, MO),

1:500; GFP (abcam, Cambridge, MA), 1:250; SM22α (abcam, Cambridge, MA), 1:250; Collagen1 (abcam, Cambridge, MA), 1:250; Collagen4 (Chemicon, Temecula, CA), 1:250; Fibronectin (Sigma), 1:500; and Laminin (Sigma), 1:250. Secondary antibodies used include α-rabbit, α-rat, and α-mouse Alexafluor 488, 543, 594, and 633 (Molecular Probes, Eugene, OR), 1:500. Antibodies used for western blots include Integrin β1 (abcam), 1:1000; Integrin β1 phospho-S785 (abcam), 1:1000; PDGFRβ (Upstate, Charlottesville, VA), 1:1000; PDGFRα (Upstate), 1:1000; and cytoskeletal actin (Novus Biologicals, Littleton, CO), 1:1000.

Realtime PCR

RNA was isolated from yolk sacs using Trizol (Invitrogen, Carlsbad, CA) and an RNeasy kit (Qiagen, Valencia, CA). Samples were isolated and homogenized in Trizol. 20% choloroform was added, mixed well, and centrifuged for layer separation. Top layer was mixed with equal volume 70% ethanol and added to an RNeasy kit minispin column and centrifuged. Washes were followed according to RNeasy protocol and eluted with DEPC H_2O. RNA was quantified and DNase treated. 1μg of RNA was used to generate cDNA using PowerScript Reverse Transcriptase (Clontech, Mountain View, CA) and random hexamers. Gene expression was quantified using standard realtime PCR methods using SYBRgreen master mix on an ABI7000 instrument (Applied Biosystems, Foster City, CA). Samples were analyzed in triplicate on a minimum of three samples per genotype. Primer sequences will be provided upon request.

MMP Assays

DQ Gelatin assay (Molecular Probes) was performed on fresh frozen tissue sections according to manufacturer's instructions. Briefly, samples were sectioned and incubated for 30 minutes in substrate buffer then transferred to DQ Gelatin (3μg/ml) at 37°C and imaged after incubation for 0, 15, and 30 minutes. Zymography was performed according to standard protocols (Leber 2001) with human MMP-2 and MMP-9 standards (Chemicon). Yolk sac lysates were quantified using Bradford reagent and equal amounts of protein were analyzed.

Allantois Assay

E8.5 allantoides were isolated from wild type and $PDGFR\alpha^{fl/fl}$; $PDGFR\beta^{fl/fl}$ embryos and plated on gelatin-coated coverslips. Media was supplemented with 1% FBS, 10% FBS, or 20ng PDGFBB (R&D Systems, Minneapolis, MN). Cultures were grown for 24-26 hours at 37°C in 5% CO_2. Samples were fixed with 4% PFA for 10 minutes and stained for PECAM as described above. Adenovirus transduction was performed using $1.4x10^7$ PFU per 1ml of media at the time of plating. PDGF receptor inhibitor (AG1296 (2μM), Calbiochem, Gibbstown, NJ) was added to appropriate stimulation media at time of plating. For collagen 4 assays, wells were coated for 1 hour with 0.5μg/ml, 5μg/ml, or 50μg/ml collagen 4 (R&D Systems) then media was added to the collagen 4 at time of allantois plating.

Image acquisition and manipulation

Whole mount and section samples were analyzed using a Nikon SMZ1000 and Zeiss Axiovert200 (Carl Zeiss, Thornwood, NY) microscopes. Images were captured using Hamamatsu ORCA-ER (Hamamatsu, Bridgewater, NJ) and Olympus DP71 (Olympus, Center Valley, PA) cameras with OpenLab 3.5.1 and DP Controller software, respectively. Fluorescent images were colored using OpenLab then processed in Adobe Photoshop. Confocal images were captured using an LSM510META confocal microscope (Carl Zeiss) and processed in ImageJ and Adobe Photoshop. Color images and western blots were processed in Adobe Photoshop for white background. Quantification and threshold measurements were calculated through ImageJ. Graphs and statistics were generated using Prism (Graphpad). Final figures were compiled using Canvas 9.

RESULTS

Generation and survival of PDGF receptor smooth muscle cell knockout embryos

Previous data from *PDGFRβ* and *PDGFB* null embryos indicates that PDGFRβ is required for formation of VSMC and that myocardial development is also affected (Leveen et al. 1994; Soriano 1994; Lindahl et al. 1998; Hellstrom et al. 1999; Van den Akker et al. 2008). Because we wanted to investigate the cell lineages dependent on PDGFRβ signal transduction, we have used loxP/Cre technology to generate animals that lack PDGFRβ in both cardiomyocytes and VSMC. We used two Cre-expressing mouse lines to accomplish the deletion, *SM22α-Cre*^{Tg} (Holtwick et al. 2002) and *myocardin*^{Cre}

(Long et al. 2007). *SM22α* is expressed as early as E8.5 in cardiomyocyte development and during VSMC terminal differentiation (Li et al. 1996), while *myocardin* is expressed by E8.5 in cardiomyocytes and is one of the earliest genes expressed in VSMC precursors (Wang et al. 2001). Surprisingly, deletion of *PDGFRβ* using either *SM22αCre*^{Tg} (referred to as *PDGFRβ*^{SKO}) or *myocardin*$^{Cre/+}$ mice (referred to as *PDGFRβ*^{MKO}) did not phenocopy *PDGFRβ*$^{-/-}$ mice. Both *PDGFRβ*^{SKO} and *PDGFRβ*^{MKO} embryos and mice were viable and fertile.

Recently, we have shown that the two PDGF receptors (α and β) act cooperatively in the neural crest-derived smooth muscle of the aortic arch (Richarte et al. 2007). To determine if PDGFRα was compensating for loss of PDGFRβ signaling in other VSMC populations, we generated mice that contained *SM22α-Cre*^{Tg} and conditional alleles of both PDGF receptors. Genotyping of offspring from these crosses revealed that few *PDGFRα*$^{fl/fl}$*;PDGFRβ*$^{fl/fl}$*; SM22α-Cre*^{Tg} (*PDGFR*^{SKO}) pups were recovered at birth, indicating that PDGF receptor signaling through both receptors was required for viability in an SM22α-expressing cell population. Using timed matings, we recovered the expected Mendelian ratios of embryos up to E10.5, but few *PDGFR*^{SKO} embryos past this time point. The few, viable mice that were doubly homozygous for the PDGF receptor floxed alleles were *SM22α-Cre*$^{Tg/0}$ (hemizygous for the transgene; data not shown). We surmised that the expression level of *Cre* in mice hemizygous for the transgene was not sufficient to recombine all four floxed alleles efficiently. Indeed, no *PDGFR*^{SKO} pups resulted from breeders that were *SM22α-Cre*$^{Tg/Tg}$. All subsequent analyses were performed using mice homozygous for *SM22α-Cre*^{Tg}. Commonly, transgenic Cre lines

are not maintained as homozygotes due to potential transgene insertion effects. We have ruled out these effects because lethality only occurs in double homozygous *PDGF receptor SM22α-Cre*$^{Tg/Tg}$ embryos not single *PDGF receptor SM22α-Cre*$^{Tg/Tg}$ embryos. Because *SM22α-Cre*^{Tg} was likely to target deletion in VSMC similar to *myocardin*^{Cre}, we predicted that excision of the two *PDGF receptors* in this mouse line (*PDGFR*^{MKO}) would phenocopy the embryonic lethality observed in *PDGFR*^{SKO} embryos. However, *PDGFR*^{MKO} embryos survived until birth.

Expression of SM22-Cre^{Tg} *before VSMC differentiation in the yolk sac*

The dramatic difference in survival between *PDGFR*^{SKO} and *PDGFR*^{MKO} embryos lead us to investigate the profile of Cre activity in the two Cre mouse lines. Using ROSA26 reporter mice, we determined *SM22α-Cre*^{Tg} and *myocardin*^{Cre} expression between E8.5 and E10.5. Cre activity was not detected in any tissue at E7.5 using either of the Cre lines. By E8.5, SM22α-Cre activity was observed in many cells of the yolk sac as well as a small number of cells in the primitive heart (Figure 2-1A). In contrast, myocardin-Cre activity was detected in the cardiac crescent, and only a few β-galactosidase positive cells were observed in *myocardin*^{Cre} yolk sacs (Figure 2-1E). Because Cre expression in the yolk sac was the most obvious difference between these lines, we examined histological sections of this tissue. At E8.5 SM22α-Cre activity was present throughout the yolk sac mesothelium, but no β-galactosidase positive cells were detected in the *myocardin*^{Cre} yolk sacs (Figure 2-1A and E). The yolk sac mesothelium is a mesoderm-derived epithelial-like component of the yolk sac that rests on a thin

basement membrane and is believed to be important for transport and movement of fluid from the yolk sac. At E9.5, β-galactosidase positive cells were present in both the mesothelial layer and surrounding some vessels in the *SM22α-Cre*^{Tg}, while *myocardin*^{Cre} activity was present in only a few cells associated with blood vessels, presumably VSMC progenitors (Figure 2-1B and F). At E10.5 *SM22α-Cre*^{Tg} and *myocardin*^{Cre} yolk sacs both possessed β-galactosidase expression in cells surrounding blood vessels, but β-galactosidase expression in *myocardin*^{Cre} was lacking in yolk sac mesoderm populations that were not vessel associated (Figure 2-1C and G). These data pointed to the possibility that deletion of the PDGF receptors in the yolk sac mesothelium caused the embryonic lethality.

Because Cre expression leads to indelible β-galactosidase expression, we could also use this marker to follow mesothelial and VSMC cell lineages in *PDGFR*^{SKO} and *PDGFR*^{MKO} embryos. In both *PDGFR*^{SKO} and *PDGFR*^{MKO} yolk sacs, few perivascular, β-galactosidase positive cells were present at E10.5 (Figure 2-1D and H). β-galactosidase positive cells were abundant in the mesothelial layer in the *PDGFR*^{SKO} yolk sac demonstrating that loss of PDGF receptors did not lead to a failure in the formation of this cell population. In addition, examination of both *PDGFR*^{SKO} and *PDGFR*^{MKO} embryos revealed abundant β-galactosidase positive cells in the hearts and trunk areas (data not shown), demonstrating that loss of the receptors did not result in a general reduction of mesoderm cells.

PDGFRα and PDGFRβ are co-expressed in the yolk sac mesothelium and perivascular cells

While PDGFRα and PDGFRβ expression has been documented as early as E6.5 in the extraembryonic endoderm and ectoplacental cone, and the ligands are expressed in chorionic ectoderm and parietal endoderm (Mercola et al. 1990; Orr-Urtreger et al. 1992; Schatteman et al. 1992), analysis of co-expression of the receptors in the yolk sac has not been determined. Therefore, we investigated expression patterns of the receptors. Expression of PDGFRα was detected using mice that express a nuclear localized GFP from the PDGFRα locus that faithfully traces PDGFRα expression (Hamilton et al. 2003) and a PDGFRβ specfic antibody. At E8.5 PDGFRα and PDGFRβ were expressed in mesothelium and endoderm, as previously reported (Figure 2-2A). At E9.5, PDGFRβ endoderm expression was reduced, but expression of both receptors was maintained in the mesothelium (Figure 2-2B and data not shown). At E10.5 both receptors were expressed in the mesothelium, but only PDGFRβ was identified in cells surrounding endothelial vessels (Figure 2-2C). Presumably these cells were VSMC. The early and persistent co-expression of PDGF receptors in the mesothelial layer (Figure 2-2D) along with lethality of $PDGFR^{SKO}$ but not $PDGFR^{MKO}$ support the possibility that PDGF receptor expression in the mesothelium is required for embryo viability.

Because multiple reports have suggested that PDGFRβ is expressed by endothelial cells and to further refine our expression analysis in the yolk sac, we examined PDGFRβ expression in $Tie2GFP^{Tg}$ mice. These mice express GFP in endothelial cells (Schlaeger et al. 1997). We found no Tie2 positive cells that expressed

detectable levels of PDGFRβ between E8.0-E10.5 (Figure 2-2E and data not shown). *Tie2GFP*^{Tg} cells were present in blood islands adjacent to PDGFRβ-expressing mesothelium at E8.5. This expression profile was consistent with a previous report that demonstrated PDGFRβ expression in mesoderm precursors in the yolk sac but not differentiated endothelial cells (Rolny et al. 2006).

PDGFR^{SKO} *results in incomplete yolk sac capillary bed reorganization*

Embryonic lethality between E9.5 and E10.5 is often a result of cardiovascular failure, but αSMA staining for cardiomyocytes and PECAM staining for endothelial cells revealed that cardiac and embryonic vascular development appeared normal in E10.5 *PDGFR*^{SKO} embryos (Figure 2-3A-D). No cardiovascular defects were observed in the embryo proper. This lack of cardiomyocyte phenotype is in agreement with gene deletion analysis of PDGF receptors using an early mesoderm expressed Cre line, *MesP1*^{Cre} (Kang et al. 2008). By contrast, whole mount views and histological sections of *PDGFR*^{SKO} embryos at E10.5 revealed an apparent cessation of blood vessel maturation within the yolk sac (Figure 2-3E and F). While endoderm and mesothelial layers appeared normal, endothelial vessels were distended and disorganized compared to vessels in control embryos. At this time point, we also observed efficient deletion of both PDGFRα and PDGFRβ in *PDGFR*^{SKO} yolk sacs (Figure 2-3G and H). Additional analyses demonstrated that these defects were not caused by abnormal proliferation or apoptosis within mutant yolk sacs as overt differences at E9.5 and E10.5 in these two processes were not observed between mutant and control samples (data not shown).

To assess yolk sac vascular development in our mutants, we performed whole mount PECAM staining. Vasculogenesis of the yolk sac begins at E7.5, and a number of signaling proteins have been implicated in this process (Argraves and Drake 2005). After E8.5 yolk sac vessels undergo a dramatic remodeling event where the primitive polygonal structure of the vasculature converts to stable and defined vessels (Flamme et al. 1997). In both control and mutant yolk sacs, we observed the typical honeycomb pattern of endothelial cells at E9.5 (Figure 2-4A and B), but at E10.5, *PDGFR*^{SKO} yolk sacs retained the characteristics of an immature yolk sac, and failed to reorganize into the normal hierarchical array of large and small vessels (Figure 2-4G).

To establish if these yolk sac defects were caused primarily by loss of one of the receptors, we analyzed yolk sac vessels by PECAM staining in single PDGF receptor mutants. Yolk sacs from *PDGFR*$\alpha^{-/-}$, *PDGFR*$\beta^{-/-}$, *PDGFR*α^{SKO}, and *PDGFR*β^{SKO} mutants developed normally, although the remodeled vessels in the E10.5 *PDGFR*$\beta^{-/-}$ yolk sacs were slightly more disorganized than control vessels (Figure 2-4D, I, J, and data not shown). We next analyzed embryos with complete deletion of both receptors to determine if this genotype would phenocopy the *PDGFR*^{SKO} embryos. To increase the probability of obtaining double mutant embryos, we crossed our conditional animals with *Meox2*^{Cre} mice. *Meox2*^{Cre} expresses Cre in all embryonic tissues and extra-embryonic mesoderm (Tallquist and Soriano 2000). Many of the mutant embryos were resorbing by E9.5 consistent with the phenotype of PDGF receptor double homozygous embryos (M.T, unpublished observation), but a few embryos were recovered. These exhibited a complete failure in yolk sac remodeling (*PDGFR*^{Meox2}; Figure 2-4E) that resembled the hyperfusion phenotype described previously (Drake and Little 1995; Dominguez et al.

2007), providing further evidence that loss of both PDGF receptors results in yolk sac vascular abnormalities.

Loss of PDGF receptors results in an increase of endothelial gene expression

Vascular remodeling is controlled by activities of multiple cell populations, including endothelial (Flamme et al. 1997) and mural (Saunders et al. 2006) cells. To examine the differentiation status of these cell populations, we analyzed yolk sac gene expression by real time PCR. First, expression analysis demonstrated an expected decrease in *PDGFR*α and *PDGFR*β in the *SM22*α*-Cre*^{Tg} mutants compared to wild type yolk sacs (Figure 2-5A). Consistent with analysis of another yolk sac remodeling mutant, *Hand1* (Morikawa and Cserjesi 2004), activated endothelial cell specific gene expression, such as *VEGFR1 (Flt1)*, *VEGFR2 (Flk1)*, and *Tie2*, was increased (Figure 2-5B). In agreement with the increased vasculogenic response, we observed slightly elevated *VEGF* ligand expression. However, two other endothelial cell specific genes, *PDGFB* and *VEcadherin*, levels were similar or when compared to controls (Figure 2-5B). The elevated level of these endothelial genes in *PDGFR*^{SKO} yolk sacs suggests that the impaired vascular development may be inducing an enhanced but non-productive angiogenic response.

To rule out a direct requirement for PDGF receptors in endothelial cells we generated embryos that lacked all PDGF receptor expression in endothelial cells using a *Tie2Cre*^{Tg} mouse line (*PDGFR*^{EKO})(Kisanuki et al. 2001). We recovered viable *PDGFR*^{EKO} mutants at E12.5 and E15.5 and no obvious defects were observed in yolk sac development (data not shown). Together these data imply that PDGF receptor signaling

is not employed by endothelial cells and that the remodeling phenotype is caused by loss of the receptors in either VSMC or the mesothelium.

Remodeling defect is not caused by loss of PDGF receptor signaling in VSMC

We next examined the expression of VSMC genes in the $PDGFR^{SKO}$ yolk sacs. Consistent with the lack of VSMC we observed by lineage tracing in Figure 1D, VSMC gene expression was reduced. *Myocardin related transcription factor B (MRTFB),* a yolk sac smooth muscle transcription factor (Wei et al. 2007), expression was reduced in $PDGFR^{SKO}$ yolk sacs (Figure 2-5C). Similarly, expression of the smooth muscle cell cytoskeletal gene *αSMA* was also reduced (Figure 2-5C). *SM22α* expression, by contrast, only exhibited a partial reduction. This result would be anticipated because mesothelial cells also express *SM22α*, and they do not appear reduced in number (Figure 2-1D and data not shown).

These expression data suggested a disruption in the VSMC population. Therefore, we examined E10.5 control, $PDGFR^{SKO}$, and $PDGFR^{MKO}$ yolk sacs for the presence of VSMC. While control yolk sacs had extensive networks of vessels that contained αSMA positive cells, in both mutant yolk sac genotypes few αSMA expressing cells were present next to endothelial vessels when compared to control yolk sacs (Fig. 2-4L-N). This result suggested that PDGF receptor signaling was required for VSMC formation. To identify if a specific receptor was important for VSMC formation, we examined αSMA staining in null and conditional mutants for *PDGFRα* and *PDGFRβ* individually (Figure 2-4 and data not shown). In $PDGFR\beta^{-/-}$ and *PDGFRβ* conditional deletion lines,

loss of PDGFRβ led to a dramatic reduction in yolk sac VSMC (Figure 2-4O-Q). Yet, despite the lack of VSMC in these mutants, yolk sac vasculature organized into vessels of different calibers. These data suggest that PDGFRβ may be the essential PDGF receptor involved in VSMC development in the yolk sac. However, the presence of normal vessel remodeling in the absence of VSMC indicated that the yolk sac phenotype we observed in $PDGFR^{SKO}$ was not caused by a failure in VSMC association. The mesothelial cells were therefore implicated as the primary cell population responsible for this phenotype as they were the only cells that expressed Cre in $SM22\alpha\text{-}Cre^{Tg}$ conditionals that did not express Cre in $myocardin^{Cre}$ conditionals.

PDGF receptor signaling affects extracellular matrix deposition

Mesothelial cells have a number of proposed functions including transport of fluids, production of growth factors, and secretion of extracellular matrix (ECM). Because the vascular defects we observed resembled retinoic acid and TGFβ signaling pathway mutants that are deficient in ECM production (Goumans et al. 1999; Bohnsack et al. 2004; Carvalho et al. 2004), we examined the distribution of ECM in wild type, $PDGFR^{SKO}$, and $PDGFR^{MKO}$ yolk sacs. Staining for fibrillar collagen by picrosirius red staining (Figure 2-6A) demonstrated that $PDGFR^{SKO}$ yolk sacs had a decreased intensity and thickness of collagen. In contrast, $PDGFR^{MKO}$ yolk sacs appeared similar to wild type samples. Immunohistochemistry for collagen 1 and collagen 4 in $PDGFR^{SKO}$ yolk sacs supported the picrosirius red findings (Figure 2-6B and C). The reduction in

collagens was limited to the mesothelium as collagen 4 was detected in close proximity to the endothelial cells. In contrast, fibronectin and laminin appeared relatively unperturbed at this stage (Figure 2-6D and E). To determine if the reduction in collagen was at the transcriptional level we performed real time PCR analysis. We detected only modest changes in transcript levels of collagens and fibronectin (Figure 2-6F).

Because we observed a greater reduction in collagen protein levels than was suggested by the realtime PCR results, we analyzed matrix metalloprotease (MMP) activity in situ and detected higher levels of MMP activity within the mesothelium (Figure 2-6G). Similarly, gelatin zymography consistently demonstrated higher levels of activated MMP-2 in $PDGFR^{SKO}$ mutant yolk sacs compared to control yolk sacs (Figure 2-6H). Taken together these data suggest that PDGF receptor signaling from the mesothelium may function to direct blood vessel remodeling in part by controlling the degradation of matrix in the yolk sac.

PDGF receptor signaling controls blood vessel morphogenesis

To further examine the role of PDGF receptors in vascular development, we used an allantois culture assay. E8.5 allantoides from wild type embryos develop rudimentary vascular structures, but when stimulated with either 10% FBS or PDGFBB, a ligand that can activate both PDGFRα and PDGFRβ, the vascular plexus expands (Figure 2-7A and C). In addition, we showed that PDGF receptor signaling in these cultures was required for the stabilization of the vessels. Using a Cre expressing adenovirus we were able to induce recombination in allantois explants from embryos homozygous for both *PDGFRα*

and *PDGFRβ* floxed alleles (*PDGFR*$^{fl/fl}$). When both PDGF receptors were deleted using Cre, vascular expansion was severely reduced (Figure 2-7B and C). Quantification of vascular expansion demonstrated that PDGF receptor stimulation yielded cultures that were comparable to serum stimulation (Figure 2-7C). Similarly, addition of a PDGF receptor specific inhibitor (AG1296) to the cultures resulted in a lack of vascular expansion similar to unstimulated cultures (Figure 2-7D). We could not examine the effects of the PDGF receptor inhibitor on PDGFBB stimulated cultures as these cultures did not adhere to the cover slip. To determine the affect of exogenous addition of matrix we plated allantois cultures on collagen 4 and found that exogenous collagen 4 resulted in increased vascular expansion in 1% serum. Treatment with collagen 4 was even capable of bypassing the effects of PDGF inhibition on cultures stimulated with either 10% FBS or PDGFBB (Figure 2-7D and data not shown).

Finally, to examine how reduced extracellular matrix could effect endothelial cell signaling, we determined if integrin function within the yolk sac was disrupted. To accomplish this, we examined the activation status of integrin β1. Integrin β1 is essential for endothelial cell function(Carlson et al. 2008) and is one of the key integrins in endothelial cell morphogenesis. Phosphorylation of integrin β1 on S785 modulates cell adhesion and migration. Using a phosphospecific antibody for S785 of β1 integrin (Mulrooney et al. 2001), we found that phosphorylation on S785 was reduced even though levels of β1 integrin were similar in control and *PDGFR*^{SKO} yolk sacs (Figure 2-7E). Taken together these data suggest that loss of PDGF receptor signaling leads to reduced vascular remodeling that may be related to a loss in matrix integrity.

DISCUSSION

Generation of mature blood vessels requires coordination between endothelial cells and their surrounding tissues. While it is established that growth factor secretion and guidance cues are necessary for appropriate vessel patterning, many of the processes involved in directing vessel remodeling remain a mystery. Here, we show that one of the signals required in yolk sac vessel formation derives from PDGF receptor signals in the mesoderm. By deleting the receptors from select cell populations we show that PDGF signaling is required for vascular remodeling. Unexpectedly, we observed normal progression of vasculogenesis in the absence of VSMC, suggesting that vascular remodeling is not due to a failure in VSMC formation. Instead, PDGF receptors in extraembryonic mesoderm provide signals for yolk sac vascular progression.

The origin of VSMC in the yolk sac is currently unclear, but there are two potential sources. One is from embryonic hemangioblasts that arise in the primitive streak and migrate to the yolk sac to form the blood islands. Clonal analysis of *brachyury* positive and *VEGFR2* positive cells has suggested that a single progenitor can give rise to endothelial, hematopoietic and vascular smooth muscle cells (Ema et al. 2003; Huber et al. 2004). Another possibility is that the yolk sac VSMC arise from yolk sac mesothelium. Evidence is accumulating to suggest that mesothelium can differentiate into components of blood vessels including VSMC and fibroblasts. The heart was the first tissue identified where the mesothelium (epicardium) differentiates and contributes to the vascular structures (Mikawa et al. 1992; Mikawa and Gourdie 1996; Dettman et al. 1998; Vrancken Peeters et al. 1999). Others have shown more recently that the serosal mesothelium can also contribute to the VSMC of the gut (Wilm et al. 2005; Kawaguchi et

al. 2007). Interestingly, stimulation of either tissue by PDGFBB results in an increase in VSMC differentiation (Lu et al. 2001; Kawaguchi et al. 2007). Although the current reagents do not permit us to conclusively prove the origin of yolk sac VSMC, our data are consistent with the possibility that yolk sac mesothelium can give rise to perivascular cells. Loss of PDGF receptors in the *SM22α–Cre* transgenic line leads to an early absence of VSMC. Thus, the mesothelium could be a source of perivascular cells that stabilize the vessels as well as a source of growth factors and extracellular matrix to direct vascular remodeling.

In addition to the uncertainty of VSMC origin, there has also been a longstanding debate over the importance of VSMC in the yolk sac. Disruption of myocardin, an SRF transcriptional cofactor and key regulator of VSMC development, leads to embryonic lethality at E9.5 (Wang et al. 2003), but it is unclear if this phenotype is caused by loss of VSMC in the yolk sac (Pipes et al. 2006). *MRTFB* mutant embryos, a second member of the myocardin family of transcription factors, display a reduction in yolk sac VSMC, but these embryos survive past E10.5 when many mutants with yolk sac phenotypes perish (Oh et al. 2005; Wei et al. 2007). Often the difficulty in interpreting known yolk sac phenotypes is that many of the genes are likely to affect yolk sac development by multiple avenues. For example, both endothelial cell differentiation and cardiac function are essential for proper yolk sac vessel maturation. Mutations in multiple components of the TGFβ signaling pathway demonstrate dramatic yolk sac vascular disruptions, but these defects could be caused by a failure in endothelial cell or VSMC function (Dickson et al. 1995; Oshima et al. 1996; Li et al. 1999; Yang et al. 1999; Arthur et al. 2000; Jadrich et al. 2006).

Studies in *PDGFRβ* and *PDGFB* null embryos have established that a subset of VSMC, sometimes referred to as pericytes, require PDGFRβ signal transduction (Soriano 1994; Lindahl et al. 1997; Hellstrom et al. 1999). The loss of PDGFRβ seems to predominantly affect VSMC of smaller vessels while VSMC of larger vessels such as the aorta are less disrupted. Here, we show that yolk sac VSMC are dependent on PDGFRβ expression. In multiple mouse lines, loss of PDGFRβ leads to a severe reduction in VSMC of the yolk sac. Surprisingly, endothelial cells in our mutants continued to mature into hierarchical vessels and early embryogenesis was undisturbed. The only abnormality caused by loss of VSMC was an increase in vessel tortuosity. Our data demonstrate that the yolk sac vasculature does not require VSMC for stability, possibly because the hemodynamic forces within these vessels are not excessive.

Although it is commonly assumed that the two PDGF receptors direct similar cellular responses, there are few *in vivo* examples of the ability of these receptors to compensate for each other. This fact is underscored by the disparate phenotypes of the individual receptor knockouts. *PDGFRα* null embryos die between E10.5 and E15.5 due to a wide range of defects (Soriano 1997), while *PDGFRβ* null embryos die perinatally from vascular defects (Soriano 1994). However, in the yolk sac, we found that if one of the receptors was expressed, blood vessel remodeling occurred normally. The observed redundancy in the yolk sac mesoderm leads to the possibility that the PDGF receptors may contribute to vessel remodeling in other tissues. Another example of receptor cooperativity in vessel remodeling was observed in cardiac neural crest cells. When PDGF receptors are removed from neural crest cells, failure of the aortic arch vessel

remodeling leads to persistent truncus arteriosus (Richarte et al. 2007). Because *PDGFRα/β* null embryos die before E10.5, this general requirement for PDGF receptor signaling and vascular remodeling may have been overlooked.

ECM disruptions have been found in several mouse mutants with yolk sac phenotypes. Mutations in collagen4, fibronectin, and laminin expression have demonstrated vascular defects (George et al. 1997; Poschl et al. 2004). TGFβ signaling is considered a key component of ECM deposition, and mutations in several components of TGFβ pathways have also demonstrated defects in yolk sac vascular formation (Goumans et al. 1999; Li et al. 1999; Yang et al. 1999; Arthur et al. 2000; Larsson et al. 2001; Cohen et al. 2007). Although disrupted ECM deposition is common to both TGFβ pathway mutant and PDGF receptor mutant yolk sacs, the cell types responsible are different. Recently, it was demonstrated that endothelial specific deletion of TGFβR1 or TGFβR2 recapitulates the knockout yolk sac phenotype (Carvalho et al. 2007). Our data now point to a second essential population of cells required for yolk sac vessel growth, the mesothelium and demonstrate that ECM secretion by endothelial cells is not sufficient to promote normal vascular development.

Control of ECM levels by PDGF receptor expressing cells via MMP activity is a relatively new concept in vascular remodeling. Currently, the few papers addressing this topic are conflicting. Some data propose that PDGF receptor stimulation results in increased levels of MMP proteins and activity (Robbins et al. 1999), while others propose that stimulation of PDGF receptors leads to inhibition of MMP activity (Karakiulakis et al. 2007). In the yolk sac we can imagine two possible mechanisms explaining increased

MMP activity. The first is that PDGF receptor interactions with MT1-MMP at the cell membrane attenuate MT1-MMP activity, but in the absence of PDGF receptors is increased MMP activity. Data supporting this scenario are: MT1-MMP can activate MMP-2 (Sato et al. 1994; Strongin et al. 1995); MT1-MMP is expressed in mesothelial cell populations (Zhong et al. 2006); and MT1-MMP can physically associate with PDGFRβ (Lehti et al. 2005). An alternative possibility is that PDGF receptor stimulation results in secretion of tissue inhibitors of metalloproteinases (TIMPS).

Our findings suggest that PDGF receptors act coordinately in the extraembryonic mesoderm and are involved in the process of vascular remodeling. We have also shown that VSMC are not required in the establishment of mature endothelial vessels in the yolk sac. These studies open up new questions on the cooperativity of the two receptors in stromal cell populations throughout the developing embryo and potentially during vascular remodeling during the disease process.

ACKNOWLEDGEMENTS

We would like to thank Drs. Ondine Cleaver, Dan Garry, and Eric Olson for providing the *Tie2Cre*^{Tg}, *Tie2GFP*^{Tg}, and *myocardin*^{Cre} mice, respectively. We would also like to thank Dr. Robert Gerard for generously providing Cre-expressing adenovirus. We would like to thank Drs. Rhonda Bassel-Duby, Rolf Brekken, Ondine Cleaver, Rita Perlingiero and our laboratory colleagues for comments on the manuscript. We would also like to thank Angie Bookout, Michelle Kazi, Haley Newton, Banu Eskiocak, and Holly Mead for excellent technical assistance.

FIGURES AND LEGENDS

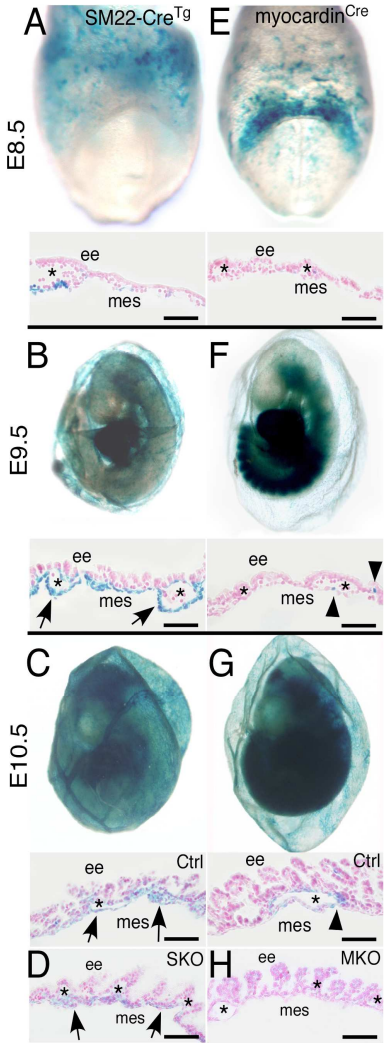

Figure 2-1. *SM22α-Cre*^{Tg} is expressed in yolk sac mesothelium and VSMC while *myocardin*^{Cre} is specific to VSMC. (A-C) Whole mount LacZ staining of yolk sac demonstrates *SM22α-Cre*^{Tg} expression at the indicated stages. (A) Yolk sac expression of *SM22α-Cre*^{Tg} can be detected as early as E8.5. (C) At E10.5, yolk sac vasculature is undergoing vascular remodeling and cre expression can be detected along the remodeled vasculature and mesothelium. (D) β-galactosidase expression in *PDGFR*^{SKO} is restricted to mesothelial cells. (E) *myocardin*^{Cre} expression is not detected in the yolk sac at E8.5 by whole mount or section analysis. (F-G) β-galactosidase expression in VSMC begins at E9.5 and is maintained at E10.5. (H) Loss of β-galactosidase positive cells in *PDGFR*^{MKO}. Black arrows indicate mesothelium. Black arrowheads point to myocardin-Cre expressing cells. Asterisks indicate blood vessels. extraembryonic endoderm (ee) and mesothelium (mes). Scale bar= 20μm.

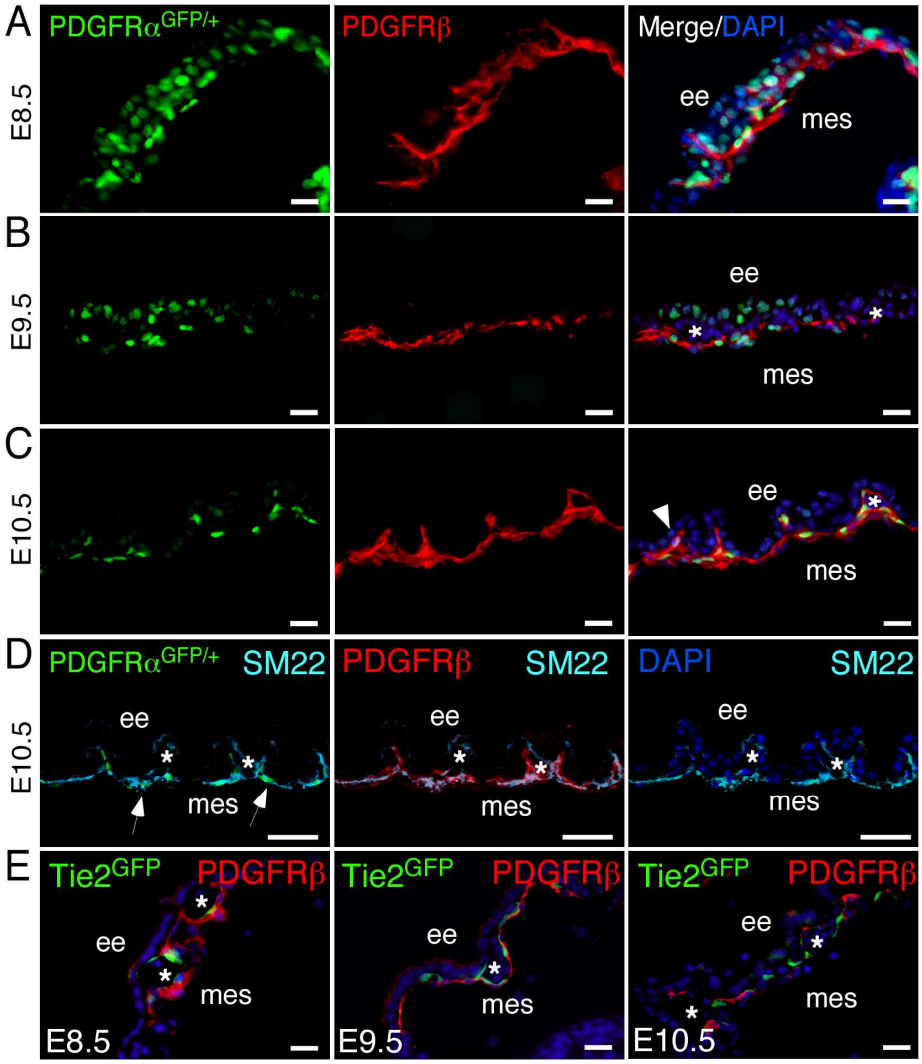

Figure 2-2. PDGFRα and PDGFRβ positive cells in yolk sac mesothelium. (A-C) Section immunohistochemistry for the PDGFRβ was performed on *PDGFRα*$^{GFP/+}$ yolk sacs. Both receptors were expressed abundantly at E8.5, but their expression pattern became more resticted to mesothelial and perivascular cells at the later stages. (D) PDGFRα and PDGFRβ coexpression with mesothelial marker, SM22. DAPI stained and SM22 negative cells represent the endoderm. (E) Immunohistochemistry for PDGFRβ and GFP on *Tie2GFP*^{Tg} frozen sections at E8.5 to E10.5 demonstrates PDGFRβ expression in close proximity to but not overlapping with Tie2GFP expression. White arrowhead indicates perivascular cells expressing only PDGFRβ. White arrows indicate PDGFRα^{GFP} and SM22 coexpressing cells. Asterisks indicate blood vessels. extraembryonic endoderm (ee) and mesothelium (mes). Scale bar= 20μm.

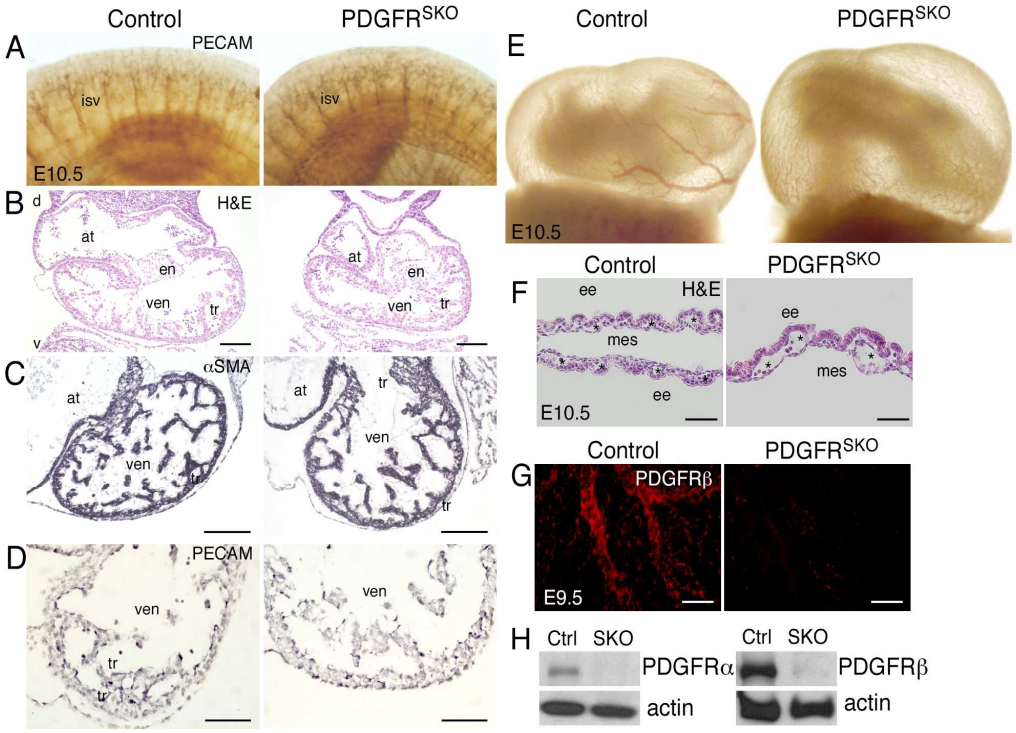

Figure 2-3. *PDGFR^{SKO}* mutants demonstrate normal cardiac and embryonic vascular development but disrupted yolk sac vasculature. (A) Whole mount PECAM staining of intersomitic vessels (isv) in E10.5 control and *PDGFR^{SKO}* embryos. (B) H&E, (C) αSMA, and (D) PECAM staining of control and *PDGFR^{SKO}* hearts. (E) E10.5 whole mount images of yolk sac blood vessels on side opposing the vitelline vessel. Embryos were imaged while attached to placenta to prevent red blood cell loss. (F) H&E stained section of yolk sac demonstrated yolk sac vascular disruptions in *PDGFR^{SKO}*. (G) Immunohistochemistry on whole mount yolk sacs demonstrated loss of PDGFRβ in *PDGFR^{SKO}* by E9.5 compared to control. (H) Deletion of both PDGFRα and PDGFRβ in *PDGFR^{SKO}* compared to control at E10.5 by western blot analysis. Asterisks indicate blood vessels. Dorsal (d), ventral (v), atria (at), ventricle (ven), endocardial cushions (en), trabeculations (tr), extraembryonic endoderm (ee), and mesothelium (mes). Scale bars = 10μm for (B) and 20μm (C-D and F-G).

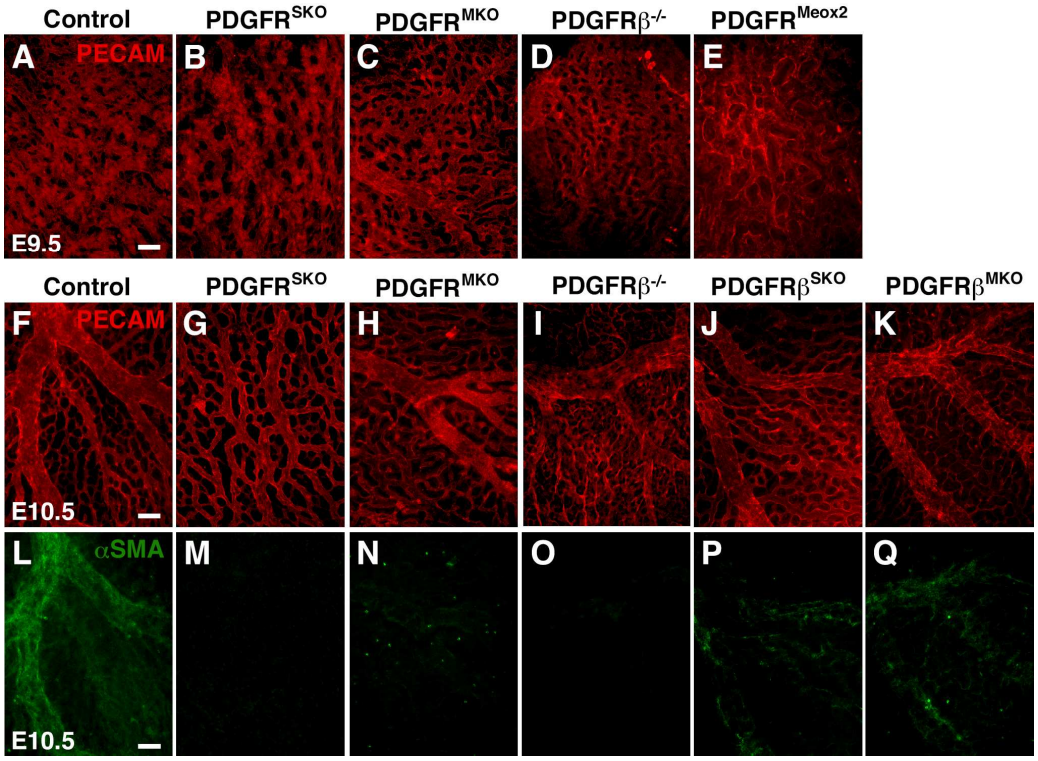

Figure 2-4. Vascular development is disrupted in *PDGFR^{SKO}* yolk sacs but not in single mutants. (A-E) Whole mount E9.5 yolk sac staining for PECAM on indicated genotypes. A normal vascular plexus was observed in control, *PDGFR^{SKO}*, *PDGFR^{MKO}*, and *PDGFRβ$^{-/-}$* yolk sacs but was disrupted in *PDGFR^{Meox2}* yolk sacs. (F-K) Yolk sac vascular remodeling progression to large defined vessels visualized by PECAM staining. *PDGFR^{SKO}* yolk sacs fail to undergo vascular remodeling, resembling the E9.5 yolk sac vascular plexus. (L-Q) αSMA staining was used to detect VSMC at E10.5 on indicated genotypes. Recruitment of VSMC to developing vasculature present in control E10.5 yolk sacs is severely reduced in *PDGFRβ^{SKO}*, *PDGFRβ^{MKO}*, and *PDGFR^{MKO}* and absent in *PDGFR^{SKO}* and *PDGFRβ$^{-/-}$*. Images represent similar regions of the yolk sac adjacent to but not including the vitelline vessels. These images are representative of a minimum of 3 yolk sacs of each genotype. Scale bar = 10μm.

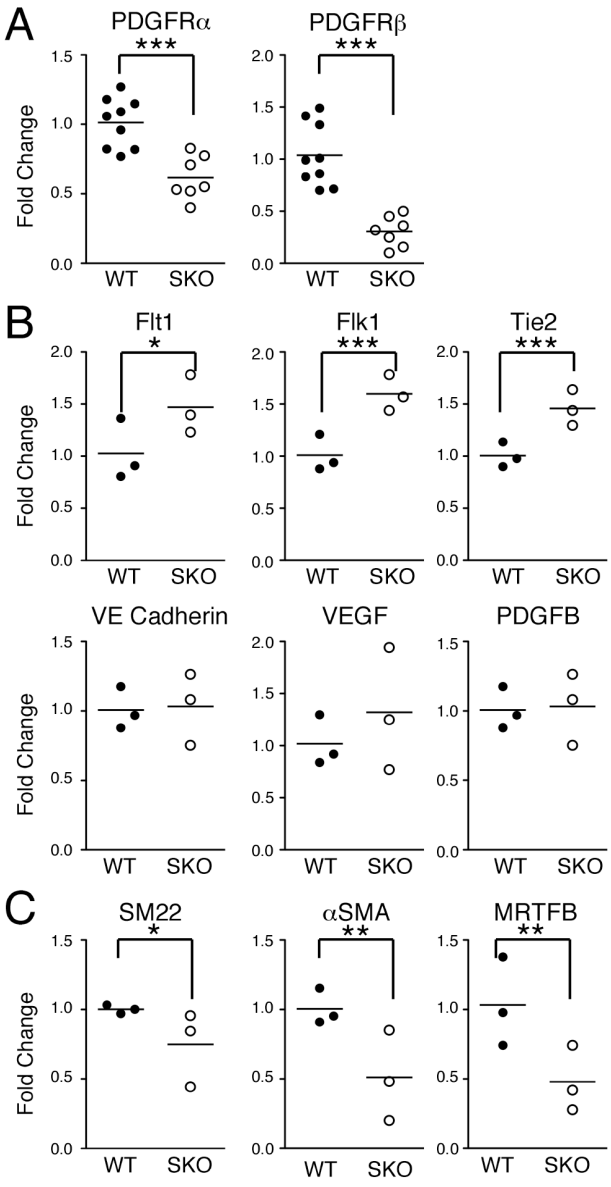

Figure 2-5. Gene expression analysis in E10.5 yolk sacs. (A) *PDGFR*^{SKO} mutants demonstrate reduced expression of *PDGFRα* and *PDGFRβ*. (B) Endothelial cell gene and growth factor expression. (C) Mesothelial and VSMC specific genes *SM22α*, *αSMA*, and *MRTFB* suggest a slight decrease in expression in PDGFR^{SKO} yolk sacs. Each symbol represents realtime PCR analysis of one sample analyzed in triplicate. A minimum of three samples were analyzed for each gene and mean bars are represented for each set of samples analyzed. Student-t test: *< 0.2, **< 0.07, ***< 0.02.

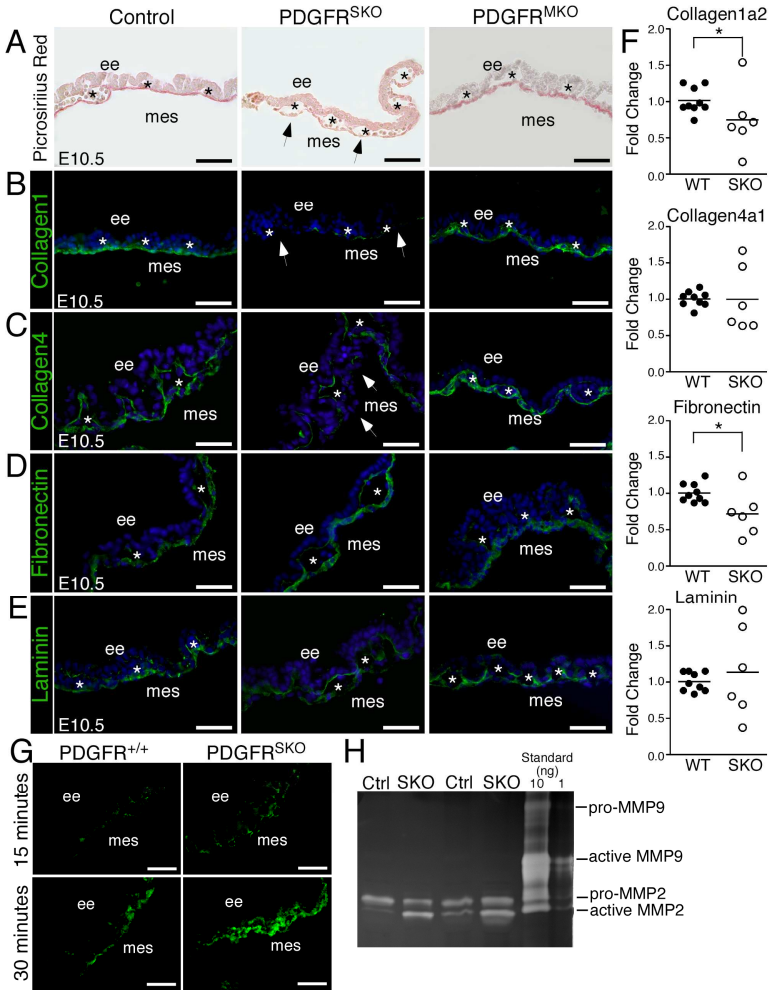

Figure 2-6. Extracellular matrix deposition disruption along the mesothelium. (A) Picrosirius red staining of paraffin sections of E10.5 yolk sacs demonstrating *PDGFR*^{SKO} yolk sac reduction in collagen compared to control and *PDGFR*^{MKO} yolk sacs. (B-E) Immunohistochemistry on E10.5 control, *PDGFR*^{SKO}, and *PDGFR*^{MKO} yolk sac sections for detection of extracellular matrix molecule expression as indicated. (F) Quantitative PCR gene expression analysis for matrix molecules in control and *PDGFR*^{SKO} E10.5 yolk sacs. Individual symbols and mean bars represent each sample analyzed in triplicate for wild type and SKO mutants. Student-t test: *< 0.15. (G) E10.5 fresh frozen yolk sac sections of control and *PDGFR*^{SKO} mutants imaged for MMP activity observed through increasing levels of fluorescence detected by in situ DQ gelatin assay. (H) Gelatin zymography demonstrating increased MMP2 activity in *PDGFR*^{SKO} E10.5 whole yolk sac lysates compared to control lysates. Arrows indicate mesothelial loss of collagen 1 and collagen 4. Asterisks indicate blood vessels. extraembryonic endoderm (ee) and mesothelium (mes). Scale bar = 40μm.

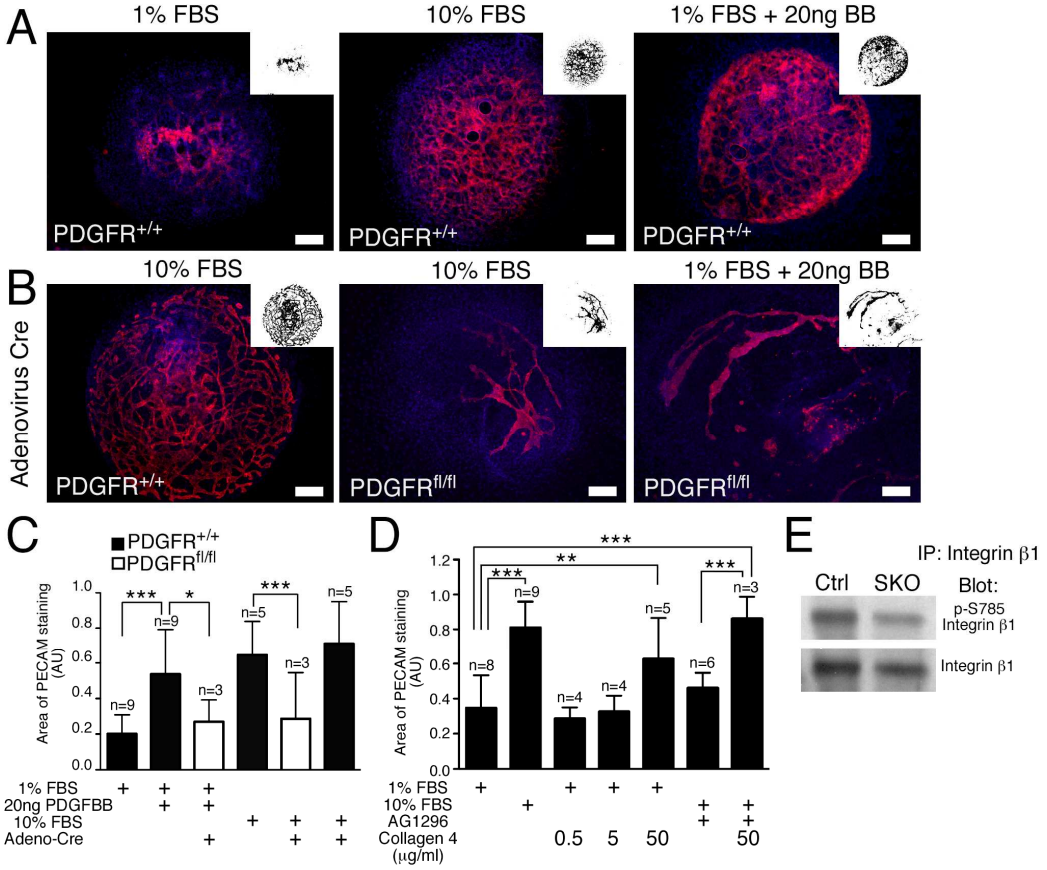

Figure 2-7. PDGF receptor signaling in allantois cultures. (A) PECAM staining on E8.5 wild type allantoides grown in culture for 24-26 hours with the varying stimulation; 1% FBS, 20ng PDGFBB, or 10% FBS. (B) PECAM staining of adenovirus Cre treated E8.5 wild type or PDGF receptor conditional (*PDGFR*$^{fl/fl}$) allantoides demonstrating deletion of PDGF receptor disrupts vasculogenesis in response to PDGFBB and 10% FBS. Insets represent threshold images of PECAM fluorescence that were used to quantify the vascular area. (C) Quantification of vasculogenesis in the allantois assays by measurement of PECAM staining in stimulated and unstimulated samples in the presence or absence of PDGF receptor expression. (D) Quantification of PECAM staining in the presence of a PDGF receptor inhibitor (AG1296) and increasing concentrations of Collagen 4 compared to 10% FBS. (E) E10.5 yolk sac lysates immunoprecipitated for integrin β1 and analyzed for activation by western blot analysis for phosphorylation of integrin β1 at S785 and integrin β1 demonstrating decreased phosphorylation yet similar levels of integrin β1. Student t-test: * <0.07, ** < 0.04, ***<0.005. Scale bar = 20μm. PECAM = red; DAPI = blue.

CHAPTER THREE
ADDITIVE EFFECTS OF PDGF RECEPTORβ SIGNALING PATHWAYS IN VASCULAR SMOOTH MUSCLE CELL DEVELOPMENT

Michelle D. Tallquist[1,2], Wendy J. French[2], and Philippe Soriano[1*]
[1]Program in Developmental Biology and Division of Basic Sciences, Fred Hutchinson Cancer Research Center, 1100 Fairview Ave North, Seattle, WA 98109, [2]Department of Molecular Biology, University of Texas Southwestern Medical Center, 5323 Harry Hines Blvd, Dallas TX 75390-9148

ABSTRACT

The platelet derived growth factor β receptor (PDGFRβ) is known to activate many molecules involved in signal transduction and has been a paradigm for receptor tyrosine kinase signaling for many years. We have sought to determine the role of individual signaling components downstream of this receptor *in vivo* by analyzing an allelic series of tyrosine-phenylalanine mutations that prevent binding of specific signal transduction components. Here we show that the incidence of vascular smooth muscle cells/pericytes (v/p), a PDGFRβ-dependent cell type, can be correlated to the amount of receptor expressed and the number of activated signal transduction pathways. A decrease in either receptor expression levels or disruption of multiple downstream signaling pathways leads to a significant reduction in v/p. Conversely, loss of RasGAP binding leads to an increase in this same cell population, implicating a potential role for this effector in attenuating the PDGFRβ signal. The combined in vivo and biochemical data suggests that the summation of pathways associated with the PDGFRβ signal transduction determines the expansion of developing v/p cells.

INTRODUCTION

Although signal transduction by receptor tyrosine kinases (RTKs) has been

studied extensively, the roles of individual signaling proteins downstream of these receptors are a matter of debate. Some studies have shown that disruption of particular pathways leads to loss of specific cellular functions (Valius and Kazlauskas 1993). Others have suggested that it is the sum of the signals that results in the unique cellular outcomes directed by each receptor (Fambrough et al. 1999). Yet, others have demonstrated that the interpretation of receptor signals is determined by the distinct cellular history (Flores et al. 2000; Halfon et al. 2000; Xu et al. 2000). Because many of these conclusions have been reached in diverse cell types and through the analysis of different RTKs, it is difficult to determine if results from one receptor system can be used to generalize the functions of RTK signaling.

Recently, several labs have dissected the roles of RTK modular signaling components by generating point mutations in cytoplasmic domains of the receptors in mice (Partanen et al. 1998; Heuchel et al. 1999; Blume-Jensen et al. 2000; Kissel et al. 2000; Tallquist et al. 2000; Klinghoffer et al. 2001; Maina et al. 2001; Klinghoffer et al. 2002). These studies have revealed a unique requirement for individual signaling components in specific cell types (Partanen et al. 1998; Blume-Jensen et al. 2000; Kissel et al. 2000; Maina et al. 2001). In contrast, similar experiments on platelet-derived growth factor receptor α (PDGFRα) signaling mutants have demonstrated that phosphatidylinositol 3' kinase (PI3K) and Src family kinase (SFK) signal transduction pathways play roles in oligodendrocyte development (Klinghoffer et al. 2002). These experiments suggest that requirements for signal transduction vary not only by the receptor under consideration but also by the cell lineage that is receiving the signal.

The platelet derived growth factor receptor β, PDGFRβ, has not only been

studied physiologically but also has been the focus of intensive biochemical analysis. Upon ligand binding, the PDGFRβ dimerizes and is autophosphorylated on as many as thirteen cytoplasmic tyrosine residues. These phosphorylated tyrosines become binding sites for SH2-domain containing proteins that initiate a number of signal transduction pathways (reviewed by (Claesson-Welsh 1994; Heldin et al. 1998)). The pathways downstream of the PDGFRβ control multiple cellular functions including proliferation, migration, matrix deposition, and immediate early gene induction (reviewed by (Heldin and Westermark 1999; Betsholtz et al. 2001)). At least ten distinct SH2 domain-containing proteins can bind the phosphorylated PDGFRβ and activate downstream signal transduction cascades. These molecules include Src family kinases (SFK; (Kypta et al. 1990)), phosphatidylinositol 3' kinase (PI3K; (Kazlauskas and Cooper 1990; Kundra et al. 1994; Wennstrom et al. 1994a; Wennstrom et al. 1994b)), Shc (Yokote et al. 1994), RasGAP (Kaplan et al. 1990; Kazlauskas et al. 1990), signal transducers and activators of transcription (STATs; (Vignais et al. 1996)), Grb2 (Arvidsson et al. 1994), Grb7 (Yokote et al. 1996), SHP-2 (Kazlauskas et al. 1993; Lechleider et al. 1993), phospholipase Cγ (PLCγ; (Meisenhelder et al. 1989; Morrison et al. 1990)) and Nck (Nishimura et al. 1993). While multiple downstream effects have been attributed to activation of these pathways, their relative importance downstream of the PDGFRβ has not been determined *in vivo*.

We have concentrated our present analyses on the signal transduction by the PDGFRβ. Previous studies using a null allele of the receptor have demonstrated that PDGFRβ signal transduction is required for a subset of vascular smooth muscle cells and

pericytes (v/p) (Leveen et al. 1994; Soriano 1994). These cells are the mesenchymal support cells that surround blood vessels (reviewed by (Hungerford and Little 1999)). Brain pericytes, kidney mesangial cells, retinal mural cells, and limb and skin pericytes have all been recognized as PDGFRβ-dependent cells (Lindahl et al. 1997; Lindahl et al. 1998; Hellstrom et al. 1999; Enge et al. 2002). Studies have indicated that the PDGFRβ is likely to play a key role in the proliferation and/or migration of a progenitor population (Hellstrom et al. 1999). These results explain why defective PDGF signal transduction results in a reduction of the v/p cell lineage and ultimately perinatal lethality due to vessel instability (Hellstrom et al. 2001).

To examine the roles of PI3K and PLCγ downstream of the PDGFRβ, we have previously disrupted their binding sites in the receptor's cytoplasmic domain (Heuchel et al. 1999; Tallquist et al. 2000). Surprisingly, no overt phenotypes were detected in homozygous mutants lacking these two pathways, and deficiencies were observed only when the animals were challenged physiologically. To assess the roles of the remaining signal transduction pathways, we have created a PDGFRβ allelic series in mice (Figure 1). We refer to this series as the F series because it contains Y-F mutations at the known phosphorylated tyrosine residues. Using v/p cell number as a readout for PDGFRβ signal transduction, we have determined that the level of receptor expressed as well as the sum of signaling pathways induced by the PDGFRβ determines the number of v/p cells that form. These results provide an example of RTK signal transduction quantitatively controlling cellular development.

MATERIALS AND METHODS

Mice

Point mutations which disrupt the designated signal transduction pathways were generated by changing the tyrosine residue to phenylalanine. The exception was Y1020 that was mutated to encode an isoleucine, thus generating a unique restriction site that facilitated identification of homologous recombinants. Mouse mutants F2 and F3 have been previously described (Heuchel et al. 1999; Tallquist et al. 2000). The targeting vector for the F1, F5, and β^{T}mutations utilized the same arms of homology as the F3 vector. The exons containing the point mutations were introduced in the arms of homology of the targeting vector by site directed mutagenesis and verified by sequence data of PCR amplified genomic DNA from homozygous mutant mice. The F7 mutation was generated by creating a targeting vector that incorporated the 5' arm of the F5 targeting vector with 5' genomic sequences that included the exons containing the Src and Grb2 binding sites. Tyrosines 578 and 715 were mutated to phenylalanine to disrupt Src and Grb2 binding, respectively. This targeting vector was transfected into F5 heterozygous ES cells and screened for homologous recombination. The truncation mutation possesses a frame shift at amino acid 780 resulting in a premature stop codon after amino acid 801, eleven amino acids downstream of the RasGAP binding site. ES cell colonies were screened initially by PCR and positive clones were further verified by Southern blot analysis for the correct recombination at the 5' and 3' arms. The PGK neo cassettes were removed by crossing mice to Meox2^{Cre} (Tallquist and Soriano 2000) and ROSA26^{FLPeR} (Farley et al. 2000) deleters.

The majority of analyses have been carried out on a mixed 129S4 x C57Bl/6

background except where indicated. The *XlacZ4* transgenic mouse (Tidhar et al. 2001) was kindly provided by Moshe Shani and crossed into the F series. We also crossed the F5 and wild type mice to the PDGFRα^{GFP} line (Hamilton et al. 2003).

Histology, immunohistochemistry, and pericyte quantitation

Embryos and tissues were processed and embedded for sectioning according to standard protocol. We have not examined the vasculature of all PDGFRβ-dependent tissues in the F series mutant animals. Those tissues not examined are lung, brown adipose tissue, and the adrenal gland.

Immunohistochemistry

Kidneys were removed and fixed for 20 minutes in 4% paraformaldehyde. 200 μm sections were then obtained by vibratome sectioning and immunofluorescence was performed. For eye immunohistochemistry the pigmented epithelium was removed from the mouse retinas and fixed for 10 minutes in 4% paraformaldehyde. Retinas and kidney slices were then blocked and subjected to immunohistochemistry for the indicated v/p marker. Antibodies: β-galactosidase (55976 Cappel), αSMA (1A4 Sigma), and desmin (D33 Dako). Photographs were obtained on a Zeiss Axiophot.

Pericyte quantitation

E14.5 embryos were divided into quarters at the following levels: head-neck, neck-liver, liver-kidney, and kidney-tail. Quarters were rinsed with PBS and fixed for 20 minutes in 2% formaldehyde; 0.2% glutaraldehyde. They were then washed 3X in PBS,

stained overnight with X-gal, transferred to PBS, photographed, post-fixed in 10% formalin, and then processed and embedded. 7μm sections were generated and X-gal positive nuclei quantitated in the neural tube at the level of the heart and the kidney. 7-10 samples were counted for each level and the mean of this data is represented in Figure 6. Pericytes surrounding the exterior of the neural tube were excluded from the sample. Positive nuclei were counted at 20X magnification and photographed at 10X magnification on Zeiss Axiophot microscopes. Retinas were prepared in a similar manner. The pigmented epithelium was removed prior to the initial fixation step, and the lens was not removed until after the final fixation to maintain retina shape. Images were obtained on a Nikon SMZ1000 with a Coolpix 900 camera.

Immunoprecipitation and western blotting.

Mouse embryonic fibroblasts were generated from E9 or E14.5 day embryos. Embryos were isolated, decapitated, and eviscerated. The remaining tissue was then treated with trypsin and plated. Cells were frozen down at passages 2 and 3. Most experiments were completed on cells at passage 3-6, except for the wild type line that was spontaneously immortalized. Cells were plated at 1-3 X 10^5 cells/well and starved for 48 hours. Receptor down-regulation was achieved by treating starved cells for 2 hours with 100 ng/ml PDGFAA (R&D). Cells were then stimulated with PDGFBB (R&D) for 5 minutes and lysed.

Immunoprecipitation and western blotting were executed as previously described (Tallquist et al. 2000). Antibodies were obtained from the following sources: PDGFRβ (06-498 Upstate Biotechnology); PDGFRα (sc-338 Santa Cruz Biotechnology); Akt

(9272 Cell Signaling Technology); PhosphoAKT (9271 Cell Signaling Technology); RasGAP (05-178 Upstate Biotechnology); Grb2 (610111 BD Transduction Laboratories); Erk1/2 (06-182 Upstate Biotechnology); c-Src (SRC2; sc-18 Santa Cruz); Phospho-Src Y418 (44-660 Biosource); Phospho Erk1/2 (9101 Cell Signaling Technology); PLCγ (05-163 Upstate Biotechnology); SH-PTP2 (sc-280 Santa Cruz Biotechnology); and phosphotyrosine [4G10] (05-321 Upstate Biotechnology). PDGFRβ 97A (kinase insert domain) and 89P (tail) were kind gifts from Andrius Kazlauskas.

RESULTS

Generation of the allelic series

Previous studies of the PDGFRβ have revealed an essential role for this receptor in v/p development, but attempts to identify key biochemical signals thus far have demonstrated that loss of certain signaling pathways only diminishes PDGFRβ driven responses (Heuchel et al. 1999; Tallquist et al. 2000). To identify key signaling pathways we have generated an allelic series of PDGFRβ mutants. Figure 3-1 illustrates the mutations that we have generated in the PDGFRβ locus and the signaling pathways that are disrupted by these mutations. Each mutant will be referred to by the number of tyrosines (Y) that have been mutated. For example, the mutation in the RasGAP binding site is the PDGFR$\beta^{F1/F1}$ or F1/F1 mutant. The truncation mutation of the PDGFRβ (β^{T}) was created by the introduction of a frameshift and subsequent premature stop codon downstream of the RasGAP binding site. Figure 3-2 illustrates the targeting events that were used to generate the series of mutants. The F1, F2, F3, F5, and β^{T}-targeted

mutations were generated by engineering Y-F, Y-I, or frame shift mutations in the same targeting vector (Figure 3-2A). The F7 mutation was generated by targeting the F5 heterozygous ES cells (Figure 3-2B; see Materials and Methods). Cells that contained all mutations on the same allele as determined by Southern blotting were used to generate the F7 line. All mutant mice were viable and fertile as homozygotes except the truncation allele, β^T, which lacks the second kinase domain and the SHP-2 and PLCγ binding sites. Embryos homozygous for the β^T allele die perinatally with a phenotype identical to that of the PDGFRβ null embryos. E18 embryos exhibit edema and hemorrhaging in multiple tissues including the kidney, brain, and skin (data not shown). These results suggest that PDGFRβ kinase activity is required for v/p development and that the receptor cannot function in the absence of kinase activity, unlike another RTK, the VEGFR-1 (Hiratsuka et al. 1998).

Identification of v/p cells

We examined the blood vessels of F series homozygous mice by histology and detected no gross abnormalities (data not shown). To obtain a more global perspective of v/p cell populations, we introduced the *XlacZ4* transgenic marker into our F series mutant mice. The *XlacZ4* transgenic mouse expresses nuclear β-galactosidase in certain populations of differentiated, non-proliferating v/p cells in the embryo and the adult (Tidhar et al. 2001). As described below, using this marker in adult animals we identified vascular defects in the F5 and F7 mice in the tissues of the eyes, hearts, and brains (Figure 3-7, 3-8, 3-9, and data not shown). This observation suggests that both the F5 and

F7 alleles function sub-optimally in tissues known to require PDGFRβ signal transduction (Lindahl et al. 1998; Hellstrom et al. 1999; Enge et al. 2002). Although both of these mutations cause notable phenotypes in some v/p populations, we have not observed pathologies in all populations of v/p cells that require PDGFRβ signal transduction. V/p cell populations with no pathological phenotype in the F5 and F7 mice include the kidney mesangial cells and pericytes in the skin and skeletal muscle (data not shown). The lack of an overt phenotype in these tissues suggests that the reduction in v/p cells is less severe than in the case of the PDGFRβ null mice or that these tissues can function adequately even with reduced v/p cell numbers. Because some populations of v/p cells appear to be more dependent on PDGFRβ signal transduction than others, we reasoned that the PDGFRα might be co-expressed in the less affected v/p populations. Although PDGFRα has been reported in a variety of mesenchymal cell lineages (Schatteman et al. 1992; Lindahl et al. 1997; Takakura et al. 1997; Zhang et al. 1998; Karlsson et al. 2000), we wanted to determine if any v/p populations express the PDGFRα, or if it may be upregulated in any of the F series mice. We crossed the PDGFRα^{GFP} line of mouse that expresses a nuclear-localized GFP under the control of the PDGFRα promoter (Hamilton et al. 2003) with the F5 mutant mice and compared the GFP expression pattern to the pattern of v/p cells in the kidney, eye, and brain (Figure 3-3 and data not shown). We have used three independent markers to designate v/p cells: αSMA, desmin, and *XlacZ4* transgene. Although PDGFRα-expressing cells are found in the same tissues as v/p cell markers, there is no overlapping expression of GFP with any of the v/p cell markers in the arteries or veins in the vessels of the eye and brain.

PDGFRα-expressing cells are also absent from the larger vessels of the kidney. A population of GFP^+ cells is detected within the kidney glomerulus, but the positive nuclei do not definitively overlap with the αSMA positive cytoplasm (Figure 3-3A). These may be the vascular adventitial fibroblasts that are known to express the PDGFRα (Seifert et al. 1998). These data indicate that PDGFRα is not expressed or up-regulated in two of the most affected tissues of the mutant mice, the eye and the brain, and is not likely to be functioning as a surrogate co-receptor with the PDGFRβ.

Vascular smooth muscle cell/pericyte development

To determine if the reduction in v/p was caused by a gradual loss or a developmental defect, we examined pericyte populations in wild type and mutant embryos. The *XlacZ4* mouse marker can be used to identify specific v/p cell populations as early as E12.5. We chose to observe pericytes at E14.5 because at this time point v/p are abundant in wild type animals in several tissues, including the developing spinal cord and intercostal vasculature. Figure 4 demonstrates whole mount visualization of the v/p cell populations in E14.5 wild type and the most severe F series mutant embryo (F7/-). After examining several litters of F series mutant embryos bearing the *XlacZ4* marker, it was clear that the entire panel of F series homozygous mutant embryos could be distinguished from wild type embryos simply by the degree that blood vessels had acquired v/p (data not shown).

To obtain a quantitative view of these results, we chose to focus on the spinal cord pericyte population. These cells begin to form at E10.5 in a rostral to caudal fashion

in the embryo and require PDGFRβ signals for development (Leveen et al. 1994). Cross sections through the developing spinal cord (neural tube) provide a relatively uniform area for quantitation. We can consistently identify a particular maturation stage of the developing vasculature based on its axial level within the embryo, and the pericytes can often be found as isolated cells (Figure 3-5). Using the entire panel of PDGFRβ mutant mice, we compared pericyte numbers between the different F series mutants (Figure 3-5 and 6). In all mutants examined with the exception of the F1 mutation, we observed a decreased incidence of pericytes when compared to the wild type embryos. The reduction in pericyte numbers ranged from 42-77%. This reduction was present at the more mature axial level of the heart as well as at the axial level of the kidney.

The F7/F7 mutant embryos are the only embryos that exhibited a difference between the number of pericytes at the heart level versus the number at the level of the kidney. All other mutants demonstrated similar numbers at both levels, indicating that pericyte development is disrupted and does not reach homeostasis as the tissue matures. Because the F7 is the most severely affected allele, it is possible that the difference between the heart and kidney levels is due to a developmental delay in v/p formation. Pericyte development may still be proceeding at the level of the kidney in these embryos. At the more mature level of the heart the F7/F7 pericyte populations have reached a steady state level and resemble v/p numbers more similar to those observed in the F5/F5 embryos.

Previously, chimeric analysis had demonstrated that PDGFRβ heterozygous cells do not contribute extensively to the smooth muscle cell compartment, suggesting that heterozygous cells may have reduced v/p developmental potential (Crosby et al. 1998).

To find out if receptor levels had any impact on v/p cells in our system, we crossed animals bearing the PDGFRβ null allele to our mutant series (Figure 3-5B and 3-6B). We observed an even further reduction in pericyte levels, resulting in a 70-92% decrease in pericytes when compared to wild type embryos. Interestingly, even the PDGFRβ$^{+/-}$embryos demonstrate a nearly 40% decrease in pericytes. This result suggests that the quantity of receptor impacts the number of pericytes that form. Another observation from this data is that even the F7/- embryos can induce cell development at levels greater than the null. In fact, the F7/- animals survive whereas the PDGFRβ nulls do not. This is a rather surprising result given that most of the downstream signal transduction molecules that directly interact with the receptor have been dissociated.

While most of the F series alleles demonstrate a decrease in v/p cells, the F1 allele results in an apparent increase in spinal cord pericytes. Although the increase is most pronounced when we compare the F1 hemizygote to the PDGFRβ heterozygote (Figure 3-6), an increase is also observed when comparing F1/F1 embryos and wild type embryos. In fact the level of pericytes in the F1/- embryos is very similar to those in the wild type. These data demonstrate two interesting findings. One is that RasGAP may play a role in PDGFRβ signal attenuation, and loss of this pathway results in increased PDGFRβ signals. The second is that v/p numbers may not be tightly controlled and PDGFRβ signaling can result in more cells.

To determine if the signaling pathways affected other v/p populations in the same manner, we have examined the v/p population in the retina. It has been shown previously that PDGFB and PDGFRβ signaling controls pericyte development in the eye (Benjamin

et al. 1998; Klinghoffer et al. 2001; Enge et al. 2002). Adult mice transheterozygous for one null allele and one F5 or F7 allele exhibited severe eye defects. These defects were first observed as an opacity and sometimes visible hemorrhage in the eye (Figure 3-7A) as previously described for PDGFRβ and PDGFB signaling mutants (Klinghoffer et al. 2001; Enge et al. 2002). The F5 and F7 hemizygous mutant mice possessed fewer, discontinuous blood vessels and overgrowth of retinal cells. This phenotype occurred with 100% penetrance but with variable severity (Figure 3-7C) and was detectable sometimes as early as four days after birth. The presence of a pathological condition suggests that the F5 and F7 alleles have compromised receptor function when compared to the wild type, F1, F2, and F3 alleles and demonstrate that retinal pericytes are also dependent on the PDGFRβ signaling pathways that we have disrupted.

To examine the retinal pericytes in the entire F series we again used mice bearing the *XlacZ4*transgene. At four weeks of age the retinal vasculature is mature and can be isolated from the lens and pigmented epithelium for visualization. Figure 3-8 illustrates that homozygotes for the F1, F2, and F3 mutant alleles are indistinguishable from wild type eyes, however F5/F5 and F7/F7 eyes exhibit reduced numbers of pericytes. Even without the ability to quantitate these differences, it is clear that the PDGFRβ$^{+/-}$, F5/F5, F7/F7, F5/-, and F7/- mutant retinas have a reduction in v/p when compared to wild type eyes, reinforcing the requirement for multiple PDGFRβ signal transduction pathways in v/p development.

A final tissue where we have examined v/p formation is the heart. F2 and F3 homozygotes and transheterozygotes were indistinguishable from wild type and heterozygous hearts, respectively. Consistent with our observations in the eye and the

nervous system, the F5 and F7 mutant alleles display abnormalities in the vascular coating of their coronary arteries and veins (Figure 3-9 and data not shown). F5/- and F7/- mice often exhibited a variety of heart abnormalities including enlarged ventricles, increased heart:body mass ratio, dilated atria, and fibrosis (data not shown). In contrast, the F1/+ mice appeared to have more extensive vasculature with extended vessels and additional branching (Figure 3-9). In agreement with the data from the nervous system and the eye, the F5 and F7 mutant alleles have a significant reduction in v/p cells.

Taken together these results demonstrate several important findings for PDGFRβ signal transduction. First, the number of pericytes formed directly correlates with the number of signaling pathways transducing PDGFRβ activity. Second, a reduction in pericytes is observed even when only the amount of receptor is affected. Finally, although SH2-domain-containing proteins impact v/p numbers, the intrinsic kinase activity of the receptor may play a role in transmitting the PDGFRβ signal because the truncation mutation does not exhibit any rescue of v/p development while the F7 mutant allele that transmits primarily through kinase activity (due to loss of the SH2-domain containing protein binding sites) still supports v/p development sufficient for viability.

Downstream signal transduction

Because F2, F3 and F5 mutant receptors have been previously studied biochemically (Valius and Kazlauskas 1993; Heuchel et al. 1999; Tallquist et al. 2000), we have focused our biochemical analysis on the F1 and F7 mutant receptors' signal transduction to verify the effects of these particular mutations on downstream signal transduction cascades. We have used mouse embryo fibroblasts (MEFs) for these

analyses. All lines of MEFs that we generated expressed both PDGFRα and PDGFRβ, albeit at different levels (data not shown). To avoid stimulation of the PDGFRα by PDGFBB, we down-regulated PDGFRα surface expression by pre-treatment with PDGFAA two hours before PDGFBB stimulation. In all cell lines examined we observed an increase in tyrosine phosphorylation in response to ligand (Figure 3-10A). The most evident phosphorylated bands are around 200 kD which are likely to be the PDGFRα and PDGFRβ. Although we have mutated seven of the thirteen tyrosines a significant amount of phosphorylation is observed in all cell lines, albeit at lower levels in the F7/- cell line (Figure 3-10A and 3-10B). In the whole cell lysate phosphotyrosine blot the phosphorylated protein detected at 200 kD is likely cytoplasmic PDGFRα, as it is reduced in F7 cells after down-regulation of the PDGFRα.

Because we have disrupted only one of the potential Src binding sites, we examined the level of Src activation downstream of our F7 cell line (Figure 3-10B). Upon PDGFBB addition there was an increase in the amount of Src phosphorylated on tyrosine 418 (a site whose phosphorylation is required for full catalytic activity; Johnson et al. 1996). In contrast, in the F7/F7 MEFs we did not observe any increase in Src activation. These results are in agreement with other reports that demonstrate that a mutation at amino acid 578 of the PDGFRβ is sufficient for reducing the level of Src binding and activation (Mori et al. 1993; Twamley et al. 1993; Vaillancourt et al. 1995; Fanger et al. 1997).

Two potential downstream targets of PDGFRβ activation are activation of ERK1/2 and AKT (Franke et al. 1995). As expected, phosphorylation of ERK1/2 and

AKT are reduced or absent in the F7 homozygous and hemizygous mutant cell lines, but cells expressing at least one copy of the wild type receptor are capable of inducing the activation of these downstream molecules (Figure 3-10C). These data demonstrate that loss of seven tyrosine residues on the PDGFRβ results in a severe loss of downstream signal transduction. In contrast, cells bearing even just one copy of the F1 receptor show increased phosphorylation of ERK 1/2. These data are in concordance with the *in vivo* data, where lack of the RasGAP binding site on the receptor results in an increase in the downstream signaling events and a subsequent increase in v/p. Therefore, the F1 mutant receptor has increased activity while the F7 receptors have decreased activation of these same pathways, despite having apparently normal levels of kinase activity.

DISCUSSION

Receptor tyrosine kinase signal transduction plays an important role in directing many cellular activities. We have used an *in vivo* system to analyze how cellular development relates to the signaling pathways downstream of the PDGFRβ. Examination of the v/p population demonstrates a quantitative relationship between the extent that signals are being transduced and the number of v/p that form. Several other studies have demonstrated that strength of signal may dictate cellular outcomes. Examples of these are T cell development in the immune system, gradients of morphogens in developmental systems, and MAP kinase activation in oocyte maturation (Heemskerk and DiNardo 1994; Nellen et al. 1996; Zecca et al. 1996; Ferrell and Machleder 1998; Gong et al. 2001).

In our system, the intensity of signal can be affected in two ways. The first is by the amount of receptor expressed at the cell surface. V/p numbers are significantly lower in PDGFRβ$^{+/-}$ embryos when compared to wild type controls. In this situation there is a decrease in overall signal but no specific, directly associated pathway is disrupted. This demonstrates a quantitative role for receptor activity. The second influence on PDGFRβ signal transmission is by the number of associated SH2-domain-containing proteins. Loss of even a single pathway results in reduction of v/p, and as the number of disrupted pathways increases, there is a concomitant decrease in v/p. There is no significant difference between the F2 and the F3 mutant alleles, but there is a noticeable difference when the number of mutations is further increased. These signaling differences as illustrated by v/p number and the presence of vascular pathologies can be categorized in the mutant alleles by the following hierarchy: F1>w.t.>F2=F3>F5>F7>null. In addition, hemizygotes show an even further reduction in v/p when compared to the F series homozygotes. This suggests that specific effector pathways may play more of a role in fine tuning PDGFRβ signals.

In total, our results demonstrate that PDGFRβ signal transduction is regulated not only by direct binding of signal transduction molecules but also by receptor expression levels possibly reflecting inherent kinase activity. In addition, no particular signaling pathway that we have analyzed is absolutely required for transmission of PDGFRβ signals, because even the F7 allele has a phenotype less severe than the null. In support of the observation that receptor levels and kinase activity may have a direct role in signal transduction, we have observed that a chimeric PDGFR that has the extracellular domain

of the PDGFRβ but the intracellular domain of the PDGFRα exhibits a more severe phenotype than the F5 allele (Klinghoffer et al. 2001). This chimeric receptor can signal through all of the same downstream components as the PDGFRβ except for RasGAP, suggesting that the more severe vascular defects in these chimeric receptor mice may be due to reduced kinase activity and/or expression levels of the chimeric receptor.

The strength of PDGFRβ's signal appears to dictate the absolute numbers of v/p that form, but how the individual pathways contribute to this phenotype remains to be tested. In fact, very little difference in numbers of v/p is observed between the F2 and the F3 mutants, suggesting that PLCγ signals may be somehow redundant with or dependent on the PI3K pathway. In contrast, loss of additional pathways leads to an incremental loss of v/p. The difference between the F3 and the F5 mutations is the ability to bind SHP-2 and RasGAP, and it has been proposed that both of these molecules play roles in down-regulating the PDGFRβ signal (Klinghoffer and Kazlauskas 1995; Ekman et al. 1999). Our results demonstrate that loss of these signaling pathways is detrimental to PDGFRβ signal transduction and that both may have positive and negative influences on receptor activity.

There are several potential ways that loss of these signaling pathways leads to v/p reduction. One mechanism would be that each pathway contributes to a specific cellular outcome. For example, SFK's predominant role could be to promote proliferation (Roche et al. 1995; Hansen et al. 1996), whereas PI3K activity could be more important for migration (Kundra et al. 1994; Wennstrom et al. 1994b). Therefore, the combined loss of these pathways results in a net reduction in v/p, albeit for entirely different cellular

reasons. A second scenario would be that all pathways lead to a single or few specific cellular conclusions. Thus, loss of any one pathway only reduces the outcome but does not ablate it. Evidence from immediate early gene expression analysis suggests that this mechanism may occur (Fambrough et al. 1999), although this possibility does not require that all pathways contribute equally. Last, some pathways may play a primary role downstream of the receptor, while others may be more secondary. Our data suggests that PI3K may be a principal pathway. The F2/F2 mutant mice have a significant reduction in v/p numbers when compared to the wild type and the heterozygous mice and additional mutations have less of an effect than PI3K on v/p numbers. A similar situation has been observed with the PDGFRα (Klinghoffer et al. 2002): the phenotype of mouse embryos with loss of the PDGFRα-PI3K pathway was just as severe as embryos expressing a PDGFRα F7 allele (which is similar to the F7 allele of the PDGFRβ). It will be interesting to determine if a mutation in only the Src binding site would yield a similar reduction in v/p cells.

Although we find that overall loss of downstream pathways attenuates receptor actions as demonstrated by v/p formation, it is surprising that the F7/F7 mice do not phenocopy the null animals. The F7 allele possesses disruptions at seven of the thirteen known phosphorylated tyrosine residues. These mutations should disrupt a majority of the signal relay molecules downstream of the receptor. The remaining tyrosines are capable of binding SFKs, Stats, and Grbs. Based on several previous reports, disruption of Y578 affects the majority of SFK binding (Mori et al. 1993; Twamley et al. 1993; Vaillancourt et al. 1995; Fanger et al. 1997), and we have shown that SFKs do not become activated after stimulation of the F7 receptor. As for the signaling roles of Stat

and Grb2 downstream of the receptor, little direct function has been demonstrated for these remaining effector molecules in PDGF induced cellular responses (Heldin et al. 1998). Therefore F7 signal transmission must use some other means than direct binding by SH2-domain containing proteins. The receptor should still have full kinase activity, unlike the lethal β^{T}mutation which is lacking only the second kinase domain and the SHP-2 and PLCγ binding sites. Possibly, the receptor is phosphorylating molecules that are only transiently associated. Another possibility is that other receptors may function as surrogates. The most likely surrogate is the PDGFRα, but we have demonstrated that in several of the v/p cell populations the PDGFRα is not expressed. Other candidate molecules for such a mechanism are integrins, ephrins, and LRP (Miyamoto et al. 1996; Schneller et al. 1997; Woodard et al. 1998; Boucher et al. 2002; Loukinova et al. 2002). Although these proteins are known to cross talk with the PDGFRβ, it is unclear if they have the capability to substitute for the PDGFRβ's own signaling components.

The F1 mutant allele is an interesting corollary to the F mutant series. While all of the other mutations appear to have a detrimental effect on PDGFRβ signal transduction, the F1 mutation results in an apparent increase in PDGFRβ activity as determined by v/p incidence. This data is in agreement with previous observations that RasGAP function decreases the Ras/MAP kinase pathway activity and migration (Kundra et al. 1994; Ekman et al. 1999). In addition, an add-back mutation of the RasGAP binding site induced a different gene profile from the PDGFRβ immediate early gene profile (Fambrough et al. 1999). This suggests that RasGAP may have different signaling capabilities from the other PDGFRβ signal transduction components.

The mutant mice not only uncover the role of RTK signal transduction *in vivo*, but they also reveal some interesting information regarding v/p cell development. For example, although v/p cell development is impaired when PDGFRβ signal transduction is disrupted, a basal level of cells forms in agreement with previous observations that propagation not initiation of v/p cell development is directed by the PDGFRβ (Lindahl et al. 1997; Hellstrom et al. 1999). Even in the null embryos, v/p cells can be found. It has been proposed that PDGFRβ signals are required for the expansion of v/p cells (Lindahl et al. 1998). While this may be the case, it is curious that even in the instance of the least affected mutation (the heterozygote) the deficiency of v/p cells persists into the adult. There are two explanations for the observation that v/p cells never reach wild type levels. The first is that there is constant turnover in the v/p population and the rate of replacement in the mutant mice is below the rate of loss, resulting in a net reduction in the v/p population. Evidence against this mechanism is the failure to observe any significant proliferation in the adult wild type animals under normal conditions or significant apoptosis in the mutant panel of mice (data not shown).

The second possibility is that there is a specific window during development when v/p cells can expand. After a specified time v/p cell number expansion could be limited, perhaps related to the ability of endothelial cells to secrete the PDGF ligand (Benjamin et al. 1998). Support for this model is the inability of nascent endothelial tubes to recruit v/p cells in tumors (Abramsson et al. 2002). The inability to develop sufficient numbers of v/p cells also appears to be recapitulated in the eye vasculature, suggesting that the maturation of the vessel is more dependent on the local environment than on the chronological age of the embryo.

Our findings demonstrate that the strength of PDGFRβ signal transduction determines the total number of v/p cells. The strength of signal can be modulated not only by the amount of receptor expressed at the cell surface but also by the number of specific downstream signaling pathways activated by the receptor. Whether these results are unique to PDGFRβ signal transduction in v/p cells, or if they can be extrapolated to other RTK remains to be demonstrated.

ACKNOWLEDGEMENTS

We thank Moshe Shani for the XlacZ4 transgenic line; Andrius Kazlauskas for antibodies; Elizabeth Behler, Philip Corrin, Jason Frazier, and Tara Swamy for excellent technical support, and our laboratory colleagues for discussions and critical comments on the manuscript. M.D.T was supported in part by a fellowship from ACS PF-98-149-01. This work was supported in part by research grant number 0330351N from the American Heart Association and 5-FY03-14 from the March of Dime Birth Defects Foundation to M.D.T and by grants HD24875 and HD25326 from the National Institute of Child Health and Human Development to P.S.

FIGURES AND LEGENDS

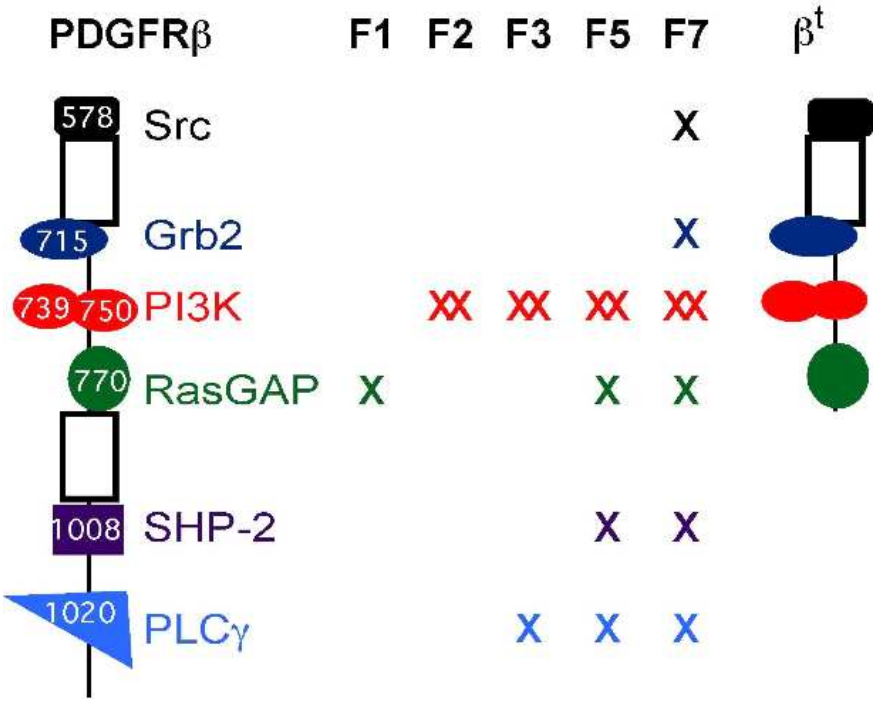

Figure 3-1. PDGFRβ allelic series. This figure depicts the mutant alleles generated in the mouse PDGFRβ genomic locus. X represents a mutation in the tyrosine binding site(s) for a particular signal transduction molecule. The F7 allele contains a disruption in one SFK binding site because loss of both sites results in diminished kinase activity (Mori et al. 1993). The truncation allele (β^T) was created by deletion and subsequent frameshift that results in a stop codon 32 amino acids past the RasGAP binding site.

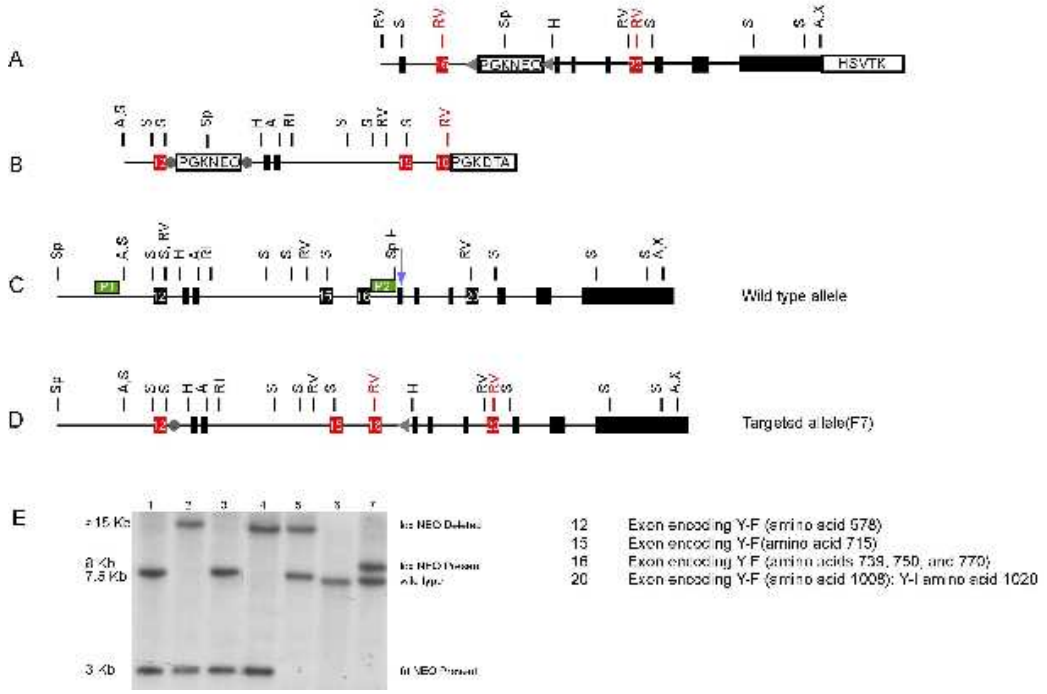

Figure 3-2. Targeting strategy and Southern blot. A. Targeting vector used to create F5 mutant allele. Two exons contain all five mutated tyrosines. B. Targeting vector containing mutations in 5' exons used to generate the F7 mutant allele. C. Wild type allele. D. Targeted allele with PGK-neo removal. Restriction enzyme abbreviations. Sp, *SpeI*; A, *Asp718*; S, *SacI*; RV, *EcoRV*; H, *HindIII*; X, *XhoI*; and RI, *EcoRI*. Green boxes indicate probes used in Southern blot for F7 targeted ES cells. Blue arrow indicates exon where point mutation causes frame-shift in truncation mutation. Black boxes indicate wild type exons. Red boxes indicate exons containing targeted mutations. Restriction enzymes in red indicate sites introduced by mutagenesis to verify proper homologous recombination by Southern blot. Circles denote FRT sites. Triangles denote loxP sites.

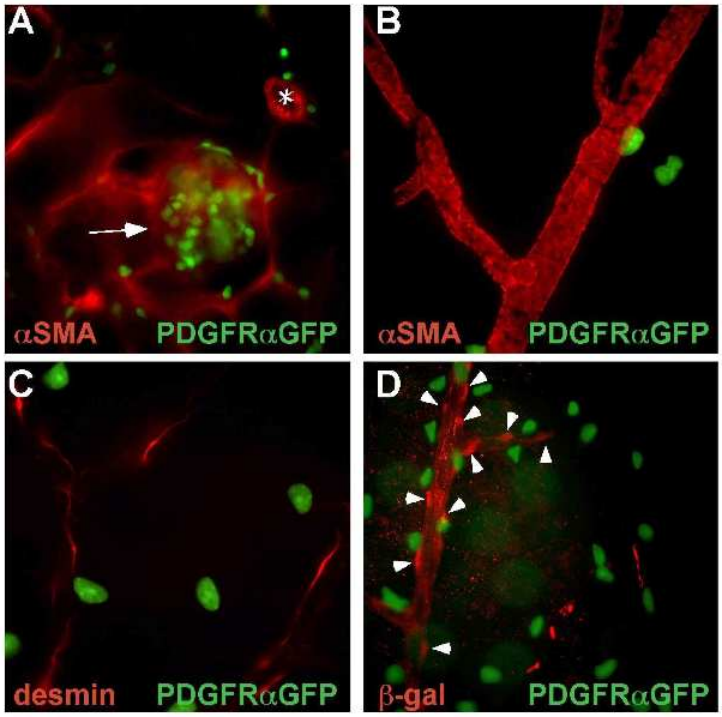

Figure 3-3. Tissue localization of v/p cell markers and PDGFRα expression. A-D. Tissue preparations from P21 PDGFRα^{GFP}; PDGFRβ$^{F5/F5}$ mutant mouse. Immunofluorescence was used to detect: A-B, αSMA; C, desmin; D, β-galactosidase; and A-D, GFP expression for PDGFRα. A. Kidney (200 μm vibratome section). Arrow indicates glomerulus. * indicates an arteriole. B-D. Retina (whole mount preparation). Arrowheads point to β-galactosidase positive nuclei.

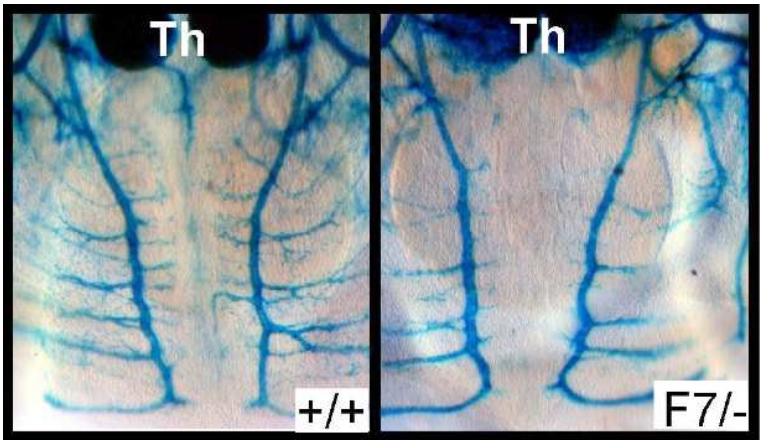

Figure 3-4. Reduction in v/p cells in the thoracic region of the E14.5 embryos. Ventral view of E14.5 wild type and F7/- littermates with the *XlacZ4* mouse marker background. β-galactosidase positive nuclei represent v/p cells. Th-thymus.

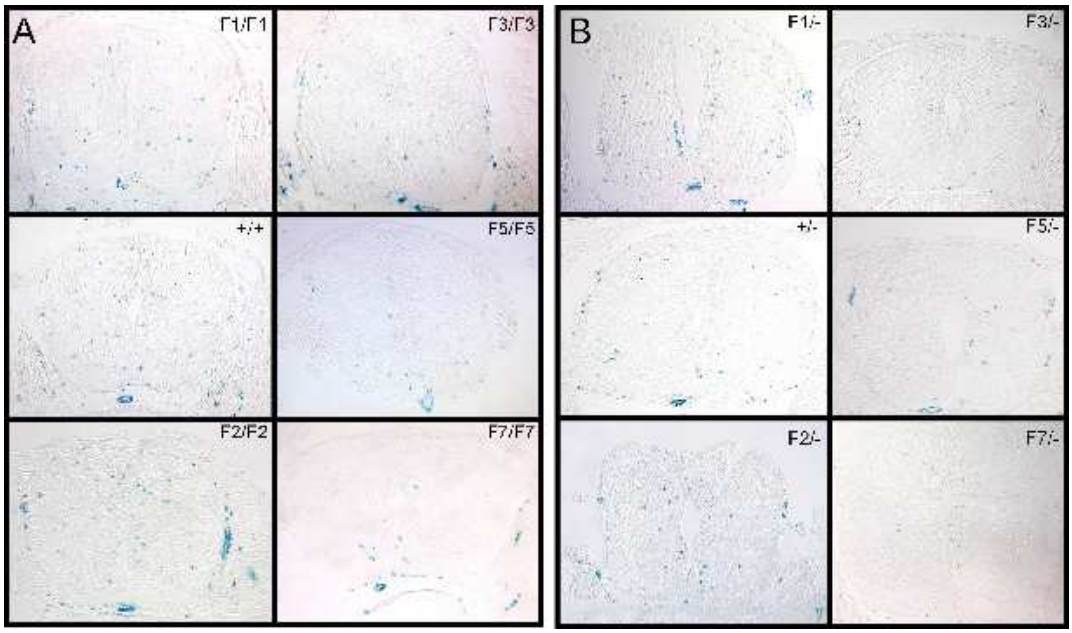

Figure 3-5. Pericytes within E14.5 nervous system of F series mutant embryos. Panel A. Representative sections through neural tubes of embryos from the homozygous F allelic series. Panel B. Representative sections of embryos from the hemizygous allelic series (F series mutant with one copy of the null allele). Sections are from the rostral level between the heart and kidney. Pericytes are visualized by nuclear localized β-galactosidase staining in cells committed to the v/p lineage. 7 μm sections.

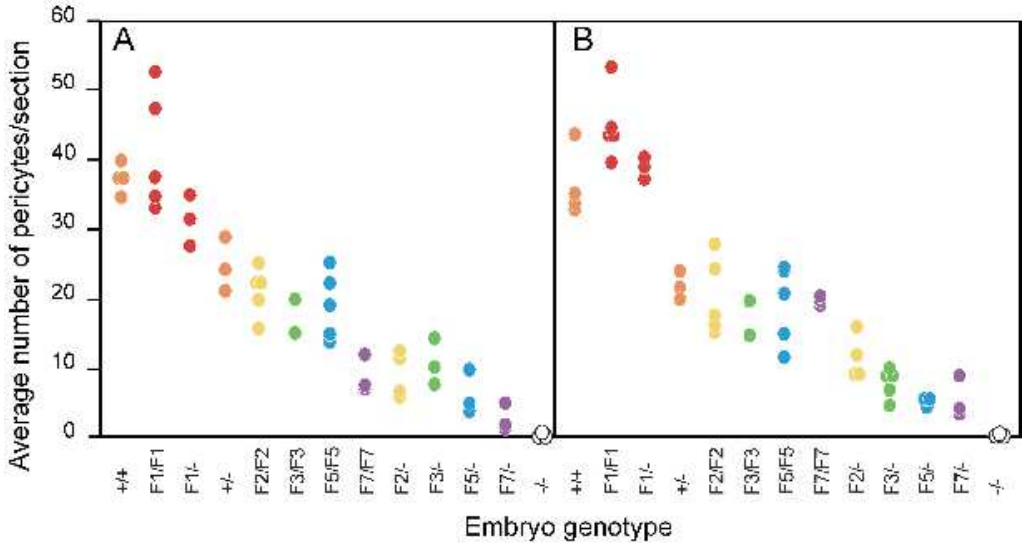

Figure 3-6. Quantitation of pericytes in nervous system. β-galactosidase-positive nuclei were counted within the neural tube. Each data point represents a mean of 7-10 sections from a single embryo. Data was gathered at two rostral levels in each embryo. The genotypes are ordered by the predicted strength of signal depending on the number of copies of the receptor being expressed and the signal transduction pathways remaining downstream of the receptor.

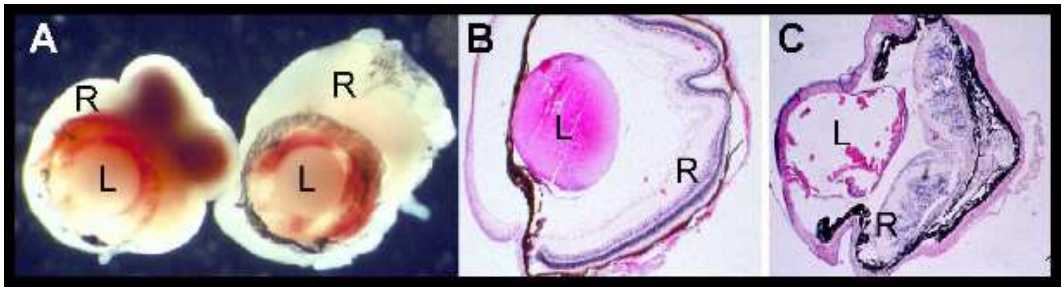

Figure 3-7. Eye defects in F5/- mice. A. Eyes from a P4 F5/- mouse demonstrating severe hemorrhaging. B and C. H/E stained sagittal sections through eyes of wild type and F5/- 3 month old mice, respectively. The absence of the lens of the F5/- eye is a histological defect and not a phenotype of the F5/- eye. L, lens. R, retina.

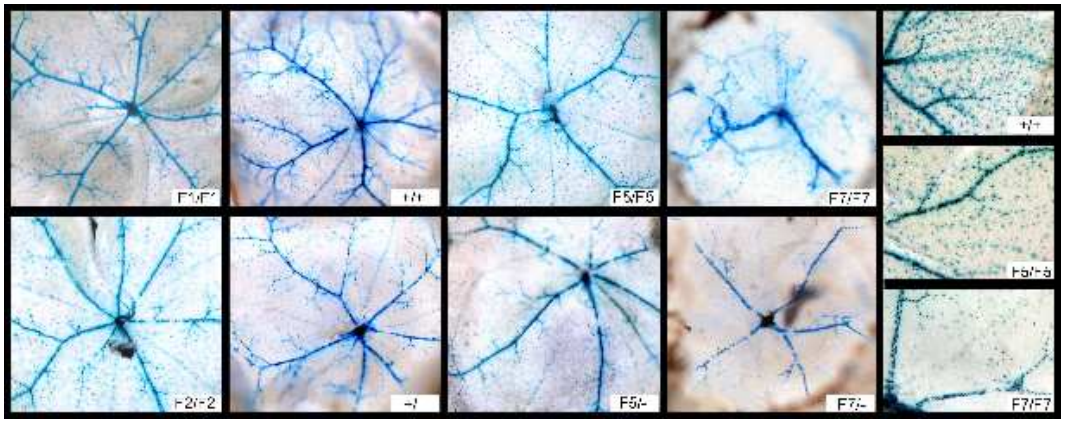

Figure 3-8. V/p populations in P28 retinas. A. Whole mount retinal preparations from wild type and mutant eyes. Pigmented epithelium was removed for visualization of β-galactosidase. Note F7/F7 and F7/- had extensive thickening of the retinal layers which resulted in a contraction of the entire retina and apparent reduction in size. B. Close-up of artery and vein of three homozygous eyes.

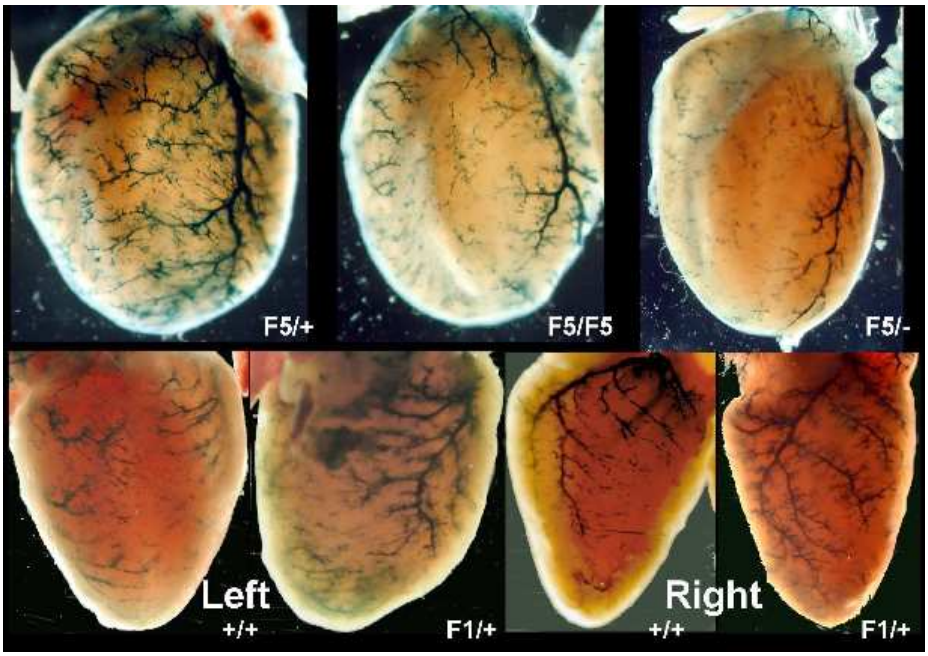

Figure 3-9. Vascular smooth muscle cells of the coronary arteries. A. Whole mount views of P21 hearts from littermates of the F5 alleles of mutant mice. Hearts were sliced coronally and the ventral surface was photographed. The F5/- heart was sliced disproportionately and therefore appears to be smaller. B. P28 hearts from wild type and F1 littermates. Hearts were sliced sagittally. Both the left and right views are shown.

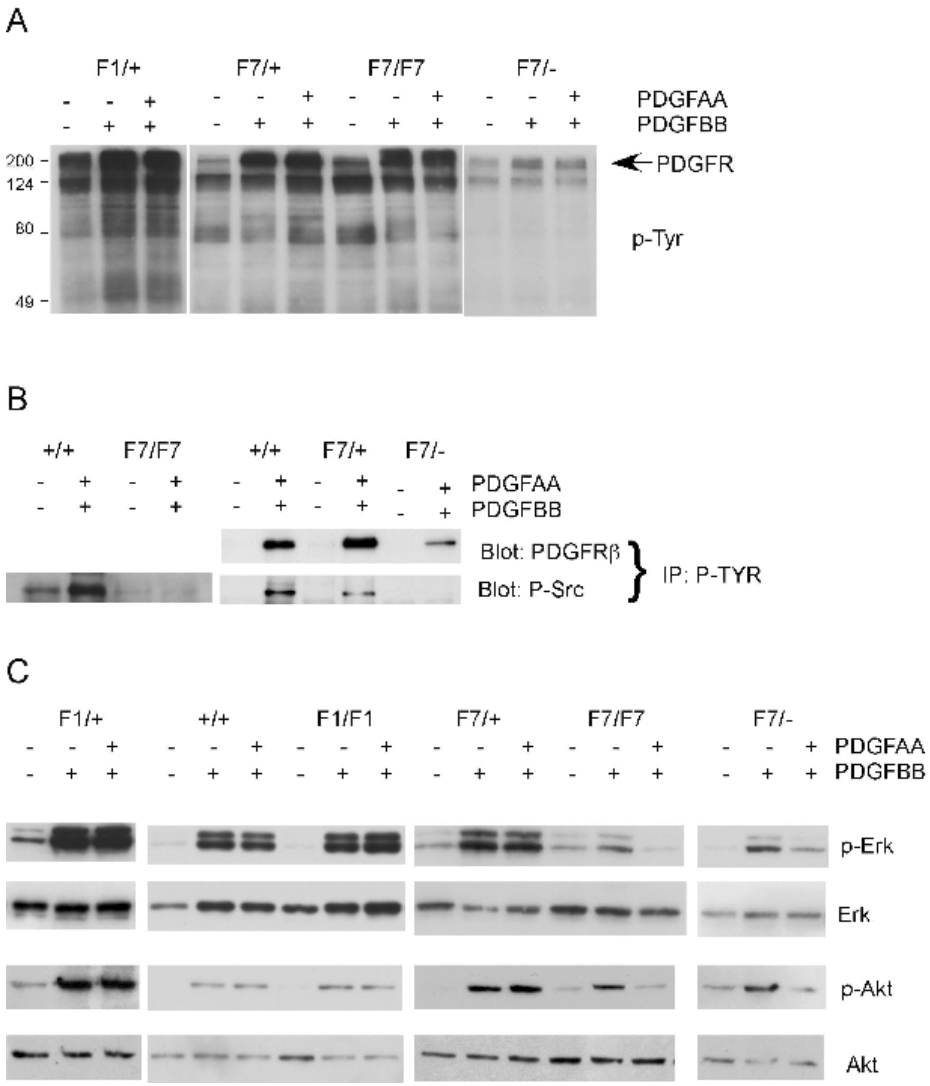

Figure 3-10. Biochemistry of MEFs from F7 and F1 mice. A. Whole cell lysates were generated from MEFs that were un-stimulated or stimulated with PDGFAA and/or PDGFBB; 100ng/ml and 30ng/ml respectively. Lysates were then subjected to SDS-PAGE and western blotting accomplished with the antiphosphotyrosine antibody (4G10). B. Immunoprecipitation of tyrosine phosphorylated proteins from wild type and F7 series of mutant MEFS. The precipitates were then run on SDS-PAGE and a western blot was performed using anti-Src [pY^{418}] antibody and anti-PDGFRβ 90A. C. Whole cell lysates from un-stimulated or stimulated MEFs. Lysates were then subjected to SDS-PAGE and western blotting accomplished with the indicated phospho-specific antibodies. Blots were stripped and blotted with antibodies to the corresponding unphosphorylated proteins to demonstrate protein loading. Data are representative of results from at least two independently-derived cell lines.

CHAPTER FOUR
MICROARRAY ANALYSIS OF VASCULAR REMODELING AND VESSEL MATURITY

INTRODUCTION

Over the years gene deletion analyses have identified molecules essential for vascular development during both early developmental stages as well as later stages for vessel stability and function. Much research has focused on understanding not only how these proteins function but also what regulates their expression. Transcriptional regulators are often found downstream of cell membrane receptors such as receptor tyrosine kinases (RTK) that activate signaling pathways including MAPK, PI3K, and Src. These pathways are often regulated by activated cell surface receptors such as VEGF, TGF, and PDGF. VEGFR and TGFR are essential in vascular development through their role in precursor cell populations and endothelial cells (Argaves and Drake, 2005). To further understand vascular development and the contribution of other cell populations this study focused on the PDGF receptors and their role in VSMC and their precursors.

Part of the challenges to identifying regulators of vasculogenesis is that it occurs throughout the development of tissues and organs. This makes it difficult to isolate components unique to vascular development due to dilution by activation of pathways and molecules not involved in vasculogenesis but moreso organogenesis. In our studies, the yolk sac provided a unique tissue source early in development that is limited in cell populations and developmental processes. The yolk sac consists of three main cell populations including the endoderm, mesoderm, and ectoderm. Formation of mature vessels has been shown to be essential for embryonic survival by several molecules

involved in mesoderm differentiation as well as those in endothelial cell functions. Mutations in these key molecules can disrupt early stages of vasculogenesis preventing the formation of endothelial tubes while others can disrupt vascular remodeling into mature vessels (Argaves and Drake, 2005).

As described in previous chapters, PDGFR play an essential role in VSMC and mesothelial cell populations for proper vascular development. In these studies, the PDGFR mutant yolk sacs were used to identify key differences in gene regulation in specific cell populations and/or cellular pathways. Wild type E10.5 yolk sacs were used as the baseline, identifying the genes expressed in normally developed yolk sac vasculature. Comparing this gene list to that of a wild type E9.5 yolk sac allowed identification of all changes in gene regulation during vascular remodeling stages. However, this analysis identified changes in gene expression of all cell types present. To more closely understand the role of the mesothelial cell population, $PDGFR^{SKO}$ yolk sacs were analyzed at E9.5 and E10.5. Because the main defect in these samples is the lack of vascular remodeling, their gene profile can be compared to wild type E9.5 and E10.5 to subtract out general yolk sac developmental gene changes from those specific to vascular development and more specifically the mesothelium and VSMC. Additionally, $PDGFR^{MKO}$ yolk sacs at E10.5, whose main defect is the absence of VSMC, were analyzed for VSMC specific genes. Finally, E10.5 $PDGFR^{PI3K}$ mutant yolk sacs, lacking PI3 kinase signaling downstream of the PDGFR, were used to identify gene expression regulated specifically by this pathway. This analysis not only identified genes that explained the phenotypes observed through changes in matrix molecules and regulators

of cell growth, but also identified genes that suggest similarities in developmental processes to cardiovascular development and disease states.

MATERIALS AND METHODS

Mouse lines

Mice used in this study include PDGFR$\alpha^{fl/fl}$ PDGFR$\beta^{fl/fl}$; SM22-Cre^{Tg}, Myocardin^{Cre}, and PDGFR$\alpha^{PI3K/PI3K}$ PDGFR$\beta^{PI3K/PI3K}$. Crosses were designed to generate yolk sacs that were doubly homozygous for the mutant alleles for PDGFα and PDGFRβ in vascular smooth cells and their precursors. Vaginal plugs were used to determine embryonic day 0.5 and yolk sacs were isolated in placed into RNAlater on days 9.5 and 10.5. Samples were stored at –20^{o}C.

RNA isolation

RNA was isolated according to recommendations from the UT Southwestern Microarray Core Facility's protocols for Microarray processing. Samples were removed from RNAlater and placed into 100µl Trizol and homogenized. Next, 20µl of Chloroform was mixed in and samples were centrifuged at 4^{o}C for 15 minutes. Supernatant was transferred to a new tube and mixed with an equal amount of 70% ethanol. Samples were mixed well and total volume was transferred into a minispin column from the RNAeasy kit (Qiagen). Binding RNA to the column and subsequent washes were performed according to manufacturer's instructions using RW1 and RPE buffers. RNA was extracted using 20-30µl of DEPC H_2O. RNA isolated from individual

samples for each genotype was tested on an Agilent 2100 bioanalyzer for quantitative and qualitative analysis.

Microarray

UT Southwestern Microarray Core Facility processed samples for cDNA synthesis, in vitro transcription and RNA labeling. Samples were then hybridized onto an Illumina Mouse-6 BeadChip 47K Array and scanned for gene expression analysis.

Analysis

Microarray data was processed using Beadchip for normalization, analysis of gene expression levels, and cluster analysis. WebGestalt and Microsoft Excel was used for analysis of differences in gene expression across different samples. Samples analyzed were expressed more than 2 fold in wild type E10.5 yolk sacs and differentially expressed by 2 fold or more in the experimental samples.

RESULTS

Using microarray analysis, these studies identified the contribution of specific cell populations and signaling molecules to gene regulation during vascular development of the yolk sac. The stages of vascular development for the different mutants at E9.5 and E10.5 are identified in Table 4-1 as honeycomb for unremodeled vessels and mature for remodeled vessels. In previous chapters it was demonstrated that $PDGFR^{SKO}$ mutants disrupt yolk sac vascular remodeling while $PDGFR^{MKO}$ mutants undergo vascular remodeling but fail to develop VSMC. $PDGFR^{PI3K}$ mutants disrupt PI3 kinase signaling downstream of both PDGFRα and PDGFRβ in all cell populations. The yolk sac

phenotype demonstrates a loose association between VSMC and endothelial cells (Fig 4-1). Initial analysis of the different yolk sac mutants demonstrates similarities in gene expression profiles through a cluster diagram (Fig 4-2). E9.5 wild type and $PDGFR^{SKO}$ yolk sacs resulted in the same branch of the diagram demonstrating similar gene profiles. Additionally, all samples with PDGFR mutations in VSMC and their precursors branched together with the $PDGFR^{MKO}$ and $PDGFR^{PI3K}$ demonstrating even greater similarities. The rest of this chapter will focus on identifying genes specific to different cell populations by comparing expression of different genotypes and developmental stages as well as analysis of key gene lists based on cellular function. Key genes from those lists were identified that could enhance the understanding the role of VSMC in vascular remodeling and vessel stability.

To identify gene profiles for individual cell populations and vascular stages, the data was compared across three genotypes at a time. All data sets demonstrate genes with a 2 fold increase or decrease compared to $PDGFR^{+}$ E10.5. Genes analyzed are listed according to level of fold change. Genes listed more than once represent duplicate spots for the genes on the microarray and are included in total numbers. For genes involved in vascular remodeling, $PDGFR^{SKO}$ E10.5, $PDGFR^{SKO}$ E9.5, and $PDGFR^{+}$ E9.5 were compared. Figure 4-3 demonstrates a venn diagram of the gene profiles of these three genotypes demonstrating that 119 genes are differentially expressed in all three of these genotypes compared to wild type E10.5. These 119 genes were not differentially expressed in $PDGFR^{MKO}$ or $PDGFR^{PI3K}$. Because the main difference between these genotypes and wild type E10.5 is the lack of vascular remodeling, the list of genes in Table 4-2 could identify regulatory genes for vascular remodeling. Similarly, $PDGFR^{SKO}$

at E10.5 and E9.5 lack PDGFR signaling in mesothelial cells suggesting that the 92 genes differentially expressed in these two samples compared to wild type E9.5 can be specific to mesothelial cell signaling (Table 4-2). Genes differentially expressed by $PDGFR^{SKO}$ E10.5, $PDGFR^{SKO}$ E9.5, and $PDGFR^{+}$ E9.5, 590, 336, and 167, respectfully, may indicate genes that are unique to each developmental condition. For example, genes unique to E9.5 $PDGFR^{+}$ may represent changes in gene expression required for the initiation of vascular remodeling that would be completely absent in both $PDGFR^{SKO}$ samples. Genes unique to $PDGFR^{SKO}$ E10.5 may represent differentially regulated genes resulting from disrupted cell to cell interactions, such that some cells are able to progress developmentally and express different genes than $PDGFR^{+}$ E9.5 but lack the proper interactions to mimic $PDGFR^{+}$ E10.5 expression. Finally genes unique to $PDGFR^{SKO}$ E9.5 may represent differential expression due to disrupted vascular development at an earlier stage.

Gene comparisons between the different E10.5 PDGFR mutants allows analysis of gene expression at a more cell/pathway specific level (Figure 4-4). Again, in this analysis, $PDGFR^{SKO}$ E10.5 represents the absence of vascular remodeling but more specifically the absence of mesothelial signaling in addition to absent VSMC and their signaling. In the $PDGFR^{MKO}$ E10.5, genes differentially regulated are specific to VSMC or influenced by the absence of VSMC. $PDGFR^{PI3K}$ samples will identify genes specifically associated to PI3 kinase signaling either directly or indirectly. There were 597, 71, and 228 genes differentially regulated solely in $PDGFR^{SKO}$, $PDGFR^{MKO}$, and $PDGFR^{PI3K}$, respectively. There were 42 genes identified in both $PDGFR^{SKO}$ and $PDGFR^{MKO}$ suggesting these genes are specific to VSMC. The differential expression

identified in both PDGFR^{MKO} and PDGFR^{PI3K} included 41 genes and may represent a disruption from the absence of cell to cell interactions between VSMC and EC. Finally, the 66 genes differentially regulated between all three of these genotypes suggest VSMC are an important component of development through PI3 kinase signaling (Table 4-3).

Analysis of the entire microarray identifies changes in gene regulation, however it can be even more interesting when differentially regulated genes function in transcriptional and translation processes. In this analysis multiple transcription factors were identified belonging to gene families including Kruppel-like, zinc finger, and FOX transcription families (Savagner et al. 1997; Katoh 2004; Haldar et al. 2007) (Table 4-6). Family members of the Kruppel-like family include *Klf7* and *Hkr3* and are range in decreased expression from 2 to 3.2 for the PDGFR mutants and 2 to 3.3 for the wild type E9.5 yolk sac. *Snai2* and *Snai3* are both zinc finger transcription factors involved in cellular differentiation. *Snai3* was reduced 5 fold in wild type E9.5 yolk sacs and 3.4 in PDGFR^{PI3K} mutants. *Snai2* is of particular interest because it is implicated in the EMT process and is completely absent in PDGFR^{SKO} yolk sacs. Three members of the Fox family demonstrated reduced expression levels including *foxa1*, *foxq1*, and *foxo3*. *Foxa1* was reduced by 2 fold in both wild type E9.5 and PDGFR^{SKO} E10.5 and 2.4 in PDGFR^{PI3K} yolk sacs. *Foxq1* resulted in reduced levels in all comparisons ranging from 3.3 to 5 fold decreases. Differences in *Foxo3* were unique to the PDGFR mutant yolk sacs resulting in 5, 2.2, and 33.3 fold decreases in PDGFR^{SKO}, PDGFR^{MKO}, and PDGF^{PI3K} yolk sacs, respectively.

Additional factors of interest involved in transcription include *Peg3*, *Wdr9*, *Rab1*, and *Hand1* (Table 4-6). *Peg3* has been studied for its role in tumorigenesis resulting

from genomic instability (Su et al. 2002). The expression of *Peg3* was reduced in all of the samples by 3.33, 2, 2.04, and 2.56 fold in wild type E9.5, PDGFR^{SKO}, PDGFR^{MKO}, and PDGFR^{PI3K}, respectively. *Wdr9* plays an important role during development and was reduced in both wild type E9.5 and PDGFR^{SKO} by 2.5 fold, suggesting it is a key factor in vascular remodeling (Huang et al. 2003). Both *Rab1* and *Hand1* play a role in cardiac development and were reduced but the differences were observed in different samples (Martindill et al. 2007; Filipeanu et al. 2008). *Rab1* was reduced 2 to 2.5 fold in wild type E9.5, PDGFR^{SKO} E10.5, and PDGFR^{PI3K} while *Hand1* was reduced by 2.22 and 5 fold in PDGFR^{MKO} and PDGFR^{SKO} E10.5, respectively. These results suggest that *Rab1* is expressed at later stages of yolk sac development and potentially regulated downstream of the PI3 kinase pathway. The expression differences observed for *Hand1* suggest that it is expressed at both E9.5 and E10.5 yolk sacs and possibly regulated by mesothelial and/or VSMC populations.

While these genes demonstrate reductions in gene expression, members of the TEAD family demonstrated increases in expression (Table 4-6). TEAD family proteins play a role in developmental growth and possibly EMT (Zhang et al. 2009). The increases in expression were solely identified in wild type E9.5 and PDGFR^{SKO} E10.5 yolk sacs (Table 4-5). This data supports the analysis of developmental similarities between E9.5 and PDGFR^{SKO} yolk sacs and the possibility of EMT occurring in the yolk sac.

The presence of new cell populations and elongated vasculature between the stages of E9.5 and E10.5 suggests proliferation, migration and cell survival are key cellular process at this time. Differential expression of genes involved in matrix, mitosis and cell survival include *Ccn1* and *Nudel pending* (Table 4-5). *Ccn1* is expressed in

vascular cells, interacts with extracellular matrix, and has been shown to promote proliferation, migration and EC tube formation (Grote et al. 2004; Yu et al. 2008). In the yolk sac mutants, *Ccn1* expression or similar family members were reduced 2.5 in wild type E9.5 and PDGFR^{SKO}, and 4 fold in PDGFR^{MKO}. *Nudel pending* is reduced 2, 2.38, and 10 fold in wild type E9.5, PDGFR^{MKO}, and PDGFR^{SKO}, respectively. Through its interaction with dynein, Nudel pending plays a role in cell motility (Shen et al. 2008).

Interestingly, analysis of genes upregulated in the E9.5 and mutant yolk sacs identified genes such as *Arpc3* that plays an essential role in trophoblast development through its role in cell motility (Yae et al. 2006) (Table 4-4). This result suggests that the yolk sac mutants may be developmentally delayed and more closely resemble the wild type E9.5 yolk sac stages. Aside from a reduction in collagen expression, wild type E9.5, PDGFR^{MKO}, and PDGFR^{SKO} exhibited similar decreases in matrix genes such as *Claudin1 (Cldn1)* and *Vitronectin (Vtn)* (Table 4-4). *Cldn1*, or *Semp1*, is part of the epithelial membrane superfamily and has been shown to play a role in tight junctions (Hoevel et al. 2002). Gene reduction levels of *Cldn1* included a 3.26, 2.32, and 2.5 fold changes for wild type E9.5, PDGFR^{SKO}, and PDGFR^{MKO}. *Vtn* has been shown to be essential for VSMC adhesion and therefore isn't surprising to see its reduced expression in samples lacking this cell population (Stepanova et al. 2002). *Vtn* expression was 17.5, 4.5, and 3.3 fold lower in wild type E9.5, PDGFR^{SKO}, and PDGFR^{MKO}, respectively, than in wild type E10.5 yolk sacs. In PDGFR^{PI3K} mutants, there was a high level of reduction in expression of *collagen* genes. The reduction of *collagen* expression could support the hypothesis that the VSMC and EC interactions are disrupted due to a reduction in ECM.

Decreases in gene regulation unique to wild type E9.5 and PDGFR^{SKO} E10.5 included *Hspg2*, *Saa4*, and *Thbs2* (Table 4-4). *Hspg2* is also known as *perlecan* and is regulated by VEGF. Its function is in the regulation of the transcription factor, *Oct1*, that is involved in cell growth and is expressed in VSMC (Weiser et al. 1997; Kaji et al. 2006). *Saa4* is suggested to regulate EC adhesion through its regulation of the adhesion molecule VCAM1 (Ashby et al. 2001). In the wild type E9.5 and PDGFR^{SKO} mutants there was a 20 and 2.7 fold decrease, respectively. *Thbs2* has been suggested to inhibit EC proliferation through caspase dependent mechanisms and deletion of gene expression results in increased microvasculature (Armstrong et al. 2002). The fold decrease in *Thbs2* was 2.3 and 4.5 for wild type E9.5 and PDGFR^{SKO}, respectively. Interestingly, there was also an 8.3 fold decrease in *Saa4* expression and 2.3 fold decrease in *Thbs2* in PDGFR^{PI3K} mutant yolk sacs suggesting they may play an important role in vessel structure and stability but not necessarily in early stages of vascular remodeling.

Additional genes differentially regulated in wild type E9.5 and mutant yolk sacs include *ADAMS, MMP's, Serpina, Lars, CamK, Pnp, DapK, Slc, Aldh, Tpmt, Lrs1*, and *Nxn*. *ADAMS* family members include *disintegrins* and *MMP's* (Table 4-7). They have been shown to play a role in cell to cell signaling, cell adhesion and cellular motility (Goldsmith et al. 2004; Kurohara et al. 2004; Kim et al. 2006; Wildeboer et al. 2006). In the yolk sac gene expression profiles, it was shown that *Adam23* and *Adamts2* were downregulated. *Adam23* was decreased by 3.3, 2.13, and 3.8 fold in PDGFR^{SKO}, PDGFR^{MKO}, and PDGFR^{PI3K}, respectively, suggesting a VSMC specific role possibly linked to the PI3 kinase signaling pathway. *Adamts2* decreased by 3.3 and 2.3 fold in

PDGFR^{SKO} and PDGFR^{PI3K}, respectively. Interestingly, *Adam19* was upregulated by 2.9 fold in wild type E9.5 yolk sacs and reduced 2 fold in PDGFR^{SKO} yolk sacs.

CONCLUSION

These studies have identified key gene regulation essential for cell differentiation and vascular development. Our mutant combinations allowed analysis of specific cell populations including mesothelial cells, VSMC, and even more specifically the PI3 kinase pathways downstream of the PDGFR. Grouping genes according to their cellular functions allowed closer analysis of potential mechanisms and function of the PDGFR in vascular remodeling.

Extracellular matrix is an important component of vascular development and overall cell to cell interactions. It was interesting to see in this analysis the multitude of matrix molecules that were downregulated in the mutant yolk sacs. In the previous chapter different matrix molecules were analyzed for differences in levels by immunohistochemistry identifying decreases in collagen. It will be important to further explore the exact role of collagen as a matrix molecule essential for vessel development as well as other matrix and adhesion components such as *vitronectin, Saa4, Hspg2,* and *Itgs5*. Additionally, the function of the matrix components can be further investigated to determine if their key role is purely structural or if there is an additional signaling activation component. Many matrix molecules signal through integrins who have been suggested to work cooperatively with PDGFR for signaling activation. On the other hand, there was a decrease in expression of Adam family proteins as well as several

MMP's. These results suggest that the delicate balance of expression needs to be analyzed alongside the actual activity in the yolk sac to fully understand the role of each protein. Altogether the changes in expression may likely be associated to the developmental stage of vasculogenesis in the yolk sac. During earlier stages matrix will be broken down to allow migration of cells for the elongation of vessels. At later stages, it is important to express proper ECM for vessel stability. Further research into the timing of expression and the site of expression would provide insight to the role of the many ECM components.

While cellular matrix and motility can be closely associated, analysis of expression of motility or migration genes could give insight to specific cellular pathways essential for yolk sac growth at E9.5 and E10.5. While *Nudel pending* and *Kifc1* stand out for their roles specific interactions and roles in the mechanics of cell motility, additional factors were identified that may be more specific to remodeling, such as *Ccn1* and *Ngfr*. Further research to understand the function of these proteins, their interactions, and the associations to PDGFR signaling will be important.

It has been a longstanding question whether the signaling pathways downstream of the PDGFR function cooperatively or separately to activate cellular mechanisms. Using the information gathered thus far in yolk sac vascular development, the F series mutant mice described previously could be used to analyze deletion of specific pathways in the $PDGFR^{SKO}$ background. Genes essential for vascular development and VSMC could then be analyzed downstream of the specific pathway mutants, similar to the $PDGFR^{PI3K}$ analysis done in this chapter. The yolk sac phenotype and high number of matrix molecules, mainly collagen genes, identified in the $PDGFR^{PI3K}$ mutant strongly

suggest that collagen production is regulated downstream of the PI3K pathway and that this expression is essential for cell to cell association between VSMC and EC.

Understanding vascular development and the key components involved could identify mechanisms for regulating vessel growth and structure at later stages and during disease states. Mutation of or misregulation of genes has been shown to contribute to abnormal cell growth and tumorigenesis, in particular alterations in transcription factors can lead to misregulation of multiple genes. In this analysis, members of several genes are identified for their up or downregulation, include *Peg3* and members of the *Serpina* family, that have been previously implicated in tumorigenesis. Finally, vascular development of the yolk sac strongly resembles that of the cardiovasculature surrounding the heart. These similarities include the honeycomb structure remodeling to mature vasculature and the derivation of VSMC from a mesothelial cell population that are important for vessel growth. Taking these similarities into consideration it is possible to hypothesize that during vasculogenesis in the yolk sac, there could be an epithelial to mesenchymal transition (EMT) that takes places and leads to proper vascular development. The microarray data supporting this hypothesis includes the changes in regulation of EMT related genes including members of the *Cldn* and *Tead* families. The downregulation of the *Cldn* gene family and upregulation of the *Tead* family upregulated in wild type E9.5 and PDGFR^{SKO} yolk sacs suggests developmental similarities in these two yolk sac genotypes and the possible occurrence of EMT prior to the remodeling events. While the hypothesis of EMT in the yolk sac requires exploration, the microarray results from these experiments provides a good starting point for genes of interest.

Future experiments analyzing expression of genes at different developmental stages and in mutant yolk sacs to confirm the changes in gene regulation at the protein and functional level will provide greater support to the molecular changes associated with vascular remodeling. However, the genes identified in this study have definitely identified key gene families and cellular process to focus on. Overall, these microarray studies have identified changes in gene regulation that may play direct roles in vascular remodeling that can be similar to development in other tissues/organs and possibly some disease states.

FIGURES AND LEGENDS

Table 4-1. Vascular development stages and cell types present.

Mouse Type at E9.5	Cells Present	Phenotype
Wild type	Mesothelium	Honeycomb
$PDGFR^{SKO}$	Mesothelium	Honeycomb
$PDGFR^{MKO}$	Mesothelium	Honeycomb
Mouse Type at E10.5		
Wild type	Mesothelium and SMC	Remodeled and defined
$PDGFR^{SKO}$	Mesothelium	Honeycomb
$PDGFR^{MKO}$	Mesothelium	Remodeled but undefined
$PDGFR^{PI3K}$	Mesothelium and SMC	Remodeled but loosely defined

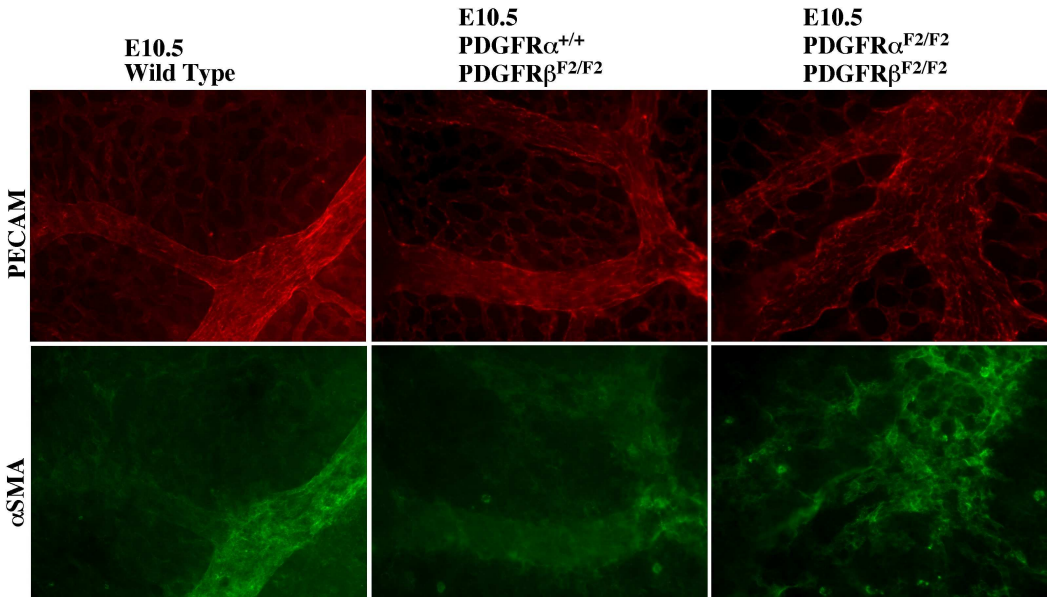

Figure 4-1. Vascular development in yolk sacs lacking PDGFR driven PI3 kinase signaling. Endothelial cell (PECAM) and VSMC (αSMA) yolk sac staining at E10.5 in wild type, PDGFRβ^{PI3K} (PDGFRβ$^{F2/F2}$), and PDGFR^{PI3K} (PDGFR$^{F2/F2}$).

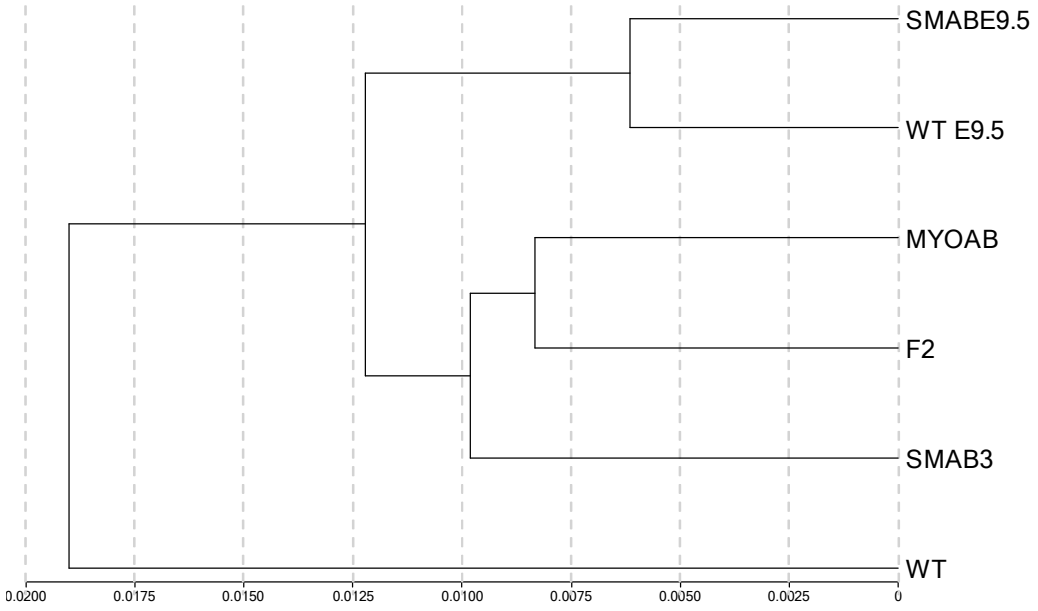

Figure 4-2. Cluster diagram analysis of gene profiles. All genotypes and ages analyzed grouped according to similarities in gene expression profiles.

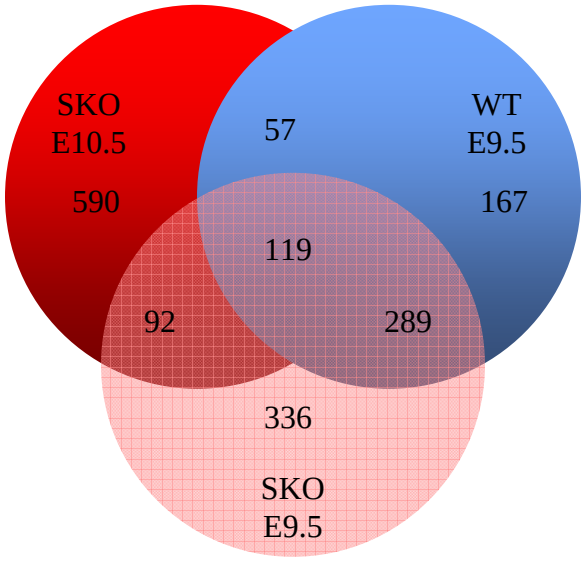

Figure 4-3. Overlapping gene expression profiles for PDGFR^{SKO} E10.5, PDGFR^{SKO} E9.5, and PDGFR^{+} E9.5. (Genes compared were identified as 2 fold difference in expression from E10.5 PDGFR^{+}).

Table 4-2. Genes differentially expressed in PDGFR^{+} E9.5, PDGFR^{SKO} E9.5, and PDGFR^{SKO} E10.5.

PDGFR^{SKO} E10.5 and PDGFR^{SKO} E9.5	PDGFR^{SKO} E10.5 and PDGFR^{+} E9.5	PDGFR^{+} E9.5 and PDGFR^{SKO} E9.5	ALL
Atp10d	Hrb	Sgk	1110018K11Rik
Gnb4	Cda	Sox18	Idb3
Shoc2	3110023B02Rik	Prss19	Adora2b
Nxt2	Slc2a2	1110025G12Rik	2310069P03Rik
8430426K15Rik	Trappc3	Aqp8	Ldb2
E130112E08Rik	3110023B02Rik	A430104N18Rik	Emb
5730409G07Rik	Calml4	Plcg2	9430073N08Rik
Amd2	Sfrs10	Prkar2b	LOC384525
4933428A15Rik	Trappc3	Rasgrp3	2400003B06Rik
LOC381801	Sfrs10	Nfe2	Car12
LOC245676	Pip5k1b	Flrt3	LOC381850
Acad9	Trappc3	Pdgfra	C730026E21Rik
BC034507	Tarbp2	6230425C21Rik	Tulp2
Galgt2	Slc2a2	Dnmt3b	Rps19
1810017F10Rik	Slc39a13	Admr	S100a1
Hemp1	Hspg2	Ppat	Adam19
Twistnb	Etohd2	Snurf	5830467P10Rik
LOC241051	Krt1-14	Agtrl1	2600013N14Rik
0610010F05Rik	Epor	Csda	Tdh
LOC383131	Mfap2	Admr	Dhrs8
2510048K03Rik	Atbf1	Fxyd6	Kifc1
Usmg5	2210008I11Rik	Paf53	Eif3s6
Rpl30	Mfap2	Leprel1	Gypc
Atp5k	Klf7	Snrpn	Gfpt2
S100a13	Leprel2	A230098A12Rik	Vapb
Polr2k	Trb	Rab25	2610042G18Rik
C330008K14Rik	0610009J05Rik	Pls3	6230427J02Rik
Pdlim4	2610001E17Rik	Rangnrf	4930553M18Rik
Ndufa5	Nope	2410008B13Rik	1700081H05Rik
LOC214738	Heph	Hoxb2	Il2rg
Slc25a4	Hspg2	1810009K13Rik	3732412D22Rik
E030006K04Rik	C430014K11Rik	Igfbp2	1810022C23Rik
Mest	Heph	Eraf	Ncf4
3110078M01Rik	Cebpa	Snrpn	Abcg5
Mmrn2	Atbf1	Cldn5	Deadc1
Plk1	1110004P15Rik	Fli1	Cbln1
Vwf	Bcl9l	Hspa4	LOC271041
2310014H01Rik	Gp5	Rangnrf	Hk2
1110014O20Rik	Susd2	Hoxb5	Abi3

PDGFR^{SKO} E10.5 and PDGFR^{SKO} E9.5	PDGFR^{SKO} E10.5 and PDGFR^{+} E9.5	PDGFR^{+} E9.5 and PDGFR^{SKO} E9.5	ALL
Kif23	AW046396	Csda	Bcap29
Socs3	9130213B05Rik	C130078N17Rik	C730026E21Rik
4933439C20Rik	Adamts9	Egfl7	Car7
Rasa3	Mfhas1	Tek	Plvap
Dguok	9330186A19Rik	Acn9	2810417H13Rik
Luc7l2	Axl	Bop1	Targ1
Vegfc	Sema3b	2810046C01Rik	Arpc3
A130092J06Rik	Col5a1	Ripk3	G431001I09Rik
Hspa12b	Col4a6	Hipk2	Upk3b
Tro	Gm22	1110001A12Rik	Nsdhl
C920013G19Rik	2610001E17Rik	Spire2	Nsdhl
Btg1	Serpina1a	Dnajc2	Tgfbi
LOC382215	Srpx	LOC381760	Emp3
9230112O05Rik	Serpina1a	Ccnd1	Faah
Wasf1	Nudel-pending	Casp7	2810403A07Rik
Popdc2	A230020G22Rik	Vamp5	9330107J05Rik
BC013481	9130213B05Rik	Ccnd1	Itgb5
Flt1		Magmas	Foxa1
2700031B12Rik		C330023M02Rik	Anxa6
Pum1		Lyl1	Gtpbp2
6030411F23Rik		Tead2	Thbs2
Ece1		Hmgn3	Hbb-b1
Ghr		Fgd5	Fdps
Bbs7		Hnrpa0	Biklk
Gja4		Xlkd1	Dhcr7
Tssc8		1110032E23Rik	Mvd
Txnl4		2310037P21Rik	Aacs
Insig2		Pthr1	Hmgcs1
6230415M23Rik		Timm8a	E030038D23Rik
Actg2		Enah	Hbb-b1
Tdrkh		BC034054	Anxa3
Foxq1		Bxdc1	Scd2
Erdr1		Ythdf2	Cyp51
Cdh5		Adcy4	A430106D13Rik
2810423A18Rik		Egfl7	Hbb-b1
Erdr1		Twist2	8430408G22Rik
Cops5		1110007M04Rik	Haao
Tnni1		Elk3	Faah
Mthfd1		Pip5k2a	Sc4mol
C530043K16Rik		Psmb10	Cyp51
A130010C12Rik		Klhl6	Hbb-b1

PDGFR^{SKO} E10.5 and PDGFR^{SKO} E9.5	PDGFR^{SKO} E10.5 and PDGFR^{+} E9.5	PDGFR^{+} E9.5 and PDGFR^{SKO} E9.5	ALL
Tgfb1i1		Exosc6	BC046404
Rgl1		Zfp68	Itgb5
E230012J19Rik		Scfd2	Hbb-b1
Hsd11b2		Rdh10	Lrp4
Uap1		Psmb10	Hbb-b1
Wdfy1		Dtymk	Raf1
Olfml3		Bckdhb	Haao
Hsd11b2		1810058I24Rik	Hbb-b1
Arrdc3		F2rl3	Hbb-b1
Snai2		3110001N18Rik	9030625A04Rik
Apoa2		6330419J24Rik	Tcea3
Fcer1g		2310040A07Rik	Pnp
		Prps1	0610006F02Rik
		LOC232680	Per2
		BC018399	2610009E16Rik
		Hip1	Peg3
		Reln	Peg3
		Gstk1	C730046C01Rik
		6720458F09Rik	Sqle
		1110002B05Rik	Serpina1b
		Recql4	Cldn1
		LOC381932	Hbb-b1
		Ftsj3	Col6a1
		3000003F02Rik	Ldlr
		Arnt	Serpina1b
		Ccnd1	D630038D15Rik
		Rpl14	Serpina1d
		Tm4sf12	Serpina1b
		5730438N18Rik	H6pd
		Wdt3-pending	Ceecam1
		Esam1	Lox
		Cfi	Tnc
		2210409B01Rik	Lss
		Acsl1	Col6a3
		Cyp2s1	Chd3
		Nedd4l	Col1a1
		Litaf	Col16a1
		Rps6kl1	1810007E14Rik
		Cry2	Arhgef6
		Sardh	
		Mucdhl	

PDGFR^{SKO} E10.5 and PDGFR^{SKO} E9.5	PDGFR^{SKO} E10.5 and PDGFR^{+} E9.5	PDGFR^{+} E9.5 and PDGFR^{SKO} E9.5	ALL
		Irak2	
		Prodh2	
		Dcn	
		6330534C20Rik	
		2900008M13Rik	
		9630015D15Rik	
		Csf2ra	
		Dhcr24	
		Tmc4	
		Lcat	
		Cpn1	
		1110067M19Rik	
		Hist2h2aa2	
		Snf1lk	
		MGC18837	
		Aldh4a1	
		Serpinf2	
		2810441C07Rik	
		Itih3	
		Hip1r	
		Atp7a	
		D930048N14Rik	
		A930002F06Rik	
		Scotin	
		MGC18837	
		Ttyh2	
		Pappa2	
		1300013F15Rik	
		2900008M13Rik	
		Gkap1	
		LOC56628	
		2310047I15Rik	
		Akp2	
		Liph	
		F2	
		Rsn	
		Muc1	
		Tob2	
		D19Ertd144e	
		Cxadr	
		C730026J16	

PDGFR^{SKO} E10.5 and PDGFR^{SKO} E9.5	PDGFR^{SKO} E10.5 and PDGFR^{+} E9.5	PDGFR^{+} E9.5 and PDGFR^{SKO} E9.5	ALL
		Glyat	
		Mocos	
		Pip5k1a	
		Apoc1	
		Sdsl	
		Glipr1	
		Stard5	
		Siat7c	
		4933425L03Rik	
		Ethe1	
		6330505N24Rik	
		D930008G03Rik	
		1810009M01Rik	
		D630014A15Rik	
		Guca1a	
		LOC380720	
		Mt2	
		Il10rb	
		Myo1d	
		Arhgap22	
		1300019J08Rik	
		0610012D14Rik	
		BC057022	
		Acas2l	
		F2rl1	
		Myadm	
		Prodh2	
		Nr1h3	
		Hsd17b2	
		C030022K24Rik	
		Mfge8	
		Hspb1	
		Dcn	
		Fga	
		Fga	
		Eps8l3	
		Elovl6	
		Zcchc14	
		0610010D20Rik	
		Apoc1	
		Arrdc4	

PDGFR^{SKO} E10.5 and PDGFR^{SKO} E9.5	PDGFR^{SKO} E10.5 and PDGFR^{+} E9.5	PDGFR^{+} E9.5 and PDGFR^{SKO} E9.5	ALL
		4833438J18Rik	
		4930402H24Rik	
		2310016A09Rik	
		Dio3	
		Ggt1	
		Rap1ga1	
		Rsn	
		Fcgrt	
		Aldh1b1	
		9130017N09Rik	
		BC031353	
		G630016D24Rik	
		Ssb4	
		Bcas3	
		1110069O07Rik	
		1700013L23Rik	
		LOC245440	
		Tnnt3	
		Serpina10	
		Gm2a	
		Selenbp1	
		Gsn	
		A230106J09Rik	
		Selenbp2	
		Dmrta2	
		2210404O07Rik	
		Mocs1	
		Clca3	
		Lamb2	
		Prosapip1	
		2410012C07Rik	
		Clmn	
		Rec8L1	
		Hs6st1	
		Maob	
		Nr1h4	
		4930402H24Rik	
		C2	
		6330408J11Rik	
		Slc28a1	
		1110028F11Rik	

PDGFR^{SKO} E10.5 and PDGFR^{SKO} E9.5	PDGFR^{SKO} E10.5 and PDGFR^{+} E9.5	PDGFR^{+} E9.5 and PDGFR^{SKO} E9.5	ALL
		Adck4	
		Tst	
		LOC245892	
		Trf	
		Pygl	
		Nrn1	
		Serpinf1	
		BC034834	
		4930569K13Rik	
		Dcn	
		Proz	
		Plg	
		Entpd2	
		Slc21a2	
		1810006K23Rik	
		Chdh	
		Serpind1	
		Krt1-23	
		2310043N10Rik	
		Adh1	
		Mfi2	
		Slc22a6	
		AI649392	
		Slc26a1	
		1810054O13Rik	
		LOC385643	
		Rbp2	
		Mgst2	
		Snai3	
		Slc6a13	
		Fcgr3	
		Dio3as	
		LOC238463	
		Slc27a2	
		Hgd	
		Slc27a2	
		Entpd3	
		Cldn4	
		Dnajc6	
		Itih2	
		Soat1	

PDGFR^{SKO} E10.5 and PDGFR^{SKO} E9.5	PDGFR^{SKO} E10.5 and PDGFR^{+} E9.5	PDGFR^{+} E9.5 and PDGFR^{SKO} E9.5	ALL
		Kng1	
		3830431G21Rik	
		Gsta3	
		Mmd2	

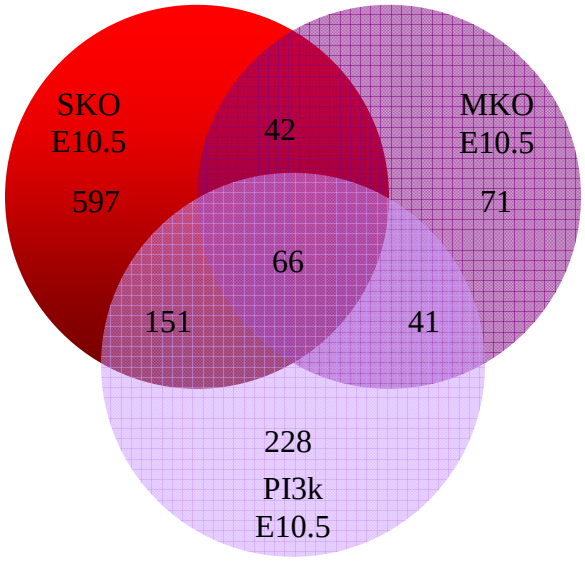

Figure 4-4. Overlapping gene expression profiles for PDGFR^{SKO}, PDGFR^{MKO}, and PDGFR^{PI3K}. (Genes compared were identified as 2 fold difference in expression from E10.5 PDGFR^{+}).

Table 4-3. Genes differentially expressed in PDGFR^{SKO} E10.5, PDGFR^{MKO} E10.5, and PDGFR^{PI3K} E10.5.

PDGFR^{SKO} and PDGFR^{MKO}	PDGFR^{SKO} and PDGFR^{PI3K}	PDGFR^{MKO} and PDGFR^{PI3K}	ALL
Targ1	Gnb4	Lgals3	Atp10d
E130112E08Rik	Gpr128	H2afz	Dhrs8
Stk4	S100a1	LOC380983	Shoc2
Hmgcs2	8430426K15Rik	LOC381292	Deadc1
4933428A15Rik	9430073N08Rik	Drbp1	Nxt2
3110023B02Rik	Emb	Bspry	2310069P03Rik
LOC245676	Kifc1	Scfd2	5730409G07Rik
4930553M18Rik	Mpst	Gng10	Idb3
3110023B02Rik	Rps19	Acy1	Adora2b
Hemp1	LOC381850	LOC211970	Hrb
Abhd3	Tpmt	Dnajc2	Cda
1110018K11Rik	Tulp2	Shmt2	2610009I02Rik
0610010F05Rik	5830467P10Rik	Acy1	Car7
Usmg5	LOC381801	1810058I24Rik	2400003B06Rik
Abcg5	Il2rg	A230098A12Rik	Vapb
Rpl30	Gfpt2	D130083G05Rik	2610042G18Rik
Atp5k	Idb2	LOC244710	1110018J18Rik
BC039632	Slc2a2	AI313915	Dhrs8
Ndufa5	5730408I21Rik	3010031K01Rik	Arpc3
Lgals9	4930471O16Rik	2310043N10Rik	1110018J18Rik
2810403A07Rik	Acad9	Cxcl7	LOC271041
Adcy6	Trappc3	D930048N14Rik	Rnase4
B230378H13Rik	Pmm2	6030458C11Rik	LOC384525
Trb	1810017F10Rik	Cldn4	Tdh
C920013G19Rik	B4galt6	G0s2	1700081H05Rik
A430106D13Rik	Ivns1abp	A530030G15Rik	BC022765
Itih4	Sfrs10	E030007N04Rik	Atbf1
Slp	Trappc3	Helz	Peg3
Anxa6	Cwf19l2	2010010M04Rik	Klf7
BC044804	Sfrs10	Chd4	Chd3
C530043K16Rik	2510048K03Rik	Iap	1810007E14Rik
P2ry14	Mbp	Iap	C730046C01Rik
E230012J19Rik	Pmm2	Slc26a1	Luc7l2
D5Ertd593e	Trappc3	Nisch	Cldn1
Wdfy1	BC016495	1300019J08Rik	9030625A04Rik
C3	S100a13	Arhgef10	1700045I19Rik
Bglap-rs1	G431001I09Rik	Rbp2	Anxa3
Srpx	C330008K14Rik	Pxmp2	Ghr

$PDGFR^{SKO}$ and $PDGFR^{MKO}$	$PDGFR^{SKO}$ and $PDGFR^{PI3K}$	$PDGFR^{MKO}$ and $PDGFR^{PI3K}$	ALL
Mrc2	2600013N14Rik	Glrx1	6720456H20Rik
Nudel-pending	Tpmt	Rpl29	Esrrb
Col9a2	Tarbp2		Cebpa
Sycn	Slc2a2		D630038D15Rik
	Hspb8		Cyp26b1
	Slc1a4		C230075M21Rik
	Etohd2		Arhgef6
	Nsdhl		Atbf1
	Ldb2		E030038D23Rik
	2210417C17Rik		Tssc8
	2810417H13Rik		Foxq1
	Zcchc3		Erdr1
	H6pd		Erdr1
	Col9a1		Pnp
	Foxa1		Serpina1d
	9530006C21Rik		Mfhas1
	Lrp4		Vtn
	Haao		Serpina1b
	Hdac5		Serpina1b
	0610006F02Rik		Serpina1b
	Per2		Ndrg1
	Gtpbp2		A130010C12Rik
	Igsf11		Lox
	4430402O11Rik		Oxr1
	Cd47		2210415K03Rik
	Leng1		Serpina1a
	Nsdhl		Col1a1
	Slc6a9		Serpina1a
	C030019I05Rik		ALL
	Nope		
	Tcea3		
	Zcchc3		
	Hbb-b1		
	Heph		
	Dact1		
	Hbb-b1		
	Usp48		
	Heph		
	Dhcr7		
	LOC381140		
	Hoxc6		

PDGFR^{SKO} and PDGFR^{MKO}	PDGFR^{SKO} and PDGFR^{PI3K}	PDGFR^{MKO} and PDGFR^{PI3K}	ALL
	Scd2		
	BC021608		
	Hbb-b1		
	Scarf2		
	Sc4mol		
	Col16a1		
	Zfp39		
	5830420C15Rik		
	Hbb-b1		
	Hbb-b1		
	Hoxc8		
	1600023A02Rik		
	Wfdc1		
	2310075G12Rik		
	5730538E15Rik		
	Smoc2		
	Nnat		
	Hmgcs1		
	1110004P15Rik		
	Bcl9l		
	Hrbl		
	Hbb-b1		
	Txnl4		
	Hbb-b1		
	Lss		
	Nnat		
	Pgam2		
	Actg2		
	Aacs		
	Zcchc3		
	Fxr2h		
	Irs1		
	AW046396		
	9130213B05Rik		
	Fkbp10		
	1600023A02Rik		
	Ntn3		
	Upk3b		
	Hbb-b1		
	Sqle		
	Hbb-b1		

$PDGFR^{SKO}$ and $PDGFR^{MKO}$	$PDGFR^{SKO}$ and $PDGFR^{PI3K}$	$PDGFR^{MKO}$ and $PDGFR^{PI3K}$	ALL
	Fbn1		
	Tnc		
	Thbs2		
	Col6a3		
	Efna5		
	9030224M15Rik		
	B130017P16Rik		
	9330186A19Rik		
	Col6a1		
	Mvd		
	Sema3b		
	1110055E19Rik		
	Col5a1		
	Col4a5		
	Rgl1		
	Hsd11b2		
	Col4a5		
	Gm22		
	Nnat		
	Ldlr		
	6720469N11Rik		
	Gm644		
	Col6a1		
	Olfml3		
	Ndrl		
	Hsd11b2		
	Arrdc3		
	9130213B05Rik		
	Pcsk9		
	Sqle		
	Fcer1g		

Table 4-4. Changes in gene regulation of matrix and cell migration genes. (Compared to wild type E10.5 yolk sacs)

E9.5 PDGFR$^{+/+}$		E10.5 PDGFR^{SKO}		E10.5 PDGFR^{MKO}		E10.5 PDGFR^{PI3K}	
Fold	Symbol	Fold	Symbol	Fold	Symbol	Fold	Symbol
2.58	Pls3	2.51	Vapb	2.83	Ipp	2.28	Arpc3
2.54	Kifc1	2.20	Arpc3	2.09	Arpc3	2.11	Mbp
2.51	Cldn5	2.15	Mbp	2.04	Vapb	2.07	Tmod3
2.48	Vapb	0.49	Hspg2	0.49	Egfl5	2.03	Pls3
2.46	Gp5	0.49	Col18a1	0.48	Ap2a1	2.01	Vapb
2.26	Msn	0.48	4933406C08 Rik	0.47	Cldn4	0.50	Emilin1
2.08	Reln	0.48	Col9a1	0.46	Catnb	0.50	Actg2
2.06	Arpc3	0.47	Itgb5	0.45	Gp5	0.43	Col3a1
2.05	Krt1-14	0.47	Epb4.9	0.43	Mrc2	0.43	Col9a1
2.01	Esam1	0.46	Myh10	0.40	Cldn1	0.43	Thbs2
0.49	Plec1	0.48	Stab2	0.40	C730046C01 Rik	0.42	Col4a5
0.49	Mucdhl	0.45	App	0.36	Col1a1	0.42	A530030G15 Rik
0.48	Hspg2	0.44	Sdc3	0.35	Notch1	0.40	1200012P04 Rik
0.47	Tgfbi	0.44	C730046C01 Rik	0.34	Col9a2	0.39	Ncam1
0.46	Hip1r	0.43	Cldn1	0.33	Tgfbi	0.36	Col6a1
0.46	Itgb5	0.42	Sdc2	0.30	Vtn	0.35	Col6a1
0.46	Pvrl1	0.41	Tro	0.30	Dst	0.35	Mrc2
0.45	Egfl5	0.40	Hspg2	0.29	Col2a1	0.34	C1qb
0.45	Muc1	0.40	Nrp	0.22	Col2a1	0.33	Col5a1
0.44	Catnb	0.40	Wasf1	0.05	Col1a2	0.29	Col6a3
0.44	Epb4.1l1	0.39	Tgfbi			0.28	Col4a6
0.43	Thbs2	0.39	Tmsb10			0.26	Diap1
0.42	Dst	0.38	Anxa3			0.25	Cldn4
0.40	Hspg2	0.38	Tpst1			0.24	Col16a1
0.40	Mfge8	0.38	Ptprb			0.20	Col1a1
0.39	Ush1c	0.38	Nrp			0.15	Spon2
0.38	Itgb5	0.38	Saa4			0.13	Col1a2
0.38	Mrc2	0.37	Col3a1			0.12	Saa4
0.34	Tnnt3	0.37	Scarf2			0.06	Col9a2
0.34	Gsn	0.36	Col16a1			0.02	Col2a1
0.34	Col5a1	0.34	Ppp1r9b			0.02	Col2a1
0.33	Col4a6	0.34	Cdh3			0.00	Tnni1
0.33	Lamb2	0.33	Egfl5				
0.31	Clmn	0.31	Gp5				

E9.5 PDGFR$^{+/+}$		E10.5 PDGFR^{SKO}		E10.5 PDGFR^{MKO}		E10.5 PDGFR^{PI3K}	
Fold	Symbol	Fold	Symbol	Fold	Symbol	Fold	Symbol
0.31	C730046C01 Rik	0.34	Wisp1				
0.31	Cldn1	0.28	Actg2				
0.30	Col6a1	0.28	Diap1				
0.29	Col6a1	0.27	Myh10				
0.28	1200012P04 Rik	0.26	Cdh5				
0.28	A530030G15 Rik	0.24	Tnni1				
0.27	Col1a2	0.23	Punc				
0.26	Col6a3	0.23	Ncam1				
0.25	Col3a1	0.23	Thbs2				
0.19	Col1a1	0.23	Col6a3				
0.16	Cldn4	0.22	Vtn				
0.15	Col16a1	0.21	Col6a1				
0.07	Col9a2	0.21	Alcam				
0.06	Vtn	0.21	Cdh3				
0.05	Saa4	0.20	Col5a2				
0.05	Col2a1	0.19	Col5a1				
0.05	Wnt9a	0.19	Col4a5				
0.04	Col2a1	0.18	Col4a6				
		0.17	Col4a5				
		0.16	Col1a2				
		0.11	Col6a1				
		0.09	Col1a1				
		0.08	Mrc2				
		0.08	Wnt9a				
		0.06	Col9a2				
		0.04	Col3a1				

Table 4-5. Changes in gene regulation of genes involved in cellular growth and survival. (Compared to wild type E10.5 yolk sacs)

E9.5 PDGFR$^{+/+}$		E10.5 PDGFR^{SKO}		E10.5 PDGFR^{MKO}		E10.5 PDGFR^{PI3K}	
Fold	Symbol	Fold	Symbol	Fold	Symbol	Fold	Symbol
2.58	Pls3	2.85	Kifc1	0.48	Polh	2.73	Kifc1
2.54	Kifc1	0.46	Myh10	0.46	Ank2	2.31	Casp7
2.30	Casp7	0.48	Mkl1	0.42	Nudel-pending	0.28	Prdx2
2.09	Hip1	0.40	Ccnd2	0.41	Bmf		
0.49	4930403J22 Rik	0.40	Wasf1	0.39	Ngfr		
0.46	Scotin	0.20	Biklk	0.25	Ccnl		
0.50	Nudel-pending	0.07	Nudel-pending				
0.48	Irak2						
0.44	Ccnl						
0.43	Biklk						
0.35	Raf1						
0.45	Rsn						
0.10	Ngfr						

Table 4-6. Changes in gene regulation of genes involved in transcription. (Compared to wild type E10.5 yolk sac)

E9.5 PDGFR$^{+/+}$		E10.5 PDGFR^{SKO}		E10.5 PDGFR^{MKO}		E10.5 PDGFR^{PI3K}	
Fold	Symbol	Fold	Symbol	Fold	Symbol	Fold	Symbol
5.6	1110018K11 Rik	2.66	Rps19	4.14	H2afz	6.28	H2afz
4.31	Sox18	2.46	Idb2	2.64	Drbp1	3.24	Drbp1
3.84	Ldb2	2.29	2210039O17 Rik	2.37	1110018K11 Rik	2.69	Rnase4
3.11	C730026E21 Rik	2.27	Hnrpk	2.21	Mist1	2.52	Zfp64
3.04	Nfe2	2.25	Sfrs10	2.20	Dnajc2	2.28	Rps19
3.02	Rps19	2.22	Zfp202	2.17	Hist1h2ab	2.23	Nr5a2
2.81	Dnmt3b	2.19	1110018K11 Rik	2.01	Rpl30	2.21	Sfrs5
2.78	Csda	2.18	Sfrs10	2.01	Mrps15	2.16	Dnajc2
2.59	Slc29a1	2.13	Tead4	2.00	2310001H12 Rik	2.15	Sfrs10
2.58	Sfrs10	2.12	Rnase4	0.49	Zfp276	2.14	Sfrs10
2.54	Hoxb2	2.12	Rpl30	0.49	Peg3	2.12	Lgtn
2.51	Eif3s6	2.1	C730026E21 Rik	0.49	Pou2f1	2.12	Sfrs5
2.51	Fli1	2.1	Eif3s6	0.48	Klf2	2.11	Npm3
2.48	Hoxb5	2.08	Ang1	0.48	Peg3	2.05	Ldb2
2.47	Csda	2.07	Polr2k	0.47	Nfat5	2.04	Skb1
2.39	Rpo1-2	2.02	G22p1	0.47	Cebpa	2.04	Rfc3
2.34	Hipk2	2.01	Tarbp2	0.46	Atbf1	2.03	Rpa2
2.32	Tarbp2	2.01	Orc4	0.46	Ank2	2	Tarbp2
2.31	Dnajc2	2	Slc25a4	0.45	Hand1	0.5	Ash1l
2.3	Sfrs10	0.5	E030006K04 Rik	0.45	Foxo3	0.49	Hoxc8
2.28	2310001H12 Rik	0.5	Ddx19	0.44	2610020C11 Rik	0.49	Hoxc6
2.27	Lyl1	0.5	E2f2	0.44	Adnp	0.49	Gtpbp2
2.27	Tead2	0.5	Rbbp2	0.43	Esrrb	0.48	Ilf2
2.27	Hmgn3	0.5	Abca7	0.42	Ank1	0.48	A930002F06 Rik
2.21	Twist2	0.49	Rbm9	0.41	D130059O18 Rik	0.48	Hdac5
2.21	Elk3	0.49	Msh3	0.41	Chd4	0.47	Trpv6
2.17	C730026E21 Rik	0.49	Ldb2	0.40	Iap	0.47	Ssa2
2.16	Skb1	0.48	Mkl1	0.38	Atbf1	0.47	Ugp2
2.13	Zfp68	0.48	Atbf1	0.37	Iap	0.47	2610016F04 Rik

E9.5 PDGFR$^{+/+}$		E10.5 PDGFR^{SKO}		E10.5 PDGFR^{MKO}		E10.5 PDGFR^{PI3K}	
Fold	Symbol	Fold	Symbol	Fold	Symbol	Fold	Symbol
2.1	3110001N18Rik	0.48	2210008I11Rik	0.37	Creb3l1	0.46	Rbm5
2.09	C79407	0.48	Foxa1	0.37	Klf7	0.46	Chd4
2.04	Eif4g2	0.47	Hdac5	0.33	Zfhx1b	0.45	Atbf1
2.04	Gata1	0.46	Peg3	0.31	Msi2h	0.45	Hmgcs1
2.03	Arnt	0.46	Klf7	0.30	Foxq1	0.45	Idb2
2.02	Rpl14	0.46	2610016F04Rik	0.30	Rora	0.44	Ppargc1a
2.01	Sfrs5	0.45	Ndn	0.25	Nr5a2	0.42	5730494J16Rik
0.5	1200002N14Rik	0.44	Notch4	0.15	C130022E19Rik	0.42	Polh
0.49	Igf2bp3	0.44	Rab1	0.01	Lars2	0.42	Fign
0.49	Nrf1	0.44	Klf2			0.41	Foxa1
0.49	Cry2	0.43	Wdr9			0.4	Hkr3
0.49	Ncoa1	0.43	Klf5			0.4	Iap
0.49	D030014N22Rik	0.42	Hkr3			0.4	Rab1
0.49	2610020C11Rik	0.41	Tcea3			0.39	Peg3
0.49	Mucdhl	0.41	Ddef1			0.38	Atbf1
0.48	Atbf1	0.4	Ankrd25			0.37	Iap
0.46	Rab1	0.4	9230112O05Rik			0.37	Esrrb
0.46	C130022E19Rik	0.39	A430091O22Rik			0.35	Rbbp2
0.46	A930002F06Rik	0.38				0.35	Peg3
0.46	Msi2h	0.38	Fign			0.34	4833412N02Rik
0.46	Foxa1	0.37	Msi2h			0.33	Zfhx1b
0.45	Wdr9	0.37	Esrrb			0.32	Txnl4
0.43	Klf7	0.37	Hoxc6			0.31	Ercc5
0.43	4933425L03Rik	0.37	Cebpa			0.31	Klf7
0.43	Fign	0.36	Zfp39			0.3	Srpr
0.43	Brca1	0.35	Atbf1			0.3	Wbscr14
0.43	Aes	0.35	Hoxc9			0.29	Fxr2h
0.42	Nr5a2	0.35	H2afy			0.29	Snai3
0.42	Ssa2	0.35	Basp1			0.28	Foxq1
0.42	2610305J24Rik	0.34	4831437C03Rik			0.26	2610020C11Rik
0.42	Bcl11b	0.33	Hoxc8			0.25	E2f2
0.41	0610012D14	0.33	Hdac7a			0.23	Cebpa

E9.5 PDGFR$^{+/+}$		E10.5 PDGFR^{SKO}		E10.5 PDGFR^{MKO}		E10.5 PDGFR^{PI3K}	
Fold	Symbol	Fold	Symbol	Fold	Symbol	Fold	Symbol
0.4	Atbf1	0.3	Txnl4			0.2	Nr1d2
0.39	Sox4	0.29	Nkx2-3			0.19	Zfp39
0.37	2210008I11Rik	0.29	C130022E19Rik			0.19	Cops5
0.36	Pou2f1	0.27	Fxr2h			0.18	Tcea3
0.35	Chd4	0.27	Sox5			0.17	2610305J24Rik
0.34	Hkr3	0.26	Foxq1			0.11	6720406L13Rik
0.34	Tcea3	0.24	Cops5			0.09	Ank1
0.32	Peg3	0.23	Pcolce			0.05	Rpl29
0.32	Peg3	0.22	Creb3l1			0.03	Foxo3
0.31	Nr1h4	0.22	Ank1				
0.29	4833412N02Rik	0.22	2610524A10Rik				
0.28	Atbf1	0.21	Zfhx1b				
0.28	Msi2h	0.21	Hand1				
0.26	H2afy	0.19	Sox4				
0.25	Sca1	0.18	2610305J24Rik				
0.23	Rora	0.17	Foxo3				
0.22	Bhlhb2	0.07	Tia1				
0.21	Snai3	0.02	Snai2				
0.2	ENPP3	0.02	Lars2				
0.16	Foxq1						
0.14	Wbscr14						
0.06	Esrrb						
0.06	Cebpa						

Table 4-7. Complete list of changes in gene regulation. (Compared to wild type E10.5 yolk sacs)

E9.5 PDGFR$^{+/+}$		E10.5 PDGFR^{SKO}		E10.5 PDGFR^{MKO}		E10.5 PDGFR^{PI3K}	
Fold	Symbol	Fold	Symbol	Fold	Symbol	Fold	Symbol
4.92	Adora2b	6.82	Atp10d	6.99	Atp10d	7.29	Atp10d
4.33	Sgk	4.22	Gnb4	2.66	Stk4	4.35	Adora2b
3.76	Prss19	4.1	Dhrs8	2.63	E130112E08 Rik	4.27	Dhrs8
3.3	Plcg2	3.99	Gpr128	2.57	Dhrs8	4.15	Gpr128
3.21	Car12	3.24	Pnliprp1	2.37	Gng10	2.96	Acy1
3.14	Prkar2b	3.02	Adora2b	2.33	Acy1	2.94	Gnb4
3.11	C730026E21 Rik	3	3110043J09R ik	2.29	Ndufb4	2.86	Gfpt2
3.05	Tulp2	2.93	Stk4	2.23	Abhd3	2.82	Mpo
2.94	Adam19	2.87	Amd2	2.19	Dusp6	2.73	Kifc1
2.85	Pdgfra	2.85	Kifc1	2.17	Shmt2	2.69	Rnase4
2.81	Dnmt3b	2.84	Mpst	2.12	Acy1	2.69	Gng10
2.81	Admr	2.76	Cdkn2a	2.10	Ndufa5	2.62	Tulp2
2.8	Ppat	2.67	Hmgcs2	2.10	Atp5k	2.58	Dhrs8
2.79	Agtrl1	2.65	Car7	2.08	Car7	2.49	Mpst
2.76	Admr	2.61	Tpmt	2.07	Tdh	2.44	Clec2
2.69	Asns	2.61	Tulp2	2.02	Ube2l6	2.43	Car7
2.68	Tdh	2.55	2400003B06 Rik	2.01	Ube2e1	2.39	B4galt6
2.58	Rab25	2.51	Il2rg	2.01	1110068E08 Rik	2.37	Pmm1
2.56	Dhrs8	2.49	Gfpt2	0.49	Ercc2	2.32	Prss19
2.53	1810009K13 Rik	2.49	2900006B13 Rik	0.48	Cyp2a12	2.31	Casp7
2.51	Igfbp2	2.41	Acad9	0.48	Phka2	2.31	Upp1
2.49	Gfpt2	2.38	Ehhadh	0.48	4833438J18R ik	2.31	Dlat
2.48	Rangnrf	2.35	Pmm2	0.48	Acas2	2.3	Tpmt
2.45	Crlf3	2.33	Dhrs8	0.48	H13	2.26	Blmh
2.42	Il2rg	2.32	Galgt2	0.48	Polh	2.25	Gng10
2.41	Tek	2.29	B4galt6	0.47	Adam23	2.24	Sgk
2.39	Rpo1-2	2.29	Serpinb1a	0.47	Man2a1	2.23	Tdh
2.36	Ripk3	2.28	Soat2	0.47	Bbox1	2.2	Acy1
2.34	Hipk2	2.24	Cyp17a1	0.46	Large	2.14	Acad9
2.3	Ccnd1	2.23	Abhd3	0.46	BC027088	2.12	Il2rg
2.3	Casp7	2.23	Bcmo1	0.44	Lox	2.12	Rangnrf
2.29	Ccnd1	2.15	Rhebl1	0.44	Hmgcs2	2.12	Ppat
2.27	Gstm6	2.15	Pmm2	0.43	Anxa6	2.1	Rdh10

E9.5 PDGFR$^{+/+}$		E10.5 PDGFR^{SKO}		E10.5 PDGFR^{MKO}		E10.5 PDGFR^{PI3K}	
Fold	Symbol	Fold	Symbol	Fold	Symbol	Fold	Symbol
2.25	Xlkd1	2.14	Abcg5	0.43	Mmp23	2.1	Ptk9
2.24	Hk2	2.12	Rnase4	0.43	9030612M13 Rik	2.07	D5Ertd33e
2.24	Pthr1	2.11	Pip5k1b	0.42	Gdi1	2.07	Plcg2
2.23	Timm8a	2.1	C730026E21 Rik	0.42	Gstm6	2.05	Pmm2
2.23	Enah	2.1	BC016495	0.42	Adcy6	2.04	Skb1
2.22	Osgepl1	2.09	Mat2a	0.42	Galgt1	2.04	Rfc3
2.22	Adcy4	2.08	Tdh	0.41	5730405I09R ik	2.04	Shmt2
2.21	Pip5k2a	2.08	Ang1	0.41	Papln	2.02	Rnf25
2.2	Bcap29	2.08	Atp5k	0.41	Chd4	2.02	Hsd17b12
2.19	Ube2l6	2.08	Fh1	0.41	ENPP3	0.5	0610012D14 Rik
2.18	Psmb10	2.07	Akr1c12	0.40	Ptprf	0.5	Prkg1
2.17	C730026E21 Rik	2.07	Polr2k	0.40	Mknk2	0.5	Rps6kl1
2.16	AA407809	2.05	Fhit	0.39	Ppp1r3c	0.49	E030007N04 Rik
2.16	Skb1	2.04	Guca2b	0.37	Ulk1	0.49	Nktr
2.16	Gstm6	2.04	Ndufa5	0.37	Aldh8a1	0.49	Pspn
2.16	Car7	2.04	Cyp3a13	0.36	Col1a1	0.49	Gtpbp2
2.13	Tfrc	2.03	Frap1	0.36	4732458O05 Rik	0.48	2810405J23R ik
2.12	Rdh10	2.03	Car12	0.35	Mmp11	0.48	Ilf2
2.12	Dctd	2.02	Tpmt	0.35	Fdps	0.48	Slc27a2
2.12	Psmb10	2.02	Cdkn2a	0.34	Hlcs	0.48	Nsdhl
2.11	Dtymk	2.02	G22p1	0.33	Zfhx1b	0.48	Hgd
2.11	Bckdhb	2.01	Rwdd2	0.33	Smpd3	0.48	Stk25
2.1	Pip5k1b	2	Slc25a4	0.32	Dapk1	0.48	Mas1
2.1	F2rl3	0.5	Mest	0.32	Arhgef10	0.48	Gpr85
2.09	Prps1	0.5	Abca7	0.29	Pnp	0.48	Hmox1
2.09	BC018399	0.49	Plk1	0.29	B4galt2	0.47	Cpn1
2.08	Arl2bp	0.49	Nsdhl	0.28	E430033B07 Rik	0.47	Mmd2
2.08	Reln	0.49	6330406L22 Rik	0.27	Cyp2a12	0.47	5730405I09R ik
2.07	Gstk1	0.49	4732458O05 Rik	0.26	Gnas	0.47	Ugp2
2.06	6720458F09 Rik	0.49	Raf1	0.23	Serpina1b	0.47	Slc27a2
2.06	Recql4	0.49	Gnaq	0.22	Serpina1d	0.47	Chst12
2.02	Ccnd1	0.48	Mmp14	0.22	Ccng2	0.47	2610016F04

E9.5 PDGFR$^{+/+}$		E10.5 PDGFR^{SKO}		E10.5 PDGFR^{MKO}		E10.5 PDGFR^{PI3K}	
Fold	Symbol	Fold	Symbol	Fold	Symbol	Fold	Symbol
2.02	Psmd13	0.48	Epor	0.22	Serpina1b	0.47	Irs1
2.01	Epor	0.48	Pemt	0.21	Faah	0.46	Lcn7
0.5	Cfi	0.48	H6pd	0.20	Bckdhb	0.46	Rdh5
0.5	Acsl1	0.48	Gpsm1	0.15	Camk4	0.46	Slc22a6
0.5	Cyp2s1	0.48	D8Ertd319e	0.15	8030402P03 Rik	0.46	Scarf2
0.5	Nedd4l	0.48	8-Sep	0.14	Mgst1	0.46	Ppap2a
0.49	Ak4	0.47	Kif23	0.14	A930030J18 Rik	0.46	Chd4
0.49	Mapk13	0.47	Hdac5	0.09	Slco1b2	0.46	0610008A10 Rik
0.49	9430043O10 Rik	0.46	0610006F02 Rik	0.05	Glrx1	0.46	Alcam
0.49	Grit	0.46	Rasa3	0.05	Col1a2	0.46	Smpd3
0.49	Rps6kl1	0.46	Pdgfa	0.02	Atp2c1	0.46	Arhgef10
0.49	Cry2	0.46	Plod2	0.01	Lars2	0.46	Serpina1b
0.49	Sardh	0.46	Fstl1			0.45	Cask
0.49	BC027088	0.46	Adam19			0.45	Atp7a
0.49	Nrk	0.45	Gtpbp2			0.45	Galgt1
0.49	Mucdhl	0.45	Rps6ka4			0.45	Rab6
0.48	Irak2	0.45	Smpd3			0.45	Hmgcs1
0.48	Prodh2	0.45	Adcy6			0.44	Nxn
0.48	Nsdhl	0.45	App			0.44	BC022133
0.48	Csf2ra	0.44	B3galt6			0.44	6030413G23 Rik
0.47	Asgr2	0.44	4631426J05R ik			0.44	Fkbp10
0.47	Dhcr24	0.44	Notch4			0.43	Adamts2
0.47	Nsdhl	0.44	Ptpn21			0.43	Dhcr7
0.47	Lcat	0.44	Dguok			0.43	Scd2
0.47	Cpn1	0.44	Rab1			0.43	Sc4mol
0.47	Pink1	0.44	Cdkl2			0.43	Prkar2b
0.47	Hsd17b12	0.44	Map4k5			0.42	5730494J16R ik
0.47	Snf1lk	0.44	Rab32			0.42	Pnp
0.47	Senp8	0.44	C730046C01 Rik			0.42	Polh
0.47	Gckr	0.43	Hspa12a			0.42	H6pd
0.47	Aldh4a1	0.43	Mod1			0.42	Itih2
0.47	Faah	0.43	V1rh1			0.42	Ndst1
0.46	Rab1	0.43	Vegfc			0.42	F13b
0.46	Serpinf2	0.43	Nsdhl			0.41	Fcgrt

E9.5 PDGFR$^{+/+}$		E10.5 PDGFR^{SKO}		E10.5 PDGFR^{MKO}		E10.5 PDGFR^{PI3K}	
Fold	Symbol	Fold	Symbol	Fold	Symbol	Fold	Symbol
0.46	2810441C07 Rik	0.43	Slc35a2			0.41	Serpina1d
0.46	Itih3	0.43	Hspa12b			0.41	Serpina1b
0.46	Atp7a	0.42	Gucy1a3			0.41	Gckr
0.46	Nktr	0.42	Sema4g			0.41	Nsdhl
0.45	C230081A13 Rik	0.42	Fgfrl1			0.41	Ghr
0.45	Akp2	0.42	Sort1			0.41	Serpina1b
0.45	Liph	0.42	Gnas			0.4	Trappc5
0.45	F2	0.41	Cxcl12			0.4	Pygl
0.45	Acadl	0.41	Slc3a1			0.4	Rab1
0.44	B4galt2	0.41	Ddef1			0.39	Atp2a3
0.44	Cxadr	0.41	P4ha2			0.39	Serpinf1
0.44	Anxa6	0.41	Efna1			0.39	Epor
0.44	Glyat	0.4	Nrp			0.39	Ncam1
0.44	Ccnl	0.4	9230112O05 Rik			0.39	Slc1a1
0.43	Pip5k1a	0.4	Ccnd2			0.39	Hspb8
0.43	Fdps	0.4	Ptp4a3			0.39	Bckdhb
0.43	Biklk	0.39	Flt1			0.38	Rab22a
0.43	Sdsl	0.39	Tgfbi			0.37	Fut10
0.43	Dhcr7	0.39	Chst12			0.37	Sqle
0.43	Mmp23	0.39	Acox2			0.37	Pgm2
0.43	Mvd	0.39	St6gal1			0.37	Esrrb
0.42	Nr5a2	0.39	Fads2			0.37	Pgam2
0.42	9630032J03 Rik	0.39	Fdps			0.36	Fcer1g
0.42	Aacs	0.39	Slc1a3			0.35	Nudt7
0.42	Hmgcs1	0.38	Anxa3			0.35	1110001A05 Rik
0.42	Gnb5	0.38	Tpst1			0.35	Sqle
0.41	Il10rb	0.38	Ptprb			0.35	Mmp11
0.41	Anxa3	0.38	Hk2			0.34	Smpdl3b
0.41	Cxcl16	0.38	Mbc2			0.34	Clca3
0.41	Dapk1	0.38	Fign			0.34	Tgfb2
0.41	Scd2	0.38	Dhcr7			0.33	Fads2
0.41	D8Ertd319e	0.37	Ghr			0.33	Serpina1a
0.41	Cyp51	0.37	Bbox1			0.33	Hsd11b2
0.41	0610012D14 Rik	0.37	Scd2			0.32	Lgals9
0.41	Fgf1	0.37	Cebpa			0.32	B4galt2
0.4	Acas2l	0.37	Siat9			0.31	Mvd

E9.5 PDGFR$^{+/+}$		E10.5 PDGFR^{SKO}		E10.5 PDGFR^{MKO}		E10.5 PDGFR^{PI3K}	
Fold	Symbol	Fold	Symbol	Fold	Symbol	Fold	Symbol
0.4	F2rl1	0.37	Scarf2			0.31	Folr2
0.4	Prodh2	0.36	Sc4mol			0.31	Mmp23
0.4	Itpka	0.36	Prkg1			0.31	Ercc5
0.4	Nr1h3	0.35	Hk1			0.31	Ldlr
0.4	Hsd17b2	0.35	Mmp2			0.31	AI838661
0.4	Faah	0.35	8430419L09 Rik			0.3	Hsd11b2
0.4	Fads2	0.35	H13			0.3	Ftcd
0.4	Sc4mol	0.34	Wisp1			0.29	Serpina1a
0.39	Ush1c	0.33	Tgfb2			0.29	Eya3
0.39	Slc13a3	0.33	Adam23			0.29	Agl
0.39	Axl	0.33	Cyp51			0.28	Prdx2
0.39	Eps8l3	0.33	Wfdc1			0.28	Rhag
0.39	Cyp51	0.33	Hdac7a			0.28	Gnb5
0.38	Elovl6	0.32	Bmp4			0.28	Ppp1r3c
0.38	Bdh	0.32	Cyp51			0.27	Slc3a1
0.38	4833438J18 Rik	0.31	Hmgcs1			0.27	Anxa6
0.38	0610038K03 Rik	0.31	Dpysl2			0.27	Atp7a
0.37	2310016A09 Rik	0.29	Pgam2			0.26	Agl
0.37	Dio3	0.29	Sbk			0.26	Adam23
0.37	Ggt1	0.29	Adamts2			0.26	4732458O05 Rik
0.37	Rps6ka4	0.28	Syngr1			0.25	Pla2g12a
0.36	Ppp1r3c	0.28	Nxn			0.24	Cxadr
0.36	Aldh1b1	0.28	Ahsg			0.24	0610006F02 Rik
0.36	9130227N12 Rik	0.28	Ppp1r3c			0.23	Rgl1
0.36	Fbp2	0.27	Irs1			0.22	Lox
0.36	Bmp1	0.26	Fkbp10			0.22	Gsta3
0.35	Raf1	0.26	1600023A02 Rik			0.21	Fxyd2
0.35	Cyp2d22	0.26	Rab22a			0.2	Nr1d2
0.35	Senp1	0.26	Anxa6			0.2	Fdps
0.35	Chd4	0.25	Ntn3			0.2	Pak1
0.35	Fdxr	0.25	Ak5			0.2	Adh1
0.34	Serpina10	0.25	Cerk			0.2	Cdkn2b
0.34	Syngr1	0.24	Mmp11			0.19	D8Ertd319e
0.34	Gsn	0.24	Sqle			0.19	Pcsk9

E9.5 PDGFR$^{+/+}$		E10.5 PDGFR^{SKO}		E10.5 PDGFR^{MKO}		E10.5 PDGFR^{PI3K}	
Fold	Symbol	Fold	Symbol	Fold	Symbol	Fold	Symbol
0.33	Clca3	0.24	Hbb-b1			0.19	Fkbp6
0.33	Lamb2	0.24	Pnp			0.18	Ccnl
0.33	Pnp	0.24	Fbn1			0.18	Atp2c1
0.33	0610006F02 Rik	0.24	Cops5			0.18	Hmbs
0.33	Cyp27a1	0.24	Tnni1			0.18	A930030J18 Rik
0.32	0610038K03 Rik	0.24	Mmp23			0.17	Camk4
0.31	Sqle	0.23	Serpina1d			0.16	Hlcs
0.31	Hs6st1	0.23	Faah			0.15	Papln
0.31	Maob	0.22	Serpina1b			0.14	Ahsg
0.31	Serpina1b	0.21	Axl			0.14	Cyp2a12
0.31	Nr1h4	0.21	Mvd			0.13	Cyp2a12
0.3	Mgat3	0.21	Alcam			0.12	9430065F12 Rik
0.3	C2	0.21	Serpina1b			0.12	Man2b1
0.3	Mmp11	0.21	Aldh8a1			0.12	Ccng2
0.3	Nr1h3	0.2	Ehd3			0.11	6720406L13 Rik
0.29	Serpina1a	0.2	Biklk			0.11	Gstm6
0.29	Tst	0.2	Serpina1b			0.11	E430033B07 Rik
0.29	Pygl	0.2	Mthfd1			0.11	Gstm6
0.29	Ldlr	0.19	Ccnd2			0.1	C3
0.29	Serpina1b	0.18	Rgl1			0.09	Esm1
0.29	Mas1	0.17	A930030J18 Rik			0.07	Faah
0.28	Serpina1d	0.17	Hsd11b2			0.07	Aldh8a1
0.28	Proz	0.17	Loxl1			0.07	Ngfr
0.28	Serpina1b	0.17	Uap1			0.06	Pnrc2
0.27	Plg	0.15	Camk4			0.04	Glrx1
0.27	H6pd	0.15	C3			0.04	Pnp
0.27	Lox	0.14	Lox			0.03	Pdgfra
0.26	Serpina1a	0.14	Ldlr			0.02	Plk1
0.26	Entpd2	0.12	Serpina1a				
0.26	Gnas	0.12	Reck				
0.26	Dhrs9	0.1	Mgst1				
0.25	Ghr	0.1	Mknk2				
0.25	Serpind1	0.08	Serpina1a				
0.24	Cxcl7	0.08	8030402P03 Rik				

E9.5 PDGFR$^{+/+}$		E10.5 PDGFR^{SKO}		E10.5 PDGFR^{MKO}		E10.5 PDGFR^{PI3K}	
Fold	Symbol	Fold	Symbol	Fold	Symbol	Fold	Symbol
0.24	Hdc	0.08	Hsd11b2				
0.24	Adh1	0.03	Pcsk9				
0.23	Trpv6	0.03	Sqle				
0.23	Rora	0.02	Lars2				
0.22	Vldlr	0.02	Fdps				
0.22	Mgst2	0	Fcer1g				
0.22	Rab22a						
0.21	Fcgr3						
0.21	Sqle						
0.2	Bbox1						
0.2	Ahsg						
0.2	ENPP3						
0.2	Abcd1						
0.2	4732458O05 Rik						
0.2	Slc27a2						
0.19	Hgd						
0.19	Slc27a2						
0.19	Slc1a1						
0.19	Ftcd						
0.18	Abhd3						
0.18	Cyp2a12						
0.17	Papln						
0.16	Entpd3						
0.16	Itih2						
0.16	8030402P03 Rik						
0.15	Gdf15						
0.15	Hgfac						
0.15	Camk4						
0.14	Cyp2a12						
0.14	Soat1						
0.13	Mgst1						
0.13	BC022133						
0.12	Wfdc1						
0.12	Fdps						
0.11	Gsta3						
0.11	Acox2						
0.11	C3						
0.08	Itih1						
0.08	Hlcs						

E9.5 PDGFR$^{+/+}$		E10.5 PDGFR^{SKO}		E10.5 PDGFR^{MKO}		E10.5 PDGFR^{PI3K}	
Fold	Symbol	Fold	Symbol	Fold	Symbol	Fold	Symbol
0.08	Mmd2						
0.07	Psmc1						
0.06	Esrrb						
0.04	Aldh8a1						
0.03	Pnp						
0.03	A930030J18 Rik						
0.02	Smpd3						

CHAPTER FIVE
Conclusions and Recommendations

Regulation of vascular development involves specific temporal and spatial expression of multiple signaling molecules for initiation, maturation, and stability of vessels. Hematopoietic and endothelial cells appear early in vascular development and have been shown to be essential for initiation and expansion of vasculature. Mural cells are also an important component of blood vessels but their function has not been clearly defined. This research demonstrated mural cells are not essential for vascular development but do play a role in vessel structure. Additionally, mesothelial cells were discovered to play an essential role in vascular remodeling through regulation of matrix composition by PDGFR signaling.

PDGFRβ signaling is essential for mural cell development

It has been suggested that vascular remodeling defects result from a lack of SMC recruitment to developing endothelial cells (Li et al. 1999; Carvalho et al. 2004; Carvalho et al. 2007). For the first time this study analyzed in vivo model systems that demonstrated PDGFRβ specific deletion leads to dramatic if not a complete decrease in SMC during vascular development without disrupting endothelial cells directly. Absence of VSMC results in remodeled but unstable vasculature determined by tortuous vessel walls. These results were not only observed in the *PDGFRβ* null embryos but also in the PDGFRβ VSMC specific deletion at early and late stages of vasculogenesis. Additionally, the specific signaling pathways leading to the SMC deletion were analyzed in signaling point mutants of PDGFRβ and determined to have a cumulative effect on the

presence of VSMC. While the tyrosine to phenylalanine point mutations on the cytoplasmic tail of the PDGFRβ eliminated activation of specific pathways there was a progressive decrease in the number VSMC that correlated to the number of signaling pathways disrupted. These results suggest the signaling pathways downstream of PDGFRβ converge to regulate specific cellular functions or the cellular functions cooperatively lead to increases in VSMC. Previous studies analyzing changes in gene expression in response to PDGFR stimulation suggest signaling pathways may converge and activate similar genes that may be translated to similar cellular functions (Fambrough et al. 1999). While these studies have contributed to the understanding of vasculogenesis, further analysis in the adult model would help define the role of VSMC in vessel stability during disease and injury.

PDGFR signaling in mesothelial cells is essential for vascular remodeling

Previous studies have demonstrated PDGFRβ plays a significant role in mural cell development. *PDGFRβ* null embryos demonstrate a dramatic decrease in VSMC/pericytes (Soriano 1994). However a few pericytes/VSMC are still present in *PDGFRβ* null embryos particularly surrounding larger vessels suggesting additional signaling pathways leading to differentiation or proliferation of these cells. Because of their similarities in downstream signaling, a candidate molecule for functional redundancy or compensation could be PDGFRα. These studies used VSMC specific gene deletion of both *PDGFRα* and *PDGFRβ* addressed this possibility and determined that the receptors function cooperatively in a precursor cell population, specifically the

mesothelium. The receptors were found to play a role in vascular remodeling prior to the recruitment of VSMC. Additionally, expression of a single receptor was sufficient to prevent lethality suggesting pathways common to both receptors are regulating vascular remodeling. Analysis of endothelial cell markers and VEGF expression was slightly upregulated in mutant yolk sacs suggesting the mesothelial cells do not inhibit proliferation or differentiation of endothelial cells. This was further supported by total yolk sac analysis of proliferation and cell survival that demonstrated no differences. Instead the mesothelial cells appear to be specifically signaling for remodeling potentially through activation of migration or cytoskeletal rearrangements. During the remodeling process, endothelial cells must migrate toward each other to redefine vessel boundaries establishing larger vessels. Endothelial cells will also become more extended to provide vessel flexibility. Mesothelial cells may aid in these processes either providing the direct signaling components for activation or indirectly by establishing the environment to facilitate these processes. The timing of PDGFR function in vasculogenesis can be analyzed by temporal and spatial specific rescue of the $PDGFR^{SKO}$ mutants. PDGFR affects vascular remodeling but it is not clear whether the receptors actively function during the remodeling stages or earlier setting up the proper environment for remodeling.

SM22 expression in mesothelial cells

While the goal of this research was to analyze the early deletion of the PDGFR using $myocardin^{cre}$ and late stage, possibly injury stage, analysis of PDGFR deletion using $SM22\text{-}Cre^{Tg}$, the mutant mice demonstrated unpredicted yet insightful results. SM22 is a cytoskeletal protein expressed in cardiac, skeletal, and smooth muscle cells

during embryogenesis and specifically in visceral and vascular smooth muscle cells into adulthood (Zhang et al. 2001). By cell tracing experiments using *SM22-Cre*^{Tg} and Rosa26Reporter LacZ it was demonstrated that the SM22 promoter is active in mesothelial cell populations prior to the differentiation of mural cells. Additional experiments not presented here using an *SM22*^{lacz} mouse line confirmed the early expression in mesothelial cells. Finally antibody specific immunohistochemistry confirmed the expression SM22 expression patterns observed by lacZ staining. It was important to use the antibody to determine that SM22 was actively expressed in mesothelial cell lines since the lacZ may not mimic the SM22 half-life and the reporter experiments additionally tag cells derived from SM22 expressing cells and do not necessarily represent active expression of SM22. Because SM22 is a cytoskeletal protein, its expression in mesothelial cells could demonstrate structural requirements essential for mesothelial function. It has been demonstrated previously that structural instability of the yolk sac is a characteristic found in mutants exhibiting vascular disruption resulting in dissociated cell layers (Dickson et al. 1995; Goumans et al. 1999; Dominguez et al. 2007).

The early mesothelial cell expression of SM22 could suggest a predetermined cell fate characteristic of precursor cells, different functions for SM22 in different cell types or developmental environments, or simply a mesothelial specific expression pattern previously uncharacterized in the yolk sac. These results suggest it is important to characterize gene expression patterns in all tissues to determine if similar cells in different environments vary in function or gene expression. Expression analysis of key

cellular markers and signaling molecules will aid in determining how which mechanisms are conserved in different tissues.

Vasculogenesis occurs throughout development in different tissues and many of the same signaling molecules involved are present in all cases. It will be interesting to see if the same holds true for the role of PDGFR in other precursor cell populations. Initial analysis to determine if other tissues/organs undergo similar vascular development would involve identification of mesothelial cell populations in tissues/organs undergoing vasculogenesis. A useful tool for this analysis would be SM22 expression to identify potential precursor or mesothelial cells. However lack of SM22 expression should not dismiss the possibility for similar mechanism because gene expression may not be identical. The mesothelium has been described in other tissues such as the gut (Wilm et al. 2005; Kawaguchi et al. 2007). Analysis of $PDGFR^{SKO}$ did not allow for exploration of vascular development in other tissue and organs due to the early lethality. To identify a role for the PDGFR in vasculogenesis of other tissues additional conditional deletion analysis can be performed using specific cre lines, such as heat inducible or tamoxifen inducible cre. In addition to analyzing the role of the PDGFR in vasculogenesis it would be interesting to compare the requirement for PDGFR in angiogenic remodeling. Retinal vasculature would be ideal for this analysis because angiogenesis occurs after birth and can be targeted directly using Adenovirus Cre. Because angiogenesis involves the dissociation of matrix to enhance vascular development, similar requirements for PDGFR signaling and matrix deposition in angiogenesis would provide great insight to the specific temporal and spatial function of specific molecules.

PDGFR signaling is essential for proper extracellular matrix composition

PDGFR signaling in mesothelial cells is essential for proper matrix composition and disruption leads to reduced EC signaling essential for vascular remodeling. Specifically collagen 1 and collagen 4 are dramatically reduced in the $PDGFR^{SKO}$ mutants. Furthermore PDGFR deletion/inhibition in vitro also leads to vascular development defects that can be rescued by the addition of collagen 4. These in vitro and in vivo studies demonstrate matrix molecules provide essential signaling for vascular development that is regulated by PDGFR signaling. Previous studies have demonstrated temporal specificity for matrix molecule expression suggesting functional specificity. Furthermore, the matrix molecule receptors have been implicated in vascular development. Analysis of integrin β1 phosphorylation demonstrated a decrease in activation in $PDGFR^{SKO}$ consistant with the decrease in collagen matrix. These PDGFR studies suggest a specific and essential role for collagen and integrin β1 in vascular remodeling. To further understand the role of collagens and integrin β1 signaling in vascular remodeling, *in vitro* stimulation experiments on endothelial cells could be analyzed for migration and cytoskeletal changes as well as changes in gene expression. It would be interesting to explore the potential vascular remodeling rescue by collagen expression. To perform this analysis a transgenic mouse would be generated to express collagens using the SM22 promoter and crossing the mice to the $PDGFR^{SKO}$. These experiments would also identify additional roles for the PDGFR in vascular remodeling if complete rescue did not occur. One caveat to these experiments is that the effects of

overexpression of collagens in vascular remodeling have not been explored and could in itself cause a phenotype.

PDGFRα and PDGFRβ cooperative function in vasculogenesis

In addition to identifying a role for PDGFR in vascular remodeling, it was interesting to determine a cooperative function for the receptors. Because both receptors are expressed in mesothelial cells in wild type yolk sacs, it can be concluded that they function cooperatively and single receptor rescue is not a compensatory role in the mutants. Pathways common to both receptors include PI3 kinase, Src, PCLγ, Shp-2, and Grb2. However preliminary analysis demonstrating remodeled yolk sac vasculature in $PDGFR^{PI3K/PI3K}$ mutants would suggest either multiple pathways play a role in vascular remodeling or at least PI3 kinase does not function alone (Data not shown). Identifying overlapping roles for the PDGF receptors is important to fully understand the roles of the receptors in development. Similar studies found cooperative function between PDGFRα and PDGFRβ specific to neural crest cells (Richarte et al. 2007). However in this system the phenotype was not rescued by expression of just one of the receptors but rather the additional loss of PDGFRβ in the PDGFRα deleted background exacerbated the phenotype.

Because only one functional allele is required for PDGFR function in vascular remodeling, it would be useful to cross the $PDGFR^{SKO}$ to the F series point mutants to rescue the phenotype. These experiments would provide *in vivo* evidence for specific pathways functions in vascular remodeling and more specifically in matrix formation. In

addition single pathway analysis can potential identify additional roles for the PDGFR in vascular remodeling. For example if matrix phenotype is rescued but remodeling remains disrupted it can be concluded that additional signaling factors are essential in vasculogenesis.

In summary, SMC are not essential for vascular remodeling but do play an essential role in vessel structure and stability. The signaling pathways downstream of the PDGFRβ each contribute to VSMC cellular function but how each pathway contributes to VSMC is still unknown. The PDGFRβ signaling point mutants are an ideal model system to analyze injury models and angiogenesis in the absence of VSMC. In contrast, PDGFR function in mesothelial cells occurs earlier in vascular development during vascular remodeling. This system not only demonstrated mesothelial cells play a role in remodeling but also identified PDGFR in regulation of this function.

APPENDIX A
Gene List for E9.5 Yolk Sac Samples

PDGFR^{+} E9.5		PDGFR^{SKO} E9.5	
Fold	Symbol	Fold	Symbol
5.597	1110018K11Rik	14.01	Abhd1
5.492	Idb3	3.388	LOC380764
4.923	Adora2b	3.15	8430426K15Rik
4.331	Sgk	3.129	Eif2s3y
4.307	Sox18	3.086	Dysf
4.298	2310069P03Rik	2.909	5730409G07Rik
3.837	Ldb2	2.888	2010309L07Rik
3.757	Prss19	2.667	Slit2
3.739	1110025G12Rik	2.62	Shoc2
3.703	Emb	2.598	Mpo
3.678	9430073N08Rik	2.493	Cdkal1
3.661	Aqp8	2.447	Cap1
3.621	LOC384525	2.438	9630025H16Rik
3.42	A430104N18Rik	2.367	3110043J09Rik
3.301	2400003B06Rik	2.307	A630034I12Rik
3.299	Plcg2	2.294	H2afz
3.211	Car12	2.275	1110014O20Rik
3.19	LOC381850	2.269	Abcb7
3.138	Prkar2b	2.251	2310037P21Rik
3.129	Rasgrp3	2.246	Pttg1
3.113	C730026E21Rik	2.242	Ncam1
3.046	Tulp2	2.242	4732462B05Rik
3.042	Nfe2	2.235	C920004C08Rik
3.016	Rps19	2.23	Mpo
2.971	S100a1	2.21	0610009J05Rik
2.94	Adam19	2.2	
2.908	Flrt3	2.176	Neurl
2.867	5830467P10Rik	2.162	4832420M10
2.847	Pdgfra	2.159	Fkbp6
2.837	A230020G22Rik	2.154	E130112E08Rik
2.823	2600013N14Rik	2.151	6430559E15Rik
2.818	6230425C21Rik	2.15	Fxyd6
2.81	Dnmt3b	2.15	Mina
2.806	Admr	2.124	C330008K14Rik
2.805	Tmc7	2.115	BC055368
2.798	Ppat	2.101	6030440P17Rik
2.796	Snurf	2.1	Hemp1
2.786	Agtrl1	2.098	D030063E12

PDGFR^{+} E9.5		PDGFR^{SKO} E9.5	
Fold	Symbol	Fold	Symbol
2.783	Csda	2.095	Nav1
2.772	Trib3	2.09	Col3a1
2.761	Admr	2.08	BC060615
2.745	Fxyd6	2.067	Hspg2
2.744	Paf53	2.064	Adamts12
2.732	Leprel1	2.058	Gnb4
2.719	2610019N19Rik	2.055	2210008I11Rik
2.694	Asns	2.044	Zfp68
2.678	Tdh	2.04	Punc
2.623	Snrpn	2.031	AU042671
2.6	A230098A12Rik	2.018	BC035291
2.589	Slc29a1	2.016	Bcat2
2.58	Rab25	2.005	Vegfc
2.579	Sfrs10	2.004	Ddef1
2.577	Pls3	2	A930008A22Rik
2.566	Rangnrf	0.5	Ythdf2
2.56	Dhrs8	0.5	Acad9
2.558	2410008B13Rik	0.499	Pygl
2.553	LOC380836	0.499	Rac3
2.539	Hoxb2	0.499	6820428D13
2.537	Kifc1	0.499	2410042D21Rik
2.529	1810009K13Rik	0.498	Hrb2
2.523	Hrb	0.498	Nudt7
2.514	Eif3s6	0.498	Ung
2.514	Igfbp2	0.497	Zcchc3
2.511	Eraf	0.497	Map17
2.508	Snrpn	0.497	Itm2a
2.506	Cldn5	0.496	Sip1
2.505	Fli1	0.493	Farp2
2.496	Gypc	0.493	Pts
2.494	Gfpt2	0.493	Olfr1371
2.488	Hspa4	0.492	Tcea3
2.485	Vapb	0.491	Hnrpk
2.484	Rangnrf	0.49	Ccne2
2.476	2610042G18Rik	0.49	1300013J15Rik
2.476	Hoxb5	0.488	Spon2
2.47	Csda	0.488	Hes6
2.456	Gp5	0.488	LOC384281
2.449	Crlf3	0.487	Rad51
2.443	6230427J02Rik	0.486	Frag1
2.44	4930553M18Rik	0.486	Rdh12

PDGFR^{+} E9.5		PDGFR^{SKO} E9.5	
Fold	Symbol	Fold	Symbol
2.439	C130078N17Rik	0.486	4930538D17Rik
2.426	Egfl7	0.485	LOC381691
2.424	1700081H05Rik	0.485	BC016495
2.423	Il2rg	0.485	AA175286
2.422	Gypa	0.484	Eif4g2
2.412	LOC380665	0.483	Rrm2
2.41	3732412D22Rik	0.483	Tpi1
2.406	Tek	0.483	2400010D15Rik
2.403	Acn9	0.483	2310061A22Rik
2.399	Mllt3	0.482	Htf9c
2.385	Rpo1-2	0.482	1700017I11Rik
2.377	Bop1	0.481	LOC224732
2.368	2810046C01Rik	0.481	Rgl1
2.364	Ripk3	0.481	Serhl
2.362	1190007I07Rik	0.48	M6pr
2.342	Hipk2	0.48	Plaur
2.333	2700083B06Rik	0.48	AA960436
2.33	Polr3g	0.479	Pga5
2.324	1110001A12Rik	0.479	LOC209281
2.324	1810022C23Rik	0.479	Snx2
2.316	Tarbp2	0.478	Cdc2l2
2.311	Spire2	0.477	4930553C05Rik
2.311	Dnajc2	0.475	Btg1
2.306	LOC381760	0.475	Hnrpk
2.305	Ccnd1	0.474	2410014A08Rik
2.305	Sfrs10	0.473	Hemgn
2.304	Ncf4	0.473	Tmem8
2.301	Phemx	0.473	Nudel-pending
2.297	LOC211970	0.472	Skb1
2.297	Casp7	0.472	Polh
2.293	Vamp5	0.472	LOC224276
2.29	Ccnd1	0.47	Bfar
2.288	Vangl1	0.469	Acad8
2.28	Magmas	0.469	Icmt
2.277	C330023M02Rik	0.468	Gp5
2.276	2310001H12Rik	0.468	Melk
2.273	Abcg5	0.467	Galns
2.272	Lyl1	0.467	Ppp2r5d
2.27	Tead2	0.466	BC025462
2.269	Deadc1	0.466	Kars
2.269	Gstm6	0.466	Decr2

PDGFR^{+} E9.5		PDGFR^{SKO} E9.5	
Fold	Symbol	Fold	Symbol
2.268	Hmgn3	0.465	
2.267	Fgd5	0.465	Lin28
2.265	Hnrpa0	0.465	2810012L14Rik
2.263	Cbln1	0.464	Agpat2
2.259	Zfp277	0.464	1810017F10Rik
2.255	Msn	0.464	Uros
2.255	Eif5a	0.462	Ubqln1
2.254	Xlkd1	0.462	AI553587
2.254	1110032E23Rik	0.461	2410003P15Rik
2.254	Adamts9	0.46	
2.252	Trappc3	0.46	Slc43a1
2.252	4631434O19Rik	0.459	2010300G19Rik
2.249	LOC271041	0.459	Haao
2.246	2010005O13Rik	0.459	LOC384538
2.245	Hk2	0.459	9430076G02Rik
2.242	5330411L03Rik	0.458	2310061I09Rik
2.24	2310037P21Rik	0.458	Slc6a4
2.239	Pthr1	0.458	Acat3
2.235	A030007L17Rik	0.458	E030030I06Rik
2.227	Timm8a	0.458	Crygn
2.226	Enah	0.457	Ube2l6
2.224	4930563C06Rik	0.456	Rab6
2.224	Abi3	0.454	Hbb-b1
2.222	Osgepl1	0.452	A230021I18Rik
2.222	BC034054	0.451	6030458C11Rik
2.221	Bxdc1	0.451	Ddx5
2.22	Ythdf2	0.451	9230112O05Rik
2.218	Adcy4	0.45	mt-Nd5
2.215	Egfl7	0.449	Cars
2.214	Twist2	0.449	E430007C11Rik
2.211	1110007M04Rik	0.449	Glipr2
2.21	Elk3	0.448	1110008H02Rik
2.207	Pip5k2a	0.448	Serpinf2
2.2	Bcap29	0.448	Rdh5
2.195	Nupl2	0.446	2810423A18Rik
2.192	Ube2l6	0.445	LOC381820
2.184	Psmb10	0.444	AI461788
2.182	Klhl6	0.443	2310003C23Rik
2.179	Stoml2	0.442	Slc39a8
2.177	Ckn1	0.441	Ftcd
2.17	Exosc6	0.44	C2

PDGFR^{+} E9.5		PDGFR^{SKO} E9.5	
Fold	Symbol	Fold	Symbol
2.169	C730026E21Rik	0.438	5230400G24Rik
2.163	AA407809	0.435	Mapk3
2.162	Skb1	0.434	
2.16	Lgals3	0.434	1700095N21Rik
2.159	Gstm6	0.434	Acad8
2.156	Car7	0.433	Sgk
2.146	Gtf3c4	0.433	Wdr4
2.14	Plvap	0.432	A730098P15
2.132	Zfp68	0.432	
2.129	Tfrc	0.429	Vcam1
2.127	Scfd2	0.429	Cdkn2b
2.126	Lin28	0.429	Tubd1
2.123	Rdh10	0.428	0610009I22Rik
2.123	Dctd	0.426	Ncoa4
2.123	C78339	0.425	Cttn
2.123	Psmb10	0.424	3830431G21Rik
2.119	M6pr	0.424	Hist1h4i
2.118	BC003236	0.424	Vasp
2.111	Dtymk	0.423	
2.107	Bckdhb	0.423	5830415F09Rik
2.107	3110023B02Rik	0.423	Rnf34
2.103	Pip5k1b	0.423	Hist1h4m
2.102	1810058I24Rik	0.422	Tssc4
2.101	F2rl3	0.42	Ipo9
2.1	3110001N18Rik	0.42	
2.096	2810417H13Rik	0.418	Sec23ip
2.096	6330419J24Rik	0.418	8430408G22Rik
2.095	1200015F23Rik	0.418	BC034507
2.095	Targ1	0.417	Ap1g1
2.095	2310040A07Rik	0.416	Mat2b
2.093	Prps1	0.416	E030024M05Rik
2.092	LOC383227	0.413	D930038J03Rik
2.092	LOC232680	0.411	Habp2
2.091	BC018399	0.411	Gin1
2.091	C79407	0.409	Srcasm
2.087	Hip1	0.407	Alg8
2.084	Arl2bp	0.405	Psmd5
2.083	Appbp1	0.403	Pdcd8
2.076	Reln	0.403	P2rx4
2.074	Cda	0.402	Cyp20a1
2.071	Sitpec	0.402	Rusc2

PDGFR^{+} E9.5		PDGFR^{SKO} E9.5	
Fold	Symbol	Fold	Symbol
2.071	Gstk1	0.401	Mcoln3
2.064	Arpc3	0.4	Sfxn2
2.064	LOC380691	0.4	1110001A23Rik
2.06	2410080P20Rik	0.399	
2.059	6720458F09Rik	0.399	5730537D05Rik
2.058	1110002B05Rik	0.398	Sec61a2
2.057	Recql4	0.398	Camp
2.055	Krt1-14	0.395	Cbx3
2.054	2610019I03Rik	0.394	Slc25a30
2.051	Trappc3	0.392	Stat1
2.047	Clec2	0.391	Hbb-b1
2.046		0.389	Tmem25
2.046	3110082I17Rik	0.388	Nt5c3
2.044	LOC381932	0.388	A930033M14Rik
2.043	Ftsj3	0.385	Arl3
2.04	Eif4g2	0.384	Apoa2
2.04	Slc2a2	0.384	Prph1
2.038	Gata1	0.384	2310042P20Rik
2.037	3000003F02Rik	0.383	Akr1c19
2.033	Blvrb	0.383	Phlda3
2.031	Arnt	0.38	Dars
2.029	Cdc45l	0.378	Hist1h4i
2.026	BC011248	0.375	4930429A08Rik
2.025	Tssc4	0.375	Pmm1
2.024	Ccnd1	0.374	Arrdc3
2.024	Rpl14	0.373	4930527B16Rik
2.023	Psmd13	0.373	1810015P03Rik
2.019	Tm4sf12	0.372	Sgk3
2.012	Epor	0.371	Erdr1
2.01	Sfrs5	0.37	Nfe2l2
2.008	5730438N18Rik	0.37	Ckap2
2.007	Wdt3-pending	0.37	Insig2
2.005	Esam1	0.368	E030022H21
2.005	G431001I09Rik	0.368	Lrrfip2
2.003	LOC244710	0.364	Neu2
0.5	Srb1	0.364	4930503L19Rik
0.5	C430041B13Rik	0.362	4930429F11Rik
0.5	Hist2h2aa1	0.361	2010004N17Rik
0.499	Cfi	0.36	Rab6
0.499	Zfyve26	0.36	BC021785
0.497	Sfmbt2	0.358	Gstm6

PDGFR^{+} E9.5		PDGFR^{SKO} E9.5	
Fold	Symbol	Fold	Symbol
0.497	5630401D06Rik	0.358	9530090G24Rik
0.497	1200002N14Rik	0.358	Spag7
0.497	2210409B01Rik	0.357	AI929863
0.496	Grina	0.357	Ddb2
0.496	Acsl1	0.356	Tera-pending
0.496	Cyp2s1	0.353	Tnni1
0.496	Nedd4l	0.351	Hist1h4a
0.496	Smad5	0.347	Hmg20a
0.496	A430070A22Rik	0.345	Glrx1
0.495	Nudel-pending	0.344	Srpr
0.495	Igf2bp3	0.343	LOC232400
0.494	4930403J22Rik	0.342	2010005E20Rik
0.494	Litaf	0.341	C920013G19Rik
0.494	Ak4	0.341	Fxyd2
0.493	Mapk13	0.338	Atf4
0.493	Abcc10	0.336	1110030E23Rik
0.493	Upk3b	0.334	Trib3
0.493	9130422H11Rik	0.333	Uap1
0.492	9430043O10Rik	0.333	Slc25a19
0.492	Mustn1	0.332	2610024N24Rik
0.492	6430567E01Rik	0.332	Plg
0.492	Leprel2	0.328	Nup54
0.491	Synpo	0.327	Nr1d2
0.49	Grit	0.326	Pnrc2
0.49	Rps6kl1	0.324	Lancl2
0.489	4832404P21Rik	0.316	Atp6v1c1
0.489	Cry2	0.315	Actc1
0.489	C030004M05Rik	0.314	Sucla2
0.489	Sardh	0.314	Wdr37
0.488	Rgpr	0.313	Fgfr1op2
0.488	Trim6	0.313	6330414G02Rik
0.488	Thsd6	0.309	Plekhf2
0.488	Asxl2	0.306	Hbb-bh1
0.487	BC027088	0.298	Olfr887
0.487	AI314180	0.297	4930427A07Rik
0.486	Nrk	0.294	Ddx58
0.485	Sema3b	0.291	Dct
0.485	Plec1	0.291	1110034A24Rik
0.485	Mucdhl	0.29	2700046G09Rik
0.485	Irak2	0.289	0610038F15Rik
0.485	A430107N12Rik	0.289	1110039B18Rik

PDGFR^{+} E9.5		PDGFR^{SKO} E9.5	
Fold	Symbol	Fold	Symbol
0.484	1110004P15Rik	0.288	Adh1
0.483	Slc12a7	0.285	Etohd2
0.481	Prodh2	0.278	Hbb-b1
0.481	2610001E17Rik	0.278	Scamp5
0.48	Oxct1	0.276	Dguok
0.48	Dcn	0.273	C1rl
0.48	6330534C20Rik	0.266	4933402B14Rik
0.48	3222402P14Rik	0.263	LOC269859
0.479	Gm22	0.261	Cdkl2
0.479	Nsdhl	0.254	Txnl4
0.479	1300010F03Rik	0.254	2400003C14Rik
0.479	Atbf1	0.252	2310010B21Rik
0.479	E030007N04Rik	0.251	2310020P08Rik
0.478	2900008M13Rik	0.246	Pak1
0.478	Cyb561	0.246	3110021A11Rik
0.477	Hspg2	0.242	Kif23
0.477	9630015D15Rik	0.237	Oxr1
0.477	E430030L01Rik	0.233	8030462N17Rik
0.476	Rhobtb1	0.231	BC024806
0.476	Csf2ra	0.229	BC033915
0.475	Fbs1	0.228	Bbs7
0.475	9430047F21Rik	0.224	Armc8
0.475	Dhcr24	0.221	G430005B15Rik
0.474	AI428936	0.219	Hmbs
0.474	Nsdhl	0.216	2810410P22Rik
0.473	Calml4	0.208	LOC243823
0.473	B2m	0.204	Srpx
0.473	BC023892	0.204	6330562C20Rik
0.473	Tmc4	0.203	Kmo
0.473	Tgfbi	0.2	Mthfd1
0.473	9330186A19Rik	0.198	Fcer1g
0.472	5830454D03Rik	0.195	Plk1
0.471	Lcat	0.185	Dct
0.471	Cpn1	0.179	Srd5a2l
0.471	1110067M19Rik	0.163	Wdfy1
0.471	Hist2h2aa2	0.162	3830402I07Rik
0.47	Chd2	0.158	C330017I15Rik
0.469	Pink1	0.151	Gjb2
0.468	2310007G05Rik	0.127	Serpina1b
0.467	Tens1	0.125	2810417H13Rik
0.467	Snf1lk	0.121	Fmo1

PDGFR^{+} E9.5		PDGFR^{SKO} E9.5	
Fold	Symbol	Fold	Symbol
0.467	D14Ertd449e	0.119	Nudt6
0.466	MGC18837	0.108	Serpina1d
0.466	Cxxc6	0.103	Serpina1b
0.465	Emp3	0.098	Serpina1b
0.465	Aldh4a1	0.087	LOC280487
0.465	A230067E15Rik	0.067	Mad
0.465	Faah	0.065	Picalm
0.465	Slc39a13	0.052	2610025M23Rik
0.465	Serpinf2	0.05	Serpina1a
0.464	2810441C07Rik	0.035	A230020G22Rik
0.464	2810403A07Rik	0.034	Fbxw5
0.464	9330107J05Rik	0.027	Serpina1a
0.463	AA175286	0.011	Zfp367
0.463	Itih3	0.007	Serhl
0.463	Hip1r	0.007	Ctsc
0.462	Etohd2	0.005	Rps13
0.461	Atp7a	0.004	2210021J22Rik
0.46	D930048N14Rik		
0.46	A930002F06Rik		
0.46	Scotin		
0.459	Itgb5		
0.458	MGC18837		
0.457	Ttyh2		
0.457	Mbl2		
0.456	Pappa2		
0.456	5730409F24Rik		
0.456	1300013F15Rik		
0.456	Foxa1		
0.455	2900008M13Rik		
0.454	Nope		
0.453	Gkap1		
0.452	B230386D16Rik		
0.451	LOC56628		
0.449	2310047I15Rik		
0.449	6030440P17Rik		
0.449	Akp2		
0.448	Liph		
0.448	F2		
0.447	Rsn		
0.447	A130070G01Rik		
0.447	Muc1		

PDGFR^{+} E9.5		PDGFR^{SKO} E9.5	
Fold	Symbol	Fold	Symbol
0.446	C430014K11Rik		
0.445	Tob2		
0.444	Catnb		
0.444	Gtl2		
0.443	D19Ertd144e		
0.443	Epb4.1l1		
0.443	C730036N12Rik		
0.442	Grcc9		
0.442	Cxadr		
0.442	Anxa6		
0.442	C730026J16		
0.44	Gtpbp2		
0.439	4930420O11Rik		
0.439	Glyat		
0.439	Susd2		
0.438	C030027H14Rik		
0.436	E130013N09Rik		
0.435	Rassf4		
0.433	Mocos		
0.433	Pip5k1a		
0.433	Thbs2		
0.432	Hist1h4h		
0.431	Apoc1		
0.431	Psap		
0.431	Abat		
0.431	Hbb-b1		
0.431	Klf7		
0.431	Fdps		
0.43	Biklk		
0.43	Sdsl		
0.43	Glipr1		
0.43	Trb		
0.43	Stard5		
0.43	2900026A02Rik		
0.429	Acy3		
0.429	Dhcr7		
0.428	Siat7c		
0.428	4933425L03Rik		
0.426	Ethe1		
0.425	Mvd		
0.425	Bcl9l		

PDGFR^{+} E9.5		PDGFR^{SKO} E9.5	
Fold	Symbol	Fold	Symbol
0.423	Plekha7		
0.423	6330505N24Rik		
0.422	Aacs		
0.422	D930008G03Rik		
0.422	1810009M01Rik		
0.42	D630014A15Rik		
0.419	Guca1a		
0.419	2700024H10Rik		
0.419	BC035947		
0.419	LOC380720		
0.418	Hmgcs1		
0.418	2900001G08Rik		
0.417	E030038D23Rik		
0.416	Mt2		
0.416	Zfp318		
0.414	Il10rb		
0.414	Hbb-b1		
0.414	Anxa3		
0.413	6430559E15Rik		
0.412	Myo1d		
0.412	Scd2		
0.411	0610009J05Rik		
0.411	Srpx		
0.411	Arhgap22		
0.41	1300019J08Rik		
0.41	Cyp51		
0.41	0610012D14Rik		
0.41	LOC381621		
0.406	BC057022		
0.406	Fgf1		
0.406	A430106D13Rik		
0.405	9130213B05Rik		
0.405	Hbb-b1		
0.405	Acas2l		
0.405	F2rl1		
0.405	8430408G22Rik		
0.404	Hspg2		
0.404	Myadm		
0.404	Mfap2		
0.403	Abcd3		
0.401	Haao		

PDGFR^{+} E9.5		PDGFR^{SKO} E9.5	
Fold	Symbol	Fold	Symbol
0.4	Prodh2		
0.4	Nr1h3		
0.399	Hsd17b2		
0.399	Atbf1		
0.399	Faah		
0.398	C030022K24Rik		
0.397	Sc4mol		
0.397	Mfge8		
0.396	9130020K20Rik		
0.395	2010309L07Rik		
0.394	Ush1c		
0.394	2900054P12Rik		
0.393	Slc13a3		
0.392	Axl		
0.391	Hspb1		
0.391	Dcn		
0.39	Fga		
0.389	Fga		
0.388	Eps8l3		
0.386	Cyp51		
0.382	Elovl6		
0.382	9430093I07Rik		
0.381	Zcchc14		
0.381	0610010D20Rik		
0.381	Apoc1		
0.38	Hbb-b1		
0.38	Arrdc4		
0.378	BC046404		
0.378	Itgb5		
0.377	4833438J18Rik		
0.376	Hrpt2		
0.376	AW046396		
0.373	Lama5		
0.373	Hbb-b1		
0.373	4930402H24Rik		
0.372	2310016A09Rik		
0.372	Dio3		
0.371	4933407C03Rik		
0.371	Ggt1		
0.37	Rap1ga1		
0.37	Lrp4		

PDGFR^{+} E9.5		PDGFR^{SKO} E9.5	
Fold	Symbol	Fold	Symbol
0.37	Hbb-b1		
0.369	Ppp1r9a		
0.367	2210008I11Rik		
0.365			
0.364	Rsn		
0.364	Fcgrt		
0.364	2010010M04Rik		
0.363	Aldh1b1		
0.362	9130017N09Rik		
0.362	BC031353		
0.361	G630016D24Rik		
0.358	6.72E+09		
0.356	Mbl1		
0.356	Fbp2		
0.355	Ssb4		
0.355	Raf1		
0.353	Bcas3		
0.352	Cyp2d22		
0.35	1110069O07Rik		
0.35	Chd4		
0.346	1700013L23Rik		
0.346	Haao		
0.345	LOC245440		
0.345	Hbb-b1		
0.344	Tnnt3		
0.344	Serpina10		
0.344	Gm2a		
0.342	Hbb-b1		
0.341	Selenbp1		
0.341	9030625A04Rik		
0.339	Tcea3		
0.339	Gsn		
0.338	A230106J09Rik		
0.337	Col5a1		
0.337	Selenbp2		
0.336	Dmrta2		
0.335	2210404O07Rik		
0.335	Col4a6		
0.335	Mocs1		
0.332	Clca3		
0.332	Lamb2		

PDGFR^{+} E9.5		PDGFR^{SKO} E9.5	
Fold	Symbol	Fold	Symbol
0.331	Pnp		
0.328	0610006F02Rik		
0.328	Heph		
0.326	Prosapip1		
0.325	2410012C07Rik		
0.324			
0.32	Per2		
0.319	2610009E16Rik		
0.319	C430014K22Rik		
0.319	Peg3		
0.316	Peg3		
0.315	Clmn		
0.315	Rec8L1		
0.314	C730046C01Rik		
0.314	Sqle		
0.314	Hs6st1		
0.313	Maob		
0.313	Helz		
0.311	Serpina1b		
0.311	Mfhas1		
0.31	Nr1h4		
0.306	Cldn1		
0.305	4930402H24Rik		
0.302	C2		
0.301			
0.3	6330408J11Rik		
0.298	Slc28a1		
0.298	Lrp2		
0.295	1110028F11Rik		
0.294	Serpina1a		
0.294	Adck4		
0.293	Tst		
0.292	LOC245892		
0.289	Trf		
0.288	Hbb-b1		
0.287	Pygl		
0.287	Col6a1		
0.287	Ldlr		
0.286	Nrn1		
0.286	Serpina1b		
0.286	1110059G02Rik		

PDGFR^{+} E9.5		PDGFR^{SKO} E9.5	
Fold	Symbol	Fold	Symbol
0.284	Serpinf1		
0.283	BC034834		
0.282	4930569K13Rik		
0.282	D630038D15Rik		
0.281	Serpina1d		
0.28	Dcn		
0.278	Proz		
0.276	Serpina1b		
0.275	Plg		
0.273	H6pd		
0.27	Ceecam1		
0.268	Lox		
0.264	Serpina1a		
0.264	Tnc		
0.263	Lss		
0.263	Entpd2		
0.263	Slc21a2		
0.261	Col6a3		
0.259	Tmem25		
0.254	1810006K23Rik		
0.251	Chdh		
0.249	Serpind1		
0.245	Krt1-23		
0.245	2310043N10Rik		
0.241	Adh1		
0.236	Mfi2		
0.233	Slc22a6		
0.233	AI649392		
0.232	Slc26a1		
0.231	1810054O13Rik		
0.226	LOC385643		
0.226	Rbp2		
0.22	Mgst2		
0.215	Snai3		
0.212	Slc6a13		
0.211	Fcgr3		
0.208	Dio3as		
0.208	Chd3		
0.2	LOC238463		
0.195	Slc27a2		
0.194	Hgd		

PDGFR^{+} E9.5		PDGFR^{SKO} E9.5	
Fold	Symbol	Fold	Symbol
0.191	Slc27a2		
0.19	Col1a1		
0.189	Ftcd		
0.165	Entpd3		
0.159	Cldn4		
0.158	Dnajc6		
0.157	Itih2		
0.153	Col16a1		
0.151	1810007E14Rik		
0.141	Soat1		
0.137	Kng1		
0.121	3830431G21Rik		
0.112	Gsta3		
0.081	Mmd2		
0.059	Cebpa		
0.049	Arhgef6		

APPENDIX B
Gene List for E10.5 Yolk Sac Samples

PDGFR^{SKO} E10.5		PDGFR^{MKO} E10.5		PDGFR^{PI3K} E10.5	
Fold	Symbol	Fold	Symbol	Fold	Symbol
6.822	Atp10d	40.351	LOC268393	7.287	Atp10d
4.218	Gnb4	6.9879	Atp10d	6.349	Lgals3
4.103	Dhrs8	5.9949	Lgals3	6.276	H2afz
4.09	Targ1	4.1442	H2afz	5.139	Nxt2
4.007	Shoc2	3.4247	5730409G07Rik	4.565	5730409G07Rik
3.989	Gpr128	3.1409	Shoc2	4.363	Shoc2
3.981	Deadc1	2.9911	2310069P03Rik	4.355	Adora2b
3.908	Nxt2	2.8654	2400003B06Rik	4.272	Dhrs8
3.327	2310069P03Rik	2.8293	Ipp	4.18	LOC380983
3.244	Pnliprp1	2.7895	LOC380983	4.151	Gpr128
3.15	S100a1	2.7854	Nxt2	3.72	2400003B06Rik
3.13	8430426K15Rik	2.7807	LOC381292	3.53	Fxyd6
3.105	E130112E08Rik	2.7597	LOC271041	3.389	D130083G05Rik
3.088	5730409G07Rik	2.7154	Deadc1	3.387	2310069P03Rik
3.077	Idb3	2.6604	Stk4	3.347	Idb3
3.019	Adora2b	2.6412	Drbp1	3.266	LOC381750
3	9430073N08Rik	2.6301	E130112E08Rik	3.244	Drbp1
3	3110043J09Rik	2.5728	Dhrs8	3.243	Ciapin1
2.976	Hrb	2.5561	Hemp1	3.201	Emb
2.965	Emb	2.5524	C330019L16	3.043	Cdkal1
2.94	Cda	2.5204	Bspry	3.037	8430426K15Rik
2.938	2610009I02Rik	2.4759	Adora2b	2.989	LOC381850
2.931	Stk4	2.4603	B930085B11Rik	2.955	Acy1
2.871	Amd2	2.417	Hdhd3	2.944	Gnb4
2.853	Kifc1	2.3975	LOC384525	2.931	
2.838	Mpst	2.387	Cda	2.908	2510048K03Rik
2.807	LOC380764	2.3745	Scfd2	2.905	A230098A12Rik
2.756	Cdkn2a	2.3741	1110018K11Rik	2.866	Cdv1
2.718	Tff3	2.3703	Gng10	2.865	4930471O16Rik
2.665	Hmgcs2	2.335	Acy1	2.864	Gfpt2
2.659	Rps19	2.3215	Cd68	2.831	Ivns1abp
2.655	Car7	2.2959	Rnase4	2.829	2610009I02Rik
2.643	LOC381850	2.2887	Ndufb4	2.823	Mpo
2.634	1810022C23Rik	2.2635	2610042G18Rik	2.805	Cda
2.634	4933428A15Rik	2.2397	LOC211970	2.782	LOC381292
2.621	Mapbpip-pending	2.2382	Abcg5	2.745	Paip1
2.609	Tpmt	2.2381	2410131K14Rik	2.733	Kifc1
2.609	Tulp2	2.2255	Abhd3	2.725	Sumf2

PDGFR^{SKO} E10.5		PDGFR^{MKO} E10.5		PDGFR^{PI3K} E10.5	
Fold	Symbol	Fold	Symbol	Fold	Symbol
2.601	5830467P10Rik	2.2222	Targ1	2.69	Rnase4
2.582	3110023B02Rik	2.2135	2610019I03Rik	2.687	Gng10
2.582	2310040A13Rik	2.2075	Mist1	2.616	Trappc3
2.554	2400003B06Rik	2.2032	Dnajc2	2.616	Tulp2
2.541	Sec15l1	2.1857	Dusp6	2.604	C230080I20Rik
2.513	LOC381801	2.1845	Cds1	2.585	Dhrs8
2.513	Il2rg	2.1841	BC039632	2.567	1810058I24Rik
2.509	Vapb	2.1759	2310037P21Rik	2.521	LOC244710
2.497	LOC245676	2.1744	Tm7sf1	2.519	Zfp64
2.489	Gfpt2	2.1738	Shmt2	2.518	Clns1a
2.485	2900006B13Rik	2.1717	4933428A15Rik	2.494	Mpst
2.485	2610042G18Rik	2.1699	Hist1h2ab	2.488	2610524H06Rik
2.476	Cidec	2.1694	1110018J18Rik	2.469	1700081H05Rik
2.461	2010309E21Rik	2.166	LOC381760	2.444	Clec2
2.458	Idb2	2.1642	Usmg5	2.438	LOC381801
2.431	Slc2a2	2.1583	3110023B02Rik	2.438	2600013N14Rik
2.424	5730408I21Rik	2.1505	LOC245676	2.436	A930005H10Rik
2.413	4930471O16Rik	2.1491	2010323F13Rik	2.433	Car7
2.412	4930553M18Rik	2.1188	Acy1	2.431	Apob
2.41	Acad9	2.1105	2410008B13Rik	2.426	9430073N08Rik
2.407	Trappc3	2.1081	1810058I24Rik	2.416	3830406C13Rik
2.379	Ehhadh	2.1036	Taf6	2.41	2810046C01Rik
2.359	Bcap29	2.0964	LOC215678	2.406	Bspry
2.345	Pmm2	2.0956	Ndufa5	2.388	B4galt6
2.345	1110018J18Rik	2.0954	Atp5k	2.367	Pmm1
2.342	BC034507	2.0883	A230098A12Rik	2.361	2610042G18Rik
2.332	Dhrs8	2.0855	Arpc3	2.344	Hemk1
2.33	Zmynd10	2.0775	Car7	2.334	LOC384525
2.319	Galgt2	2.0753	D130083G05Rik	2.319	Prss19
2.306	3110023B02Rik	2.072	Tdh	2.314	S100a1
2.303	5033406O09Rik	2.0651	0610010F05Rik	2.31	Casp7
2.303	1810017F10Rik	2.0639	Idb3	2.306	Upp1
2.296	2510004L01Rik	2.0596	Hrb	2.305	Dlat
2.295	2210039O17Rik	2.045	Vapb	2.304	Tpmt
2.289	B4galt6	2.0447	4930553M18Rik	2.284	C330008K14Rik
2.285	Serpinb1a	2.0288	BC038311	2.284	Deadc1
2.283	Soat2	2.0288	1700081H05Rik	2.282	Trappc3
2.282	Ivns1abp	2.0266	Zfp277	2.282	Rps19
2.274	Hnrpk	2.0192	Ube2l6	2.279	Arpc3
2.271	Calml4	2.0144	LOC244710	2.263	Blmh
2.257	Hemp1	2.013	Rpl30	2.262	Appbp1

PDGFR^{SKO} E10.5		PDGFR^{MKO} E10.5		PDGFR^{PI3K} E10.5	
Fold	Symbol	Fold	Symbol	Fold	Symbol
2.246	Sfrs10	2.0124	Pthr1	2.252	Gng10
2.244	Trappc3	2.0123	Ube2e1	2.245	Prss35
2.242	Cyp17a1	2.0117	Mrps15	2.241	Sgk
2.235	Cwf19l2	2.0081	1110068E08Rik	2.239	Slc2a2
2.227	Abhd3	2.0059	2610009I02Rik	2.234	Slc25a12
2.227	Bcmo1	2.0028	2310001H12Rik	2.23	2010005O13Rik
2.225	Twistnb	0.499	BC035947	2.227	Nr5a2
2.217	Zfp202	0.4978	BC044804	2.227	Tdh
2.203		0.4976	Tulp4	2.213	1810015C11Rik
2.197	Arpc3	0.4971	AI313915	2.212	1110018J18Rik
2.192	1110018K11Rik	0.497	1700020I14Rik	2.21	Sfrs5
2.191	LOC241051	0.4957	D230050J18Rik	2.209	Daf1
2.183	0610010F05Rik	0.4936	4921518A06Rik	2.201	S100a16
2.182	Sfrs10	0.4934	Ercc2	2.197	6330419J24Rik
2.178	LOC383131	0.493	Chd3	2.197	Acy1
2.165	2510048K03Rik	0.4923	D930008G03Rik	2.189	Cap1
2.162	1110018J18Rik	0.4915	Rhobtb1	2.186	AI480653
2.16	Usmg5	0.4909	LOC386192	2.177	Scfd2
2.151	Rhebl1	0.4906	3010031K01Rik	2.17	Emd
2.15	Mbp	0.4904	2310043N10Rik	2.162	Dnajc2
2.148	Pmm2	0.4895	Peg3	2.162	Acbd4
2.142	1700019N12Rik	0.4891	Pou2f1	2.153	Sfrs10
2.14	LOC271041	0.4876	Itih4	2.153	Gadd45gip1
2.136	Abcg5	0.485	Zcchc14	2.152	BC016495
2.135	Tead4	0.4835	Cxcl7	2.143	LOC271041
2.127	2410004F06Rik	0.4831	Imap38	2.142	5730408I21Rik
2.122	Rnase4	0.4831	4930527B16Rik	2.14	Acad9
2.122	Rpl30	0.4827		2.139	Cdc45l
2.114	Ncf4	0.4815	4833438J18Rik	2.139	LOC211970
2.11	2610024E20Rik	0.4814	Acas2	2.139	2310035C23Rik
2.11	Pip5k1b	0.4796	Gs2na-pending	2.136	Sfrs10
2.109	LOC381066	0.4793	Npc1	2.129	Ciapin1
2.102	Trappc3	0.4787	Peg3	2.128	LOC382162
2.1	C730026E21Rik	0.4784	Gkap1	2.126	Hnrpa0
2.099	BC016495	0.4783	D930048N14Rik	2.124	Lgtn
2.097	Eif3s6	0.4755	D5Ertd593e	2.123	Il2rg
2.092	Rnf34	0.4742	6030458C11Rik	2.121	Sfrs5
2.09	Sh3bgrl2	0.474	Ndrg1	2.119	Rangnrf
2.089	LOC384525	0.474	2210404O07Rik	2.119	Ppat
2.087	Mat2a	0.4733	AI316807	2.115	Mbp
2.08	Tdh	0.4721	Nfat5	2.109	C330027I04Rik

PDGFR^{SKO} E10.5		PDGFR^{MKO} E10.5		PDGFR^{PI3K} E10.5	
Fold	Symbol	Fold	Symbol	Fold	Symbol
2.08	Ang1	0.4688	Cldn4	2.109	Npm3
2.077	Atp5k	0.4686	Man2a1	2.101	Rdh10
2.076	Fh1	0.4681	E030038D23Rik	2.099	D4Ertd765e
2.075	S100a13	0.4678	9030625A04Rik	2.097	2810408I11Rik
2.072	Gpr39	0.4675	3632413B07Rik	2.097	Ptk9
2.07	Akr1c12	0.4669	Cyp26b1	2.093	L259
2.069	Zdhhc13	0.4662	Cebpa	2.083	LOC381681
2.068	Polr2k	0.4657	G0s2	2.079	1110017O10Rik
2.067	G431001I09Rik	0.4653	Bglap-rs1	2.077	Hrb
2.067	3300005D01Rik	0.4652	Srpx	2.076	Magmas
2.064	C330008K14Rik	0.4649	Oxr1	2.076	Rohn
2.054	BC039632	0.4645	BC022765	2.075	Tmod3
2.048	1600014K23Rik	0.4608	A530030G15Rik	2.073	D5Ertd33e
2.047	Fhit	0.4607	Atbf1	2.069	Plcg2
2.044	Pdlim4	0.4583	BC027088	2.068	LOC226135
2.043	D330023A14Rik	0.4582	2210415K03Rik	2.067	Sec23b
2.042	Guca2b	0.458	Catnb	2.057	Snapc3
2.04	Slc39a8	0.458	E030007N04Rik	2.055	Gpr124
2.039	Ndufa5	0.4575	2310047L21Rik	2.049	Tm4sf12
2.037	Cyp3a13	0.4574	Helz	2.049	S100a13
2.032	Frap1	0.4555	C530043K16Rik	2.046	Ldb2
2.029	1700081H05Rik	0.4516	A130070G01Rik	2.045	Pmm2
2.028	Car12	0.4504	B230378H13Rik	2.045	Skb1
2.024	C630041L24Rik	0.4492	Akr1c19	2.042	Rfc3
2.019	Rbm4	0.4487	C430041B13Rik	2.039	Slc30a2
2.019	Mtch2	0.4436	LOC237436	2.036	LOC218805
2.018	LOC214738	0.4409	C730036N12Rik	2.036	Shmt2
2.017	2600013N14Rik	0.4403	Mfhas1	2.034	Rpa2
2.017	Tpmt	0.4402	Lox	2.033	5830467P10Rik
2.017	Cdkn2a	0.44	2810403A07Rik	2.029	Pls3
2.015	G22p1	0.4399	6720456H20Rik	2.027	1110018J18Rik
2.015	Zfyve16	0.4393	Itgb4	2.023	0610009I22Rik
2.014	Tarbp2	0.4392	Hmgcs2	2.019	Rnf25
2.014	Rwdd2	0.436	Adnp	2.019	Hsd17b12
2.011	Orc4	0.435	Anxa6	2.017	Cwf19l2
2.003	Slc25a4	0.4346	Mrc2	2.012	Vapb
2.002	1110034G24Rik	0.4324	Esrrb	2.012	G431001I09Rik
2.002	Slc2a2	0.4281	Trb	2.01	C330027I04Rik
2.001	4930405D11Rik	0.4236	2010010M04Rik	2.009	LOC381683
2	Lasp1	0.4196	Nudel-pending	2.007	Stoml2
0.5	D14Abb1e	0.4188	2010300G19Rik	2.003	Tarbp2

PDGFR^{SKO} E10.5		PDGFR^{MKO} E10.5		PDGFR^{PI3K} E10.5	
Fold	Symbol	Fold	Symbol	Fold	Symbol
0.5	E030006K04Rik	0.4162	Adcy6	0.5	Ash1l
0.499	A930004J17Rik	0.4156	C230075M21Rik	0.499	Fer1l3
0.499	Hspb8	0.4152	A430106D13Rik	0.499	5330401F18Rik
0.499	Sepn1	0.4106	Papln	0.499	0610012D14Rik
0.499	Ddx19	0.4071	Chd4	0.499	6720456H20Rik
0.498	1110062M06Rik	0.4065	2010309L07Rik	0.499	2010007K12Rik
0.498	9530053J19Rik	0.4038	Cldn1	0.498	Lrp4
0.498	Mest	0.4027	D630038D15Rik	0.497	Sema3b
0.498	Slc39a13	0.3984	Anxa3	0.497	Stoml1
0.497	Ppfia1	0.3969	Iap	0.497	Emilin1
0.497	Ifitm2	0.3953	C730046C01Rik	0.497	Rps6kl1
0.497	AI173486	0.3886	Lgals9	0.496	Actg2
0.497	3110078M01Rik	0.3815	Arhgef6	0.496	4432404P07Rik
0.496	E2f2	0.3809	9130020K20Rik	0.495	Glipr1
0.495	Rbbp2	0.3732	Iap	0.495	Abcd3
0.495	Abca7	0.3718	Slc26a1	0.495	E030007N04Rik
0.495	1810045K06Rik	0.3709	Ulk1	0.494	Gtl2
0.494	Myl9	0.3676	Nisch	0.494	Zcchc3
0.494	Hspg2	0.3652	Klf7	0.494	Hoxc8
0.494	Rbm9	0.3641	C920013G19Rik	0.493	Nope
0.494	Slc1a4	0.3618	1300019J08Rik	0.493	4430402O11Rik
0.494	9130229H14Rik	0.36	Sycn	0.491	2510042H12Rik
0.493	Msh3	0.3562	Col1a1	0.491	Ntn3
0.493	Etohd2	0.3543	E230012J19Rik	0.49	Hoxc6
0.493	Mmrn2	0.3525	Luc7l2	0.49	Rgpr
0.492		0.3511	Tssc8	0.49	2210417C17Rik
0.491	Plk1	0.3509	1700045I19Rik	0.49	2410001C21Rik
0.49	Nsdhl	0.3438	P2ry14	0.488	Cyp26b1
0.49	Stxbp1	0.3385	Col9a2	0.488	1110059G02Rik
0.489	D930010J01Rik	0.336	Ghr	0.485	Gtpbp2
0.489	Ldb2	0.3333	Hpxn	0.485	2810405J23Rik
0.489	2810046M22Rik	0.328	Plekhf2	0.485	Nisch
0.487	BC022765	0.3265	Erdr1	0.484	Trp53bp2
0.487	6330406L22Rik	0.321	Arhgef10	0.484	Slc27a2
0.486	Dock11	0.3081	Krt1-23	0.484	A930002F06Rik
0.486	4732458O05Rik	0.2995	Foxq1	0.484	Nsdhl
0.486	Antxr2	0.2973	Vtn	0.484	9430093I07Rik
0.486	Col18a1	0.2945	Pnp	0.482	Hgd
0.486	Raf1	0.2935	Slp	0.482	Stk25
0.486	Gnaq	0.2889	Col2a1	0.482	2010002H18Rik
0.486	Vwf	0.2862	A130010C12Rik	0.482	1700034P13Rik

PDGFR^{SKO} E10.5		PDGFR^{MKO} E10.5		PDGFR^{PI3K} E10.5	
Fold	Symbol	Fold	Symbol	Fold	Symbol
0.486	Krt1-14	0.284	E430033B07Rik	0.481	Aacs
0.486	Lgals9	0.2765	Erdr1	0.481	LOC268350
0.485	2210417C17Rik	0.2719	1810007E14Rik	0.48	Gpr85
0.485	2310014H01Rik	0.2398	Serpina1b	0.479	2700024H10Rik
0.485	2810403A07Rik	0.2344	C3	0.478	Hdac5
0.484	Top2b	0.2279	Serpina1b	0.477	Dio3as
0.484	2810417H13Rik	0.2225	Serpina1d	0.477	Alg8
0.483	Mmp14	0.2168	Serpina1b	0.477	Hmox1
0.483	Epor	0.1901	Rbp2	0.476	Leng1
0.483	Zcchc3	0.1528	Serpina1a	0.476	Slc6a9
0.483	Stab2	0.1284	Wdfy1	0.475	Slc6a4
0.482	4933406C08Rik	0.1129	Pxmp2	0.474	Treml1
0.482	Mfap2	0.0518	Glrx1	0.474	9430002A10Rik
0.482	Mkl1	0.0309	Rpl29	0.473	Cpn1
0.482	Pemt			0.472	Slc4a1
0.481	1110014O20Rik			0.472	Mmd2
0.48	H6pd			0.472	5830407P18Rik
0.48	Col9a1			0.472	Mustn1
0.48	Atbf1			0.472	Ugp2
0.479	2310047C04Rik			0.47	Smoc2
0.479	2210008I11Rik			0.47	Selenbp1
0.478	A330081F11Rik			0.469	Mrps27
0.478	D930001I22Rik			0.468	B930044G13Rik
0.478	2210417D09Rik			0.467	Slc27a2
0.477	Gpsm1			0.467	Tssc8
0.477	Ifitm2			0.466	BC017643
0.477	Icam4			0.466	Helz
0.477	Foxa1			0.466	9330186A19Rik
0.476	D8Ertd319e			0.465	C230043G09Rik
0.476	9-Sep			0.465	Irs1
0.475	9530006C21Rik			0.465	Lcn7
0.475	5730406F04Rik			0.464	Rdh5
0.475	A130022F02Rik			0.464	Slc22a6
0.474	Kif23			0.463	Scarf2
0.473	Itgb5			0.463	Ppap2a
0.473	Lrp4			0.462	Rbm5
0.473	Mfap2			0.462	Chd4
0.472	B130052G07Rik			0.461	0610008A10Rik
0.472	4930545L23Rik			0.459	G0s2
0.472	Epb4.9			0.457	D930048N14Rik
0.471	Haao			0.456	Arhgef10

PDGFR^{SKO} E10.5		PDGFR^{MKO} E10.5		PDGFR^{PI3K} E10.5	
Fold	Symbol	Fold	Symbol	Fold	Symbol
0.471	Xylb			0.455	Serpina1b
0.469	F730017E11Rik			0.455	Efna5
0.468	Prnp			0.455	Usp48
0.467	9130415E20Rik			0.454	Atbf1
0.466	Plxnb1			0.454	5830420C15Rik
0.466	Socs3			0.453	5830407P18Rik
0.466	Gig1			0.453	1600023A02Rik
0.466	Hdac5			0.452	1600023A02Rik
0.465	4933439C20Rik			0.452	Dact1
0.464	0610006F02Rik			0.451	A730008H23
0.464	AI839920			0.45	1110004P15Rik
0.463	Nrp			0.449	LOC385643
0.463	Rasl12			0.449	Ccrn4l
0.463	Rasa3			0.449	Rab6
0.462	Whsc1l1			0.447	Hrbl
0.462	Peg3			0.447	Hmgcs1
0.462	C030025P15Rik			0.446	1190028F09
0.462	Myh10			0.446	6430544H17Rik
0.462	Rnf125			0.445	Idb2
0.462	2700049H19Rik			0.445	Pfc
0.462	Pdgfa			0.444	Ntn3
0.461	D15Mit260			0.441	Villp
0.461	Klf7			0.441	Glt25d1
0.461	Plod2			0.44	1190012C08Rik
0.461	Per2			0.439	BC022133
0.461				0.438	Gm644
0.459	Fstl1			0.438	Selenbp2
0.456	LOC382050			0.436	Fkbp10
0.456	Adam19			0.436	Bcas3
0.455	2610016F04Rik			0.436	Scoc
0.454	Pitpnm1			0.435	0610009B14Rik
0.453	BC046404			0.434	Fbn1
0.453				0.434	Cxcl7
0.453	B230104P22Rik			0.431	Col9a1
0.453	2700033B16Rik			0.43	Dhcr7
0.452	B930075F07			0.43	BC022765
0.452	Kcnn4			0.428	2010010M04Rik
0.452	Lims2			0.428	Ubc
0.452	Gtpbp2			0.428	Scd2
0.451	5730421K10Rik			0.428	2210415K03Rik
0.451	Chd3			0.427	Haao

PDGFR^{SKO} E10.5		PDGFR^{MKO} E10.5		PDGFR^{PI3K} E10.5	
Fold	Symbol	Fold	Symbol	Fold	Symbol
0.45	Tm9sf2			0.426	
0.45	Igsf11			0.426	Sc4mol
0.45				0.426	Thbs2
0.45	Phlda3			0.426	Nnat
0.449	Leprel2			0.425	Apoc1
0.449	1110003A17Rik			0.425	Prkar2b
0.449	Ndn			0.425	6030458C11Rik
0.449	A530083M17Rik			0.424	LOC238463
0.449	A430073A17Rik			0.423	5730494J16Rik
0.448	Rps6ka4			0.423	Erdr1
0.448	BC019731			0.421	Pnp
0.448	LOC381138			0.42	Col4a5
0.448	Smpd3			0.419	H6pd
0.448	B130066H02Rik			0.419	1700013L23Rik
0.448	D6Ertd253e			0.418	1810023B24Rik
0.448	Adcy6			0.418	Itih2
0.447	App			0.417	E030038D23Rik
0.446	4430402O11Rik			0.417	A530030G15Rik
0.445	Dpf3			0.416	F13b
0.445	Emp3			0.416	Haao
0.444	6230427J02Rik			0.415	Nrn1
0.444	B130020A07Rik			0.415	Ttc17
0.443	E130206E21Rik			0.415	Gm22
0.443	Sdc3			0.413	Fcgrt
0.443	B3galt6			0.413	Slc1a4
0.442	Mid1ip1			0.413	Serpina1d
0.442	C030005I21Rik			0.412	Alg8
0.442	4631426J05Rik			0.412	BC057022
0.441	Notch4			0.412	Serpina1b
0.441	B230378H13Rik			0.412	Ndrl
0.44	Ptpn21			0.411	1810045K07Rik
0.44	4933407L23Rik			0.411	Mfhas1
0.439	Dguok			0.409	Foxa1
0.439	Rab1			0.408	Nsdhl
0.438	9530029F08Rik			0.408	Igsf11
0.438	Cdkl2			0.408	3010031K01Rik
0.437	1810007E14Rik			0.408	Ghr
0.437	Cd47			0.407	Serpina1b
0.437	Klf2			0.405	
0.436	Map4k5			0.404	Acas2l
0.436	Rab32			0.403	LOC381591

PDGFR^{SKO} E10.5		PDGFR^{MKO} E10.5		PDGFR^{PI3K} E10.5	
Fold	Symbol	Fold	Symbol	Fold	Symbol
0.436	C730046C01Rik			0.403	Erdr1
0.435	6720407G21Rik			0.402	Wfdc1
0.435	Pop4			0.402	B130017P16Rik
0.434	Trb			0.401	B130008O17Rik
0.434	Luc7l2			0.4	Bcl9l
0.433	LOC215996			0.399	Anxa3
0.433	Cldn1			0.399	C030019I05Rik
0.433	9430065F12Rik			0.398	Iap
0.433	9930104M19Rik			0.397	1190002F15Rik
0.432	Hspa12a			0.397	Etohd2
0.431	Wdr9			0.396	Pygl
0.431	Mod1			0.395	C730046C01Rik
0.43	V1rh1			0.393	Dhrsx
0.429	Leng1			0.393	Per2
0.429	Vegfc			0.392	Lss
0.429	Klf5			0.391	Serpinf1
0.428	A130092J06Rik			0.391	Oxr1
0.427	Nsdhl			0.39	Slc1a1
0.427	Crim1			0.388	1110055E19Rik
0.426	Slc35a2			0.388	Hspb8
0.425	D7Ertd791e			0.387	C230075M21Rik
0.425	Hspa12b			0.386	9030224M15Rik
0.425	0610009J05Rik			0.386	Luc7l2
0.423	D230021E06Rik			0.385	Peg3
0.423	A930034L06Rik			0.384	1810054O13Rik
0.423	Colec11			0.384	9130213B05Rik
0.423	Slc35d1			0.382	Fabp3
0.422	Slc6a9			0.382	2310043N10Rik
0.422	D630004K10Rik			0.381	LOC381140
0.421	B130020M22Rik			0.381	Upk3b
0.421	Gucy1a3			0.379	Apoc1
0.421	Amotl1			0.377	LOC245440
0.42	C030019I05Rik			0.377	Gas7
0.42	Sema4g			0.375	Map17
0.42	Abi3			0.375	6330415F13Rik
0.419	Fgfrl1			0.374	5830454D03Rik
0.419	Sort1			0.373	Iap
0.418	AW124722			0.371	Siat7c
0.418	Zfp236			0.371	Sqle
0.418	2610001E17Rik			0.371	Heph
0.418	Sdc2			0.37	Pgm2

PDGFR^{SKO} E10.5		PDGFR^{MKO} E10.5		PDGFR^{PI3K} E10.5	
Fold	Symbol	Fold	Symbol	Fold	Symbol
0.418	Nope			0.369	BC031407
0.417	2610312F20Rik			0.369	Esrrb
0.416	Gnas			0.368	Pgam2
0.416	Ceecam1			0.367	1810007E14Rik
0.416	Usp54			0.364	Fcer1g
0.416	Hkr3			0.361	
0.416	D14Ertd231e			0.359	Trib3
0.415	Pdcd6ip			0.359	9530006C21Rik
0.415	Tmc6			0.357	Col6a1
0.415	E530020K13Rik			0.357	D630038D15Rik
0.414	Tcea3			0.356	Srd5a2l
0.414	4933411D12Rik			0.356	1300006C19Rik
0.413	Cxcl12			0.355	Slc6a13
0.412	Zcchc3			0.354	Ndrg1
0.411	2600011C06Rik			0.353	Col6a1
0.411	Slc3a1			0.35	Peg3
0.41	9030625A04Rik			0.35	Sqle
0.41	Tro			0.348	Flnb
0.41	Hbb-b1			0.346	Kng1
0.409	Heph			0.342	Smpdl3b
0.409	C920013G19Rik			0.34	Clca3
0.409	Ddef1			0.338	Olfml3
0.408	2610009E16Rik			0.336	1300019J08Rik
0.408	9030607L20Rik			0.335	Col5a1
0.408	L3mbtl3			0.334	9030625A04Rik
0.407	A230050P20Rik			0.334	2610002D18Rik
0.406	P4ha2			0.333	Sgcd
0.406	Btg1			0.33	Cd47
0.405	LOC98434			0.327	Serpina1a
0.405	Efna1			0.326	1810017F10Rik
0.405	A830083H19Rik			0.326	Hsd11b2
0.404	Hspg2			0.323	Txnl4
0.404	LOC382215			0.314	Mvd
0.404	Braf			0.313	6720469N11Rik
0.404	Ankrd25			0.313	AW046396
0.404	Fnbp1			0.31	Ldlr
0.403	A830085I22Rik			0.31	2310075G12Rik
0.403	Nrp			0.31	AI838661
0.402	9230112O05Rik			0.309	Klf7
0.402	Ccnd2			0.303	Srpr
0.401	Hemgn			0.302	Hsd11b2

PDGFR^{SKO} E10.5		PDGFR^{MKO} E10.5		PDGFR^{PI3K} E10.5	
Fold	Symbol	Fold	Symbol	Fold	Symbol
0.401	9430029L20Rik			0.302	2700046G09Rik
0.401	Syt11			0.298	Drctnnb1a
0.4	Wasf1			0.296	Tex19
0.399	2310047A01Rik			0.295	Ftcd
0.399	2410146L05Rik			0.293	2610018I03Rik
0.399	C430014K11Rik			0.293	Serpina1a
0.398	Ptp4a3			0.29	A130010C12Rik
0.398	Plvap			0.29	Eya3
0.398	A430106D13Rik			0.289	Agl
0.398	Awp1-pending			0.286	Fxr2h
0.397	1700045I19Rik			0.286	Snai3
0.396	Popdc2			0.286	Bst2
0.395	Mxd3			0.285	Gtpbp2
0.395	BC013481			0.285	Col6a3
0.395	Flt1			0.284	1110028F11Rik
0.395	Tgfbi			0.283	Tnc
0.394	Chst12			0.28	Foxq1
0.394	5830406C17Rik			0.28	Prdx2
0.394	Dact1			0.279	Chd3
0.394	Acox2			0.277	Eva1
0.393	St6gal1			0.27	Timd2
0.391	A130067E09Rik			0.267	Atp7a
0.391	Fads2			0.267	AI313915
0.39	Etnk2			0.266	BC021608
0.389	4832408C21Rik			0.264	Agl
0.389	2700031B12Rik			0.258	2810417H13Rik
0.389	Gypc			0.257	5730538E15Rik
0.389	Hbb-b1			0.254	Pla2g12a
0.388	BC014699			0.249	Rbp2
0.388	A430091O22Rik			0.246	Cldn4
0.388	Slc39a9			0.242	Cldn1
0.388	Nol3			0.242	Col16a1
0.387	Fdps			0.241	Cxadr
0.386	Tmsb10			0.24	1110063F24Rik
0.386	Olfr887			0.239	2410012C07Rik
0.385	Slc1a3			0.238	0610006F02Rik
0.384	1810073H04Rik			0.235	BC034834
0.384	Pum1			0.229	Rgl1
0.384	Usp48			0.229	Slc26a1
0.384	Kcnk1			0.227	Cebpa
0.383	A630076E03Rik			0.225	Hbb-b1

PDGFR^{SKO} E10.5		PDGFR^{MKO} E10.5		PDGFR^{PI3K} E10.5	
Fold	Symbol	Fold	Symbol	Fold	Symbol
0.383	Anxa3			0.221	Lox
0.383	5830427D02Rik			0.221	Rhoe
0.382	Tpst1			0.22	Gsta3
0.382	4930572L20Rik			0.218	Thap4
0.382	Ptprb			0.216	4833421E05Rik
0.382	Heph			0.213	Fxyd2
0.382	C130080N23Rik			0.211	Vtn
0.381	Nrp			0.209	2210012G02Rik
0.381	Hmgcr			0.198	Adh1
0.381	LOC218877			0.197	Hbb-b1
0.381	6030411F23Rik			0.196	Col1a1
0.381	Itih4			0.195	Hbb-b1
0.38	Hk2			0.194	Zfp39
0.379	AI850995			0.19	Pcsk9
0.379	BC021381			0.185	Hbb-b1
0.378	Ece1			0.184	Hbb-b1
0.378	Mbc2			0.181	Arhgef6
0.377	AW536289			0.179	Tcea3
0.376	E030003O11Rik			0.179	Hmbs
0.376	Msi2h			0.175	Hbb-b1
0.376	Hhip			0.16	1110067L22Rik
0.375	2310075E07Rik			0.159	Hbb-b1
0.375	Fign			0.154	Spon2
0.375	Saa4			0.142	1700045I19Rik
0.375	Lpin2			0.132	Hbb-b1
0.375	Islr			0.131	Ipo9
0.375	Dhcr7			0.123	Man2b1
0.374	Ghr			0.117	Arrdc3
0.374	Bbox1			0.104	Pxmp2
0.374	6330562C20Rik			0.05	Rpl29
0.374	Msi2h			0.049	Cops8
0.374	6720456H20Rik			0.044	Glrx1
0.373	LOC381140			0.028	Apoc2
0.373	Esrrb				
0.373	D4Ertd681e				
0.372	E330018D03Rik				
0.372	Chrd				
0.372	Lgi2				
0.371	Stim1				
0.371	B230373P09Rik				
0.37	Copz2				

PDGFR^{SKO} E10.5		PDGFR^{MKO} E10.5		PDGFR^{PI3K} E10.5	
Fold	Symbol	Fold	Symbol	Fold	Symbol
0.37	Hoxc6				
0.37	MAp19				
0.369	Scd2				
0.369	Col3a1				
0.369	E030026I10Rik				
0.369	5430432M24Rik				
0.369	3732412D22Rik				
0.369	Cebpa				
0.368	Siat9				
0.367	D630038D15Rik				
0.367	Cyp26b1				
0.367	Pex13				
0.366	LOC240261				
0.366	BC021608				
0.366	Hbb-b1				
0.365	BC025872				
0.365	Scarf2				
0.365	Itpkb				
0.365	3110038B19Rik				
0.365	Sc4mol				
0.364	Col16a1				
0.364	Kif27				
0.364	Prkg1				
0.363	Zfp39				
0.361	6430537I21Rik				
0.361	Slitl2				
0.36	C230084O18Rik				
0.359	5830420C15Rik				
0.359	5830411I20				
0.359	BC042423				
0.359	Armcx2				
0.358	6530411B15Rik				
0.358	Copz2				
0.355	Slc9a3r2				
0.354	Hk1				
0.354	Ttyh3				
0.353	C230075M21Rik				
0.353	Aard				
0.353	Arhgef6				
0.353	4921505C17Rik				
0.352	Atbf1				

PDGFR^{SKO} E10.5		PDGFR^{MKO} E10.5		PDGFR^{PI3K} E10.5	
Fold	Symbol	Fold	Symbol	Fold	Symbol
0.352	Angptl6				
0.352	D1Bwg0491e				
0.352	1810027I20Rik				
0.352	E030030I06Rik				
0.351	Mmp2				
0.35	AI875142				
0.35	8430419L09Rik				
0.349	Hbb-b1				
0.349	Hoxc9				
0.349	H2afy				
0.348	Basp1				
0.348	Lrg1				
0.346	Ylpm1				
0.346	8430408G22Rik				
0.345	H13				
0.345	Clic5				
0.345	Stab1				
0.344	E230011G24Rik				
0.344	BC060615				
0.342	C1qb				
0.342	Ifi35				
0.341	E130307J07Rik				
0.341	Bbs7				
0.341	Wisp1				
0.341	Ppp1r9b				
0.339	Esm1				
0.336	D5Ertd689e				
0.336	Cdh3				
0.336	Hbb-b1				
0.336	Cryab				
0.336	4831437C03Rik				
0.335	Rcn3				
0.335	1110060I01Rik				
0.334	4930427A07Rik				
0.333	Egfl5				
0.333	Aqp1				
0.333	Gja4				
0.332	A130052D22				
0.332	Tgfb2				
0.331	Gli2				
0.33	AU020939				

PDGFR^{SKO} E10.5		PDGFR^{MKO} E10.5		PDGFR^{PI3K} E10.5	
Fold	Symbol	Fold	Symbol	Fold	Symbol
0.33	Hoxc8				
0.33	Adam23				
0.329	Cyp51				
0.328	BC043114				
0.327	1600023A02Rik				
0.327	Slc43a1				
0.327	Wfdc1				
0.326					
0.326	D230017C05Rik				
0.326	2310075G12Rik				
0.326	Hdac7a				
0.325	5730538E15Rik				
0.323	E030038D23Rik				
0.321	Cpeb3				
0.321	Smoc2				
0.321	Bmp4				
0.321	Cyp51				
0.32	LOC381132				
0.319	Six5				
0.319	Axot				
0.317	C230029D21Rik				
0.316	Fads1				
0.316					
0.316	2510009E07Rik				
0.315	D130059P03Rik				
0.315	Nnat				
0.315	Hmgcs1				
0.315	1110004P15Rik				
0.314	Smyd4				
0.313	Bcl9l				
0.313	Tnpo1				
0.313	Lgi2				
0.312	Hrbl				
0.312	Dpysl2				
0.312	Ly6e				
0.309	Gja5				
0.309	Glipr2				
0.309	Hbb-b1				
0.308	Fabp5				
0.308	Gp5				
0.308	A830030H10Rik				

PDGFR^{SKO} E10.5		PDGFR^{MKO} E10.5		PDGFR^{PI3K} E10.5	
Fold	Symbol	Fold	Symbol	Fold	Symbol
0.306	Trpv6				
0.306	Amotl1				
0.305	Tssc8				
0.304	1110067B18Rik				
0.304	Txnl4				
0.303	E130203B14Rik				
0.303	Insig2				
0.3	6030446I19Rik				
0.299					
0.298	Polydom				
0.298	Jarid1b				
0.294	A030001L21Rik				
0.294	Hbb-b1				
0.293	Cdc42ep5				
0.293	Lss				
0.293	D730035F11Rik				
0.293	4931440L10Rik				
0.293	Nnat				
0.292	Nkx2-3				
0.291	9130229N11				
0.29	Pgam2				
0.29	Rusc2				
0.289	LOC239102				
0.287	A130086G11Rik				
0.287	6230415M23Rik				
0.287	Sbk				
0.286	Adamts2				
0.285	C130022E19Rik				
0.284	Syngr1				
0.282	Nxn				
0.282	Ahsg				
0.281	5730406O18Rik				
0.28	Actg2				
0.279	Sfxn3				
0.278	Emid2				
0.277	Aacs				
0.277	Diap1				
0.276	Cblb				
0.276	9830143E02Rik				
0.275	Ppp1r3c				
0.275	5830471E12Rik				

PDGFR^{SKO} E10.5		PDGFR^{MKO} E10.5		PDGFR^{PI3K} E10.5	
Fold	Symbol	Fold	Symbol	Fold	Symbol
0.275	Zcchc3				
0.275	Fxr2h				
0.274	2310058A03Rik				
0.272	Myh10				
0.271	Tdrkh				
0.27	Islr				
0.268	9030024J15Rik				
0.267	Ddhd1				
0.267	Sox5				
0.267	Susd2				
0.266	C730009D12				
0.266	Irs1				
0.265	AW046396				
0.264	Foxq1				
0.263	D930024H10Rik				
0.263	B930095G15Rik				
0.262	Erdr1				
0.262	9130213B05Rik				
0.262	C730049P21				
0.259	4632401N01Rik				
0.258	Cdh5				
0.258	Fkbp10				
0.257	3110021A11Rik				
0.256	Slp				
0.256	2010011I20Rik				
0.256	1600023A02Rik				
0.256	Rab22a				
0.255	Anxa6				
0.255	2310008B10Rik				
0.254	Slc15a2				
0.251	6230400G14Rik				
0.251	Ntn3				
0.25	Upk3b				
0.249	Ak5				
0.249	Tspyl1				
0.248	Hbb-b1				
0.248	Dusp23				
0.248	Lphn1				
0.247	Cerk				
0.245	A630012P03Rik				
0.245	Golph4				

PDGFR^{SKO} E10.5		PDGFR^{MKO} E10.5		PDGFR^{PI3K} E10.5	
Fold	Symbol	Fold	Symbol	Fold	Symbol
0.245	Adamts9				
0.245	2810423A18Rik				
0.244	A530020H22Rik				
0.243	Mmp11				
0.243	Erdr1				
0.242	Sqle				
0.242	Hbb-b1				
0.242	Pnp				
0.242	1700030E05Rik				
0.24	Fbn1				
0.239	2610030P05Rik				
0.239	Cops5				
0.236	Tnc				
0.235	Tnni1				
0.235	Mmp23				
0.235	A530017D24Rik				
0.234	D330001F19Rik				
0.234	Serpina1d				
0.234	Faah				
0.234	Punc				
0.233	BC044804				
0.233	Ncam1				
0.232	Pcolce				
0.231	LOC233529				
0.231	Sema3f				
0.23	Zfp367				
0.227	Thbs2				
0.227	Col6a3				
0.227	9330107J05Rik				
0.227	Efna5				
0.226	LOC381691				
0.224	9030224M15Rik				
0.223	B130017P16Rik				
0.223	Mfhas1				
0.222	Creb3l1				
0.221	Vtn				
0.22	Ank1				
0.22	Mapbpip				
0.219	6430407L02Rik				
0.218	Serpina1b				
0.217	LOC270599				

PDGFR^{SKO} E10.5		PDGFR^{MKO} E10.5		PDGFR^{PI3K} E10.5	
Fold	Symbol	Fold	Symbol	Fold	Symbol
0.216	6720403M19Rik				
0.215	2610524A10Rik				
0.214	Ddx26				
0.212	Zfhx1b				
0.212	1110001A05Rik				
0.212	4930422J18Rik				
0.212	9330186A19Rik				
0.211	Col6a1				
0.21	Axl				
0.21	D130027M04Rik				
0.21	Mvd				
0.209	Sema3b				
0.209	Alcam				
0.208	Serpina1b				
0.207	9930108O06Rik				
0.207	Hand1				
0.207	2010204O13Rik				
0.206	Cdh3				
0.206	Aldh8a1				
0.205	1110055E19Rik				
0.205	Ehd3				
0.204	Biklk				
0.203	Col5a2				
0.202	Serpina1b				
0.201	Mthfd1				
0.201	C530043K16Rik				
0.201	Ndrg1				
0.2	Apof				
0.195	1110008H02Rik				
0.194	Pga5				
0.194	0610037B23Rik				
0.189	Ccnd2				
0.188	Sox4				
0.187	BC023741				
0.187	A130010C12Rik				
0.186	Col5a1				
0.186	Col4a5				
0.183	Tgfb1i1				
0.182	9030625A11Rik				
0.179	Rgl1				
0.179	LOC385780				

PDGFR^{SKO} E10.5		PDGFR^{MKO} E10.5		PDGFR^{PI3K} E10.5	
Fold	Symbol	Fold	Symbol	Fold	Symbol
0.178	2610305J24Rik				
0.178	Gas6				
0.177	Mt3				
0.177	P2ry14				
0.175	Col4a6				
0.175	E230012J19Rik				
0.173	G430005B15Rik				
0.172	Foxo3				
0.172	2900045G02Rik				
0.169	A930030J18Rik				
0.169	Hsd11b2				
0.168	Loxl1				
0.167	Uap1				
0.167	Creld1				
0.166	Col4a5				
0.163	6820427D17Rik				
0.162	Trim10				
0.162	Gm22				
0.16					
0.159	1110017F19Rik				
0.159	D5Ertd593e				
0.159	Col1a2				
0.158	C130092E12				
0.156	Bglap2				
0.155	Camk4				
0.151	Wdfy1				
0.147	6330414G02Rik				
0.147	F830002E14Rik				
0.147	6030432P03Rik				
0.146	Nnat				
0.146	C3				
0.139	Lox				
0.139	Ldlr				
0.135	4933427D14Rik				
0.134	6720469N11Rik				
0.129	Oxr1				
0.127	2210415K03Rik				
0.126	Gm644				
0.121	0610005C13Rik				
0.121	2610001E17Rik				
0.12	Serpina1a				

PDGFR^{SKO} E10.5		PDGFR^{MKO} E10.5		PDGFR^{PI3K} E10.5	
Fold	Symbol	Fold	Symbol	Fold	Symbol
0.12	B230114H05Rik				
0.118	Reck				
0.111	Col6a1				
0.111	3110040M04Rik				
0.11	Olfml3				
0.106	B230369L08Rik				
0.101	Mgst1				
0.099	Mknk2				
0.096	Ndrl				
0.096	Bglap-rs1				
0.094	Srpx				
0.092	Col1a1				
0.085	Serpina1a				
0.085	8030402P03Rik				
0.084	Mrc2				
0.083	8030481K01Rik				
0.081	Insig1				
0.08	2210021J22Rik				
0.079	Wnt9a				
0.078	Hsd11b2				
0.075	AI115600				
0.074	Nudel-pending				
0.072	Tia1				
0.069	B930036M14Rik				
0.066	Arrdc3				
0.066	C130098C10Rik				
0.062	Col9a2				
0.061	1700009P17Rik				
0.054	1810018P12Rik				
0.053	4931426K16Rik				
0.052	A230020G22Rik				
0.051	Ctgf				
0.05	Cbln1				
0.045	9130213B05Rik				
0.044	Sparc				
0.041	Col3a1				
0.028	Pcsk9				
0.026	D430030C18Rik				
0.025	Sqle				
0.024	Sycn				
0.023	Snai2				

PDGFR^{SKO} E10.5		PDGFR^{MKO} E10.5		PDGFR^{PI3K} E10.5	
Fold	Symbol	Fold	Symbol	Fold	Symbol
0.019	Nudt6				
0.019	Slc17a1				
0.018	Lars2				
0.017	Apoa2				
0.016	Fdps				
0.003	BC021614				
0.002	Fcer1g				

BIBLIOGRAPHY

Abramsson, A., Berlin, O., Papayan, H., Paulin, D., Shani, M., and Betsholtz, C. 2002. Analysis of mural cell recruitment to tumor vessels. *Circulation* **105**(1): 112-117.

Argraves, W.S. and Drake, C.J. 2005. Genes critical to vasculogenesis as defined by systematic analysis of vascular defects in knockout mice. *Anat Rec A Discov Mol Cell Evol Biol* **286**(2): 875-884.

Armstrong, L.C., Bjorkblom, B., Hankenson, K.D., Siadak, A.W., Stiles, C.E., and Bornstein, P. 2002. Thrombospondin 2 inhibits microvascular endothelial cell proliferation by a caspase-independent mechanism. *Mol Biol Cell* **13**(6): 1893-1905.

Arthur, H.M., Ure, J., Smith, A.J., Renforth, G., Wilson, D.I., Torsney, E., Charlton, R., Parums, D.V., Jowett, T., Marchuk, D.A., Burn, J., and Diamond, A.G. 2000. Endoglin, an ancillary TGFbeta receptor, is required for extraembryonic angiogenesis and plays a key role in heart development. *Dev Biol* **217**(1): 42-53.

Arvidsson, A.K., Rupp, E., Nanberg, E., Downward, J., Ronnstrand, L., Wennstrom, S., Schlessinger, J., Heldin, C.H., and Claesson-Welsh, L. 1994. Tyr-716 in the platelet-derived growth factor beta-receptor kinase insert is involved in GRB2 binding and Ras activation. *Mol Cell Biol* **14**(10): 6715-6726.

Ashby, D., Gamble, J., Vadas, M., Fidge, N., Siggins, S., Rye, K., and Barter, P.J. 2001. Lack of effect of serum amyloid A (SAA) on the ability of high-density lipoproteins to inhibit endothelial cell adhesion molecule expression. *Atherosclerosis* **154**(1): 113-121

Baldwin, H.S. 1996. Early embryonic vascular development. *Cardiovasc Res* **31 Spec No**: E34-45.

Benjamin, L.E., Hemo, I., and Keshet, E. 1998. A plasticity window for blood vessel remodelling is defined by pericyte coverage of the preformed endothelial network and is regulated by PDGF-B and VEGF. *Development* **125**(9): 1591-1598.

Betsholtz, C., Karlsson, L., and Lindahl, P. 2001. Developmental roles of platelet-derived growth factors. *Bioessays* **23**(6): 494-507.

Blume-Jensen, P., Jiang, G., Hyman, R., Lee, K.F., O'Gorman, S., and Hunter, T. 2000. Kit/stem cell factor receptor-induced activation of phosphatidylinositol 3'-kinase is essential for male fertility. *Nat Genet* **24**(2): 157-162.

Bohnsack, B.L., Lai, L., Dolle, P., and Hirschi, K.K. 2004. Signaling hierarchy downstream of retinoic acid that independently regulates vascular remodeling and endothelial cell proliferation. *Genes Dev* **18**(11): 1345-1358.

Bohnsack, B.L., Lai, L., Northrop, J.L., Justice, M.J., and Hirschi, K.K. 2006. Visceral endoderm function is regulated by quaking and required for vascular development. *Genesis* **44**(2): 93-104.

Boucher, P., Liu, P., Gotthardt, M., Hiesberger, T., Anderson, R.G., and Herz, J. 2002. Platelet-derived growth factor mediates tyrosine phosphorylation of the cytoplasmic domain of the low Density lipoprotein receptor-related protein in caveolae. *J Biol Chem* **277**(18): 15507-15513.

Byrd, N., Becker, S., Maye, P., Narasimhaiah, R., St-Jacques, B., Zhang, X., McMahon, J., McMahon, A., and Grabel, L. 2002. Hedgehog is required for murine yolk sac angiogenesis. *Development* **129**(2): 361-372.

Carlson, T.R., Hu, H., Braren, R., Kim, Y.H., and Wang, R.A. 2008. Cell-autonomous requirement for {beta}1 integrin in endothelial cell adhesion, migration and survival during angiogenesis in mice. *Development* **135**(12): 2193-2202.

Carmeliet, P., Ferreira, V., Breier, G., Pollefeyt, S., Kieckens, L., Gertsenstein, M., Fahrig, M., Vandenhoeck, A., Harpal, K., Eberhardt, C., Declercq, C., Pawling, J., Moons, L., Collen, D., Risau, W., and Nagy, A. 1996. Abnormal blood vessel development and lethality in embryos lacking a single VEGF allele. *Nature* **380**(6573): 435-439.

Carvalho, R.L., Itoh, F., Goumans, M.J., Lebrin, F., Kato, M., Takahashi, S., Ema, M., Itoh, S., van Rooijen, M., Bertolino, P., Ten Dijke, P., and Mummery, C.L. 2007. Compensatory signalling induced in the yolk sac vasculature by deletion of TGF{beta} receptors in mice. *J Cell Sci*.

Carvalho, R.L., Jonker, L., Goumans, M.J., Larsson, J., Bouwman, P., Karlsson, S., Dijke, P.T., Arthur, H.M., and Mummery, C.L. 2004. Defective paracrine signalling by TGFbeta in yolk sac vasculature of endoglin mutant mice: a paradigm for hereditary haemorrhagic telangiectasia. *Development* **131**(24): 6237-6247.

Claesson-Welsh, L. 1994. Signal transduction by the PDGF receptors. *Prog Growth Factor Res* **5**(1): 37-54.

Cohen, T.V., Kosti, O., and Stewart, C.L. 2007. The nuclear envelope protein MAN1 regulates TGFbeta signaling and vasculogenesis in the embryonic yolk sac. *Development* **134**(7): 1385-1395.

Copp, A.J. 1995. Death before birth: clues from gene knockouts and mutations. *Trends Genet* **11**(3): 87-93.

Crosby, J.R., Seifert, R.A., Soriano, P., and Bowen-Pope, D.F. 1998. Chimaeric analysis reveals role of Pdgf receptors in all muscle lineages. *Nat Genet* **18**(4): 385-388.

Cross, M.J., Dixelius, J., Matsumoto, T., and Claesson-Welsh, L. 2003. VEGF-receptor signal transduction. *Trends Biochem Sci* **28**(9): 488-494.

Das, A., Fanslow, W., Cerretti, D., Warren, E., Talarico, N., and McGuire, P. 2003. Angiopoietin/Tek interactions regulate mmp-9 expression and retinal neovascularization. *Lab Invest* **83**(11): 1637-1645.

Dettman, R.W., Denetclaw, W., Jr., Ordahl, C.P., and Bristow, J. 1998. Common epicardial origin of coronary vascular smooth muscle, perivascular fibroblasts, and intermyocardial fibroblasts in the avian heart. *Dev Biol* **193**(2): 169-181.

Dickson, M.C., Martin, J.S., Cousins, F.M., Kulkarni, A.B., Karlsson, S., and Akhurst, R.J. 1995. Defective haematopoiesis and vasculogenesis in transforming growth factor-beta 1 knock out mice. *Development* **121**(6): 1845-1854.

Dominguez, M.G., Hughes, V.C., Pan, L., Simmons, M., Daly, C., Anderson, K., Noguera-Troise, I., Murphy, A.J., Valenzuela, D.M., Davis, S., Thurston, G., Yancopoulos, G.D., and Gale, N.W. 2007. Vascular endothelial tyrosine phosphatase (VE-PTP)-null mice undergo vasculogenesis but die embryonically because of defects in angiogenesis. *Proc Natl Acad Sci U S A* **104**(9): 3243-3248.

Drake, C.J. and Little, C.D. 1995. Exogenous vascular endothelial growth factor induces malformed and hyperfused vessels during embryonic neovascularization. *Proc Natl Acad Sci U S A* **92**(17): 7657-7661.

Ekman, S., Thuresson, E.R., Heldin, C.H., and Ronnstrand, L. 1999. Increased mitogenicity of an alphabeta heterodimeric PDGF receptor complex correlates with lack of RasGAP binding. *Oncogene* **18**(15): 2481-2488.

Ema, M., Faloon, P., Zhang, W.J., Hirashima, M., Reid, T., Stanford, W.L., Orkin, S., Choi, K., and Rossant, J. 2003. Combinatorial effects of Flk1 and Tal1 on vascular and hematopoietic development in the mouse. *Genes Dev* **17**(3): 380-393.

Enge, M., Bjarnegard, M., Gerhardt, H., Gustafsson, E., Kalen, M., Asker, N., Hammes, H.P., Shani, M., Fassler, R., and Betsholtz, C. 2002. Endothelium-specific platelet-derived growth factor-B ablation mimics diabetic retinopathy. *Embo J* **21**(16): 4307-4316.

Fambrough, D., McClure, K., Kazlauskas, A., and Lander, E.S. 1999. Diverse signaling pathways activated by growth factor receptors induce broadly overlapping, rather than independent, sets of genes. *Cell* **97**(6): 727-741.

Fanger, G.R., Vaillancourt, R.R., Heasley, L.E., Montmayeur, J.P., Johnson, G.L., and Maue, R.A. 1997. Analysis of mutant platelet-derived growth factor receptors expressed in PC12 cells identifies signals governing sodium channel induction during neuronal differentiation. *Mol Cell Biol* **17**(1): 89-99.

Farley, F.W., Soriano, P., Steffen, L.S., and Dymecki, S.M. 2000. Widespread recombinase expression using FLPeR (flipper) mice. *Genesis* **28**(3-4): 106-110.

Ferrell, J.E., Jr. and Machleder, E.M. 1998. The biochemical basis of an all-or-none cell fate switch in Xenopus oocytes. *Science* **280**(5365): 895-898.

Filipeanu, C.M., Zhou, F., and Wu, G. 2008. Analysis of Rab1 function in cardiomyocyte growth. *Methods Enzymol* **438**: 217-226.

Fischer, A., Schumacher, N., Maier, M., Sendtner, M., and Gessler, M. 2004. The Notch target genes Hey1 and Hey2 are required for embryonic vascular development. *Genes Dev* **18**(8): 901-911.

Flamme, I., Frolich, T., and Risau, W. 1997. Molecular mechanisms of vasculogenesis and embryonic angiogenesis. *J Cell Physiol* **173**(2): 206-210.

Flores, G.V., Duan, H., Yan, H., Nagaraj, R., Fu, W., Zou, Y., Noll, M., and Banerjee, U. 2000. Combinatorial signaling in the specification of unique cell fates. *Cell* **103**(1): 75-85.

Fong, G.H., Rossant, J., Gertsenstein, M., and Breitman, M.L. 1995. Role of the Flt-1 receptor tyrosine kinase in regulating the assembly of vascular endothelium. *Nature* **376**(6535): 66-70.

Francis, S.E., Goh, K.L., Hodivala-Dilke, K., Bader, B.L., Stark, M., Davidson, D., and Hynes, R.O. 2002. Central roles of alpha5beta1 integrin and fibronectin in vascular development in mouse embryos and embryoid bodies. *Arterioscler Thromb Vasc Biol* **22**(6): 927-933.

Franke, T.F., Yang, S.I., Chan, T.O., Datta, K., Kazlauskas, A., Morrison, D.K., Kaplan, D.R., and Tsichlis, P.N. 1995. The protein kinase encoded by the Akt proto-

oncogene is a target of the PDGF-activated phosphatidylinositol 3-kinase. *Cell* **81**(5): 727-736.

Gariano, R.F. and Gardner, T.W. 2005. Retinal angiogenesis in development and disease. *Nature* **438**(7070): 960-966.

Gehling, U.M., Ergun, S., Schumacher, U., Wagener, C., Pantel, K., Otte, M., Schuch, G., Schafhausen, P., Mende, T., Kilic, N., Kluge, K., Schafer, B., Hossfeld, D.K., and Fiedler, W. 2000. In vitro differentiation of endothelial cells from AC133-positive progenitor cells. *Blood* **95**(10): 3106-3112.

George, E.L., Baldwin, H.S., and Hynes, R.O. 1997. Fibronectins are essential for heart and blood vessel morphogenesis but are dispensable for initial specification of precursor cells. *Blood* **90**(8): 3073-3081.

Gerhardt, H., Golding, M., Fruttiger, M., Ruhrberg, C., Lundkvist, A., Abramsson, A., Jeltsch, M., Mitchell, C., Alitalo, K., Shima, D., and Betsholtz, C. 2003. VEGF guides angiogenic sprouting utilizing endothelial tip cell filopodia. *J Cell Biol* **161**(6): 1163-1177.

Goldsmith, A.P., Gossage, S.J., and ffrench-Constant, C. 2004. ADAM23 is a cell-surface glycoprotein expressed by central nervous system neurons. *J Neurosci Res* **78**(5): 647-658.

Gong, Q., Cheng, A.M., Akk, A.M., Alberola-Ila, J., Gong, G., Pawson, T., and Chan, A.C. 2001. Disruption of T cell signaling networks and development by Grb2 haploid insufficiency. *Nat Immunol* **2**(1): 29-36.

Goumans, M.J., Valdimarsdottir, G., Itoh, S., Rosendahl, A., Sideras, P., and ten Dijke, P. 2002. Balancing the activation state of the endothelium via two distinct TGF-beta type I receptors. *Embo J* **21**(7): 1743-1753.

Goumans, M.J., Zwijsen, A., van Rooijen, M.A., Huylebroeck, D., Roelen, B.A., and Mummery, C.L. 1999. Transforming growth factor-beta signalling in extraembryonic mesoderm is required for yolk sac vasculogenesis in mice. *Development* **126**(16): 3473-3483.

Grote, K., Bavendiek, U., Grothusen, C., Flach, I., Hilfiker-Kleiner, D., Drexler, H., and Schieffer, B. 2004. Stretch-inducible expression of the angiogenic factor CCN1 in vascular smooth muscle cells is mediated by Egr-1. *J Biol Chem* **279**(53): 55675-55681.

Haldar, S.M., Ibrahim, O.A., and Jain, M.K. 2007. Kruppel-like Factors (KLFs) in muscle biology. *J Mol Cell Cardiol* **43**(1): 1-10.

Halfon, M.S., Carmena, A., Gisselbrecht, S., Sackerson, C.M., Jimenez, F., Baylies, M.K., and Michelson, A.M. 2000. Ras pathway specificity is determined by the integration of multiple signal-activated and tissue-restricted transcription factors. *Cell* **103**(1): 63-74.

Hamilton, T.G., Klinghoffer, R.A., Corrin, P.D., and Soriano, P. 2003. Evolutionary divergence of platelet-derived growth factor alpha receptor signaling mechanisms. *Mol Cell Biol* **23**(11): 4013-4025.

Hansen, K., Johnell, M., Siegbahn, A., Rorsman, C., Engstrom, U., Wernstedt, C., Heldin, C.H., and Ronnstrand, L. 1996. Mutation of a Src phosphorylation site in the PDGF beta-receptor leads to increased PDGF-stimulated chemotaxis but decreased mitogenesis. *Embo J* **15**(19): 5299-5313.

Heemskerk, J. and DiNardo, S. 1994. Drosophila hedgehog acts as a morphogen in cellular patterning. *Cell* **76**(3): 449-460.

Heldin, C.H., Ostman, A., and Ronnstrand, L. 1998. Signal transduction via platelet-derived growth factor receptors. *Biochim Biophys Acta* **1378**(1): F79-113.

Heldin, C.H. and Westermark, B. 1999. Mechanism of action and in vivo role of platelet-derived growth factor. *Physiol Rev* **79**(4): 1283-1316.

Hellstrom, M., Gerhardt, H., Kalen, M., Li, X., Eriksson, U., Wolburg, H., and Betsholtz, C. 2001. Lack of pericytes leads to endothelial hyperplasia and abnormal vascular morphogenesis. *J Cell Biol* **153**(3): 543-553.

Hellstrom, M., Kalen, M., Lindahl, P., Abramsson, A., and Betsholtz, C. 1999. Role of PDGF-B and PDGFR-beta in recruitment of vascular smooth muscle cells and pericytes during embryonic blood vessel formation in the mouse. *Development* **126**(14): 3047-3055.

Heuchel, R., Berg, A., Tallquist, M., Ahlen, K., Reed, R.K., Rubin, K., Claesson-Welsh, L., Heldin, C.H., and Soriano, P. 1999. Platelet-derived growth factor beta receptor regulates interstitial fluid homeostasis through phosphatidylinositol-3' kinase signaling. *Proc Natl Acad Sci U S A* **96**(20): 11410-11415.

Hiratsuka, S., Minowa, O., Kuno, J., Noda, T., and Shibuya, M. 1998. Flt-1 lacking the tyrosine kinase domain is sufficient for normal development and angiogenesis in mice. *Proc Natl Acad Sci U S A* **95**(16): 9349-9354.

Hirschi, K.K., Rohovsky, S.A., Beck, L.H., Smith, S.R., and D'Amore, P.A. 1999. Endothelial cells modulate the proliferation of mural cell precursors via platelet-derived growth factor-BB and heterotypic cell contact. *Circ Res* **84**(3): 298-305.

Hirschi, K.K., Rohovsky, S.A., and D'Amore, P.A. 1998. PDGF, TGF-beta, and heterotypic cell-cell interactions mediate endothelial cell-induced recruitment of 10T1/2 cells and their differentiation to a smooth muscle fate. *J Cell Biol* **141**(3): 805-814.

Hogan, B., Beddington, R., Costantini, F., and Lacy, E. 1994. *Manipulating the Mouse Embryo: a laboratory manual*. Cold Spring Harbor Laboratory Press, Plainview, NY.

Holmgren, L., Glaser, A., Pfeifer-Ohlsson, S., and Ohlsson, R. 1991. Angiogenesis during human extraembryonic development involves the spatiotemporal control of PDGF ligand and receptor gene expression. *Development* **113**(3): 749-754.

Holtwick, R., Gotthardt, M., Skryabin, B., Steinmetz, M., Potthast, R., Zetsche, B., Hammer, R.E., Herz, J., and Kuhn, M. 2002. Smooth muscle-selective deletion of guanylyl cyclase-A prevents the acute but not chronic effects of ANP on blood pressure. *Proc Natl Acad Sci U S A* **99**(10): 7142-7147.

Hoevel, T., Macek, R., Mundigl, O., Swisshelm, K., and Kubbies, M. 2002. Expression and targeting of the tight junction protein CLDN1 in CLDN1-negative human breast tumor cells. *J Cell Physiol* **191**(1): 60-68.

Huang, H., Rambaldi, I., Daniels, E., and Featherstone, M. 2003. Expression of the Wdr9 gene and protein products during mouse development. *Dev Dyn* **227**(4): 608-614.

Huber, T.L., Kouskoff, V., Fehling, H.J., Palis, J., and Keller, G. 2004. Haemangioblast commitment is initiated in the primitive streak of the mouse embryo. *Nature* **432**(7017): 625-630.

Hughes, S. and Chan-Ling, T. 2004. Characterization of smooth muscle cell and pericyte differentiation in the rat retina in vivo. *Invest Ophthalmol Vis Sci* **45**(8): 2795-2806.

Hungerford, J.E. and Little, C.D. 1999. Developmental biology of the vascular smooth muscle cell: building a multilayered vessel wall. *J Vasc Res* **36**(1): 2-27.

Jadrich, J.L., O'Connor, M.B., and Coucouvanis, E. 2006. The TGF beta activated kinase TAK1 regulates vascular development in vivo. *Development* **133**(8): 1529-1541.

Jain, R.K. 2003. Molecular regulation of vessel maturation. *Nat Med* **9**(6): 685-693.

Johansson, B.M. and Wiles, M.V. 1995. Evidence for involvement of activin A and bone morphogenetic protein 4 in mammalian mesoderm and hematopoietic development. *Mol Cell Biol* **15**(1): 141-151.

Johnson, D.W., Berg, J.N., Baldwin, M.A., Gallione, C.J., Marondel, I., Yoon, S.J., Stenzel, T.T., Speer, M., Pericak-Vance, M.A., Diamond, A., Guttmacher, A.E., Jackson, C.E., Attisano, L., Kucherlapati, R., Porteous, M.E., and Marchuk, D.A. 1996. Mutations in the activin receptor-like kinase 1 gene in hereditary haemorrhagic telangiectasia type 2. *Nat Genet* **13**(2): 189-195.

Kaji, T., Yamamoto, C., Oh-i, M., Fujiwara, Y., Yamazaki, Y., Morita, T., Plaas, A.H., and Wight, T.N. 2006. The vascular endothelial growth factor VEGF165 induces perlecan synthesis via VEGF receptor-2 in cultured human brain microvascular endothelial cells. *Biochim Biophys Acta* **1760**(9): 1465-1474.

Kang, J., Gu, Y., Li, P., Johnson, B.L., Sucov, H.M., and Thomas, P.S. 2008. PDGF-A as an epicardial mitogen during heart development. *Dev Dyn* **237**(3): 692-701.

Kaplan, D.R., Morrison, D.K., Wong, G., McCormick, F., and Williams, L.T. 1990. PDGF beta-receptor stimulates tyrosine phosphorylation of GAP and association of GAP with a signaling complex. *Cell* **61**(1): 125-133.

Karakiulakis, G., Papakonstantinou, E., Aletras, A.J., Tamm, M., and Roth, M. 2007. Cell type-specific effect of hypoxia and platelet-derived growth factor-BB on extracellular matrix turnover and its consequences for lung remodeling. *J Biol Chem* **282**(2): 908-915.

Karlsson, L., Lindahl, P., Heath, J.K., and Betsholtz, C. 2000. Abnormal gastrointestinal development in PDGF-A and PDGFR-(alpha) deficient mice implicates a novel mesenchymal structure with putative instructive properties in villus morphogenesis. *Development* **127**(16): 3457-3466.

Katoh, M. 2004. Human FOX gene family (Review). *Int J Oncol* **25**(5): 1495-1500.

Kawaguchi, M., Bader, D.M., and Wilm, B. 2007. Serosal mesothelium retains vasculogenic potential. *Dev Dyn* **236**(11): 2973-2979.

Kazlauskas, A. and Cooper, J.A. 1990. Phosphorylation of the PDGF receptor beta subunit creates a tight binding site for phosphatidylinositol 3 kinase. *Embo J* **9**(10): 3279-3286.

Kazlauskas, A., Ellis, C., Pawson, T., and Cooper, J.A. 1990. Binding of GAP to activated PDGF receptors. *Science* **247**(4950): 1578-1581.

Kazlauskas, A., Feng, G.S., Pawson, T., and Valius, M. 1993. The 64-kDa protein that associates with the platelet-derived growth factor receptor beta subunit via Tyr-1009 is the SH2-containing phosphotyrosine phosphatase Syp. *Proc Natl Acad Sci U S A* **90**(15): 6939-6943.

Kim, E., Yamashita, M., Nakanishi, T., Park, K.E., Kimura, M., Kashiwabara, S., and Baba, T. 2006. Mouse sperm lacking ADAM1b/ADAM2 fertilin can fuse with the egg plasma membrane and effect fertilization. *J Biol Chem* **281**(9): 5634-5639.

Kim, I., Kim, H.G., Moon, S.O., Chae, S.W., So, J.N., Koh, K.N., Ahn, B.C., and Koh, G.Y. 2000. Angiopoietin-1 induces endothelial cell sprouting through the activation of focal adhesion kinase and plasmin secretion. *Circ Res* **86**(9): 952-959.

Kisanuki, Y.Y., Hammer, R.E., Miyazaki, J., Williams, S.C., Richardson, J.A., and Yanagisawa, M. 2001. Tie2-Cre transgenic mice: a new model for endothelial cell-lineage analysis in vivo. *Dev Biol* **230**(2): 230-242.

Kissel, H., Timokhina, I., Hardy, M.P., Rothschild, G., Tajima, Y., Soares, V., Angeles, M., Whitlow, S.R., Manova, K., and Besmer, P. 2000. Point mutation in kit receptor tyrosine kinase reveals essential roles for kit signaling in spermatogenesis and oogenesis without affecting other kit responses. *Embo J* **19**(6): 1312-1326.

Klinghoffer, R.A., Hamilton, T.G., Hoch, R., and Soriano, P. 2002. An allelic series at the PDGFalphaR locus indicates unequal contributions of distinct signaling pathways during development. *Dev Cell* **2**(1): 103-113.

Klinghoffer, R.A. and Kazlauskas, A. 1995. Identification of a putative Syp substrate, the PDGF beta receptor. *J Biol Chem* **270**(38): 22208-22217.

Klinghoffer, R.A., Mueting-Nelsen, P.F., Faerman, A., Shani, M., and Soriano, P. 2001. The two PDGF receptors maintain conserved signaling in vivo despite divergent embryological functions. *Mol Cell* **7**(2): 343-354.

Krebs, L.T., Xue, Y., Norton, C.R., Shutter, J.R., Maguire, M., Sundberg, J.P., Gallahan, D., Closson, V., Kitajewski, J., Callahan, R., Smith, G.H., Stark, K.L., and Gridley, T. 2000. Notch signaling is essential for vascular morphogenesis in mice. *Genes Dev* **14**(11): 1343-1352.

Kundra, V., Escobedo, J.A., Kazlauskas, A., Kim, H.K., Rhee, S.G., Williams, L.T., and Zetter, B.R. 1994. Regulation of chemotaxis by the platelet-derived growth factor receptor-beta. *Nature* **367**(6462): 474-476.

Kurohara, K., Komatsu, K., Kurisaki, T., Masuda, A., Irie, N., Asano, M., Sudo, K., Nabeshima, Y., Iwakura, Y., and Sehara-Fujisawa, A. 2004. Essential roles of Meltrin beta (ADAM19) in heart development. *Dev Biol* **267**(1): 14-28.

Kypta, R.M., Goldberg, Y., Ulug, E.T., and Courtneidge, S.A. 1990. Association between the PDGF receptor and members of the src family of tyrosine kinases. *Cell* **62**(3): 481-492.

Larsson, J., Goumans, M.J., Sjostrand, L.J., van Rooijen, M.A., Ward, D., Leveen, P., Xu, X., ten Dijke, P., Mummery, C.L., and Karlsson, S. 2001. Abnormal angiogenesis but intact hematopoietic potential in TGF-beta type I receptor-deficient mice. *Embo J* **20**(7): 1663-1673.

Larsson, J. and Karlsson, S. 2005. The role of Smad signaling in hematopoiesis. *Oncogene* **24**(37): 5676-5692.

Leber, T.M.a.N., R.P.M. 2001. *Detection and Quantitation of Matrix Metalloproteases by Zymography*. Humana Press, Totowa, NJ.

Lechleider, R.J., Sugimoto, S., Bennett, A.M., Kashishian, A.S., Cooper, J.A., Shoelson, S.E., Walsh, C.T., and Neel, B.G. 1993. Activation of the SH2-containing phosphotyrosine phosphatase SH-PTP2 by its binding site, phosphotyrosine 1009, on the human platelet-derived growth factor receptor. *J Biol Chem* **268**(29): 21478-21481.

Lehti, K., Allen, E., Birkedal-Hansen, H., Holmbeck, K., Miyake, Y., Chun, T.H., and Weiss, S.J. 2005. An MT1-MMP-PDGF receptor-beta axis regulates mural cell investment of the microvasculature. *Genes Dev* **19**(8): 979-991.

Leveen, P., Pekny, M., Gebre-Medhin, S., Swolin, B., Larsson, E., and Betsholtz, C. 1994. Mice deficient for PDGF B show renal, cardiovascular, and hematological abnormalities. *Genes Dev* **8**(16): 1875-1887.

Li, D.Y., Sorensen, L.K., Brooke, B.S., Urness, L.D., Davis, E.C., Taylor, D.G., Boak, B.B., and Wendel, D.P. 1999. Defective angiogenesis in mice lacking endoglin. *Science* **284**(5419): 1534-1537.

Li, L., Miano, J.M., Cserjesi, P., and Olson, E.N. 1996. SM22 alpha, a marker of adult smooth muscle, is expressed in multiple myogenic lineages during embryogenesis. *Circ Res* **78**(2): 188-195.

Lindahl, P., Hellstrom, M., Kalen, M., Karlsson, L., Pekny, M., Pekna, M., Soriano, P., and Betsholtz, C. 1998. Paracrine PDGF-B/PDGF-Rbeta signaling controls mesangial cell development in kidney glomeruli. *Development* **125**(17): 3313-3322.

Lindahl, P., Johansson, B.R., Leveen, P., and Betsholtz, C. 1997. Pericyte loss and microaneurysm formation in PDGF-B-deficient mice. *Science* **277**(5323): 242-245.

Lohler, J., Timpl, R., and Jaenisch, R. 1984. Embryonic lethal mutation in mouse collagen I gene causes rupture of blood vessels and is associated with erythropoietic and mesenchymal cell death. *Cell* **38**(2): 597-607.

Long, X., Creemers, E.E., Wang, D.Z., Olson, E.N., and Miano, J.M. 2007. Myocardin is a bifunctional switch for smooth versus skeletal muscle differentiation. *Proc Natl Acad Sci U S A* **104**(42): 16570-16575.

Loukinova, E., Ranganathan, S., Kuznetsov, S., Gorlatova, N., Migliorini, M.M., Loukinov, D., Ulery, P.G., Mikhailenko, I., Lawrence, D.A., and Strickland, D.K. 2002. Platelet-derived growth factor (PDGF)-induced tyrosine phosphorylation of the low density lipoprotein receptor-related protein (LRP). Evidence for integrated co-receptor function betwenn LRP and the PDGF. *J Biol Chem* **277**(18): 15499-15506.

Lu, J., Landerholm, T.E., Wei, J.S., Dong, X.R., Wu, S.P., Liu, X., Nagata, K., Inagaki, M., and Majesky, M.W. 2001. Coronary smooth muscle differentiation from proepicardial cells requires rhoA-mediated actin reorganization and p160 rho-kinase activity. *Dev Biol* **240**(2): 404-418.

Maina, F., Pante, G., Helmbacher, F., Andres, R., Porthin, A., Davies, A.M., Ponzetto, C., and Klein, R. 2001. Coupling Met to specific pathways results in distinct developmental outcomes. *Mol Cell* **7**(6): 1293-1306.

Martindill, D.M., Risebro, C.A., Smart, N., Franco-Viseras Mdel, M., Rosario, C.O., Swallow, C.J., Dennis, J.W., and Riley, P.R. 2007. Nucleolar release of Hand1 acts as a molecular switch to determine cell fate. *Nat Cell Biol* **9**(10): 1131-1141.

McAllister, K.A., Grogg, K.M., Johnson, D.W., Gallione, C.J., Baldwin, M.A., Jackson, C.E., Helmbold, E.A., Markel, D.S., McKinnon, W.C., Murrell, J., and et al. 1994. Endoglin, a TGF-beta binding protein of endothelial cells, is the gene for hereditary haemorrhagic telangiectasia type 1. *Nat Genet* **8**(4): 345-351.

Medvinsky, A. and Dzierzak, E. 1996. Definitive hematopoiesis is autonomously initiated by the AGM region. *Cell* **86**(6): 897-906.

Meisenhelder, J., Suh, P.G., Rhee, S.G., and Hunter, T. 1989. Phospholipase C-gamma is a substrate for the PDGF and EGF receptor protein-tyrosine kinases in vivo and in vitro. *Cell* **57**(7): 1109-1122.

Mercola, M., Wang, C.Y., Kelly, J., Brownlee, C., Jackson-Grusby, L., Stiles, C., and Bowen-Pope, D. 1990. Selective expression of PDGF A and its receptor during early mouse embryogenesis. *Dev Biol* **138**(1): 114-122.

Mikawa, T., Borisov, A., Brown, A.M., and Fischman, D.A. 1992. Clonal analysis of cardiac morphogenesis in the chicken embryo using a replication-defective retrovirus: I. Formation of the ventricular myocardium. *Dev Dyn* **193**(1): 11-23.

Mikawa, T. and Gourdie, R.G. 1996. Pericardial mesoderm generates a population of coronary smooth muscle cells migrating into the heart along with ingrowth of the epicardial organ. *Dev Biol* **174**(2): 221-232.

Mikkola, H.K. and Orkin, S.H. 2002. The search for the hemangioblast. *J Hematother Stem Cell Res* **11**(1): 9-17.

Miyamoto, S., Teramoto, H., Gutkind, J.S., and Yamada, K.M. 1996. Integrins can collaborate with growth factors for phosphorylation of receptor tyrosine kinases and MAP kinase activation: roles of integrin aggregation and occupancy of receptors. *J Cell Biol* **135**(6 Pt 1): 1633-1642.

Mori, S., Ronnstrand, L., Yokote, K., Engstrom, A., Courtneidge, S.A., Claesson-Welsh, L., and Heldin, C.H. 1993. Identification of two juxtamembrane autophosphorylation sites in the PDGF beta-receptor; involvement in the interaction with Src family tyrosine kinases. *Embo J* **12**(6): 2257-2264.

Morikawa, Y. and Cserjesi, P. 2004. Extra-embryonic vasculature development is regulated by the transcription factor HAND1. *Development* **131**(9): 2195-2204.

Morrison, D.K., Kaplan, D.R., Rhee, S.G., and Williams, L.T. 1990. Platelet-derived growth factor (PDGF)-dependent association of phospholipase C-gamma with the PDGF receptor signaling complex. *Mol Cell Biol* **10**(5): 2359-2366.

Mulrooney, J.P., Hong, T., and Grabel, L.B. 2001. Serine 785 phosphorylation of the beta1 cytoplasmic domain modulates beta1A-integrin-dependent functions. *J Cell Sci* **114**(Pt 13): 2525-2533.

Nagase, T., Nagase, M., Yoshimura, K., Machida, M., and Yamagishi, M. 2006. Defects in aortic fusion and craniofacial vasculature in the holoprosencephalic mouse embryo under inhibition of sonic hedgehog signaling. *J Craniofac Surg* **17**(4): 736-744.

Nellen, D., Burke, R., Struhl, G., and Basler, K. 1996. Direct and long-range action of a DPP morphogen gradient. *Cell* **85**(3): 357-368.

Nishimura, R., Li, W., Kashishian, A., Mondino, A., Zhou, M., Cooper, J., and Schlessinger, J. 1993. Two signaling molecules share a phosphotyrosine-containing binding site in the platelet-derived growth factor receptor. *Mol Cell Biol* **13**(11): 6889-6896.

Oh, J., Richardson, J.A., and Olson, E.N. 2005. Requirement of myocardin-related transcription factor-B for remodeling of branchial arch arteries and smooth muscle differentiation. *Proc Natl Acad Sci U S A* **102**(42): 15122-15127.

Orlidge, A. and D'Amore, P.A. 1987. Inhibition of capillary endothelial cell growth by pericytes and smooth muscle cells. *J Cell Biol* **105**(3): 1455-1462.

Orr-Urtreger, A., Bedford, M.T., Do, M.S., Eisenbach, L., and Lonai, P. 1992. Developmental expression of the alpha receptor for platelet-derived growth factor, which is deleted in the embryonic lethal Patch mutation. *Development* **115**(1): 289-303.

Oshima, M., Oshima, H., and Taketo, M.M. 1996. TGF-beta receptor type II deficiency results in defects of yolk sac hematopoiesis and vasculogenesis. *Dev Biol* **179**(1): 297-302.

Park, C., Afrikanova, I., Chung, Y.S., Zhang, W.J., Arentson, E., Fong Gh, G., Rosendahl, A., and Choi, K. 2004. A hierarchical order of factors in the generation of FLK1- and SCL-expressing hematopoietic and endothelial progenitors from embryonic stem cells. *Development* **131**(11): 2749-2762.

Partanen, J., Schwartz, L., and Rossant, J. 1998. Opposite phenotypes of hypomorphic and Y766 phosphorylation site mutations reveal a function for Fgfr1 in anteroposterior patterning of mouse embryos. *Genes Dev* **12**(15): 2332-2344.

Pearson, S., Sroczynska, P., Lacaud, G., and Kouskoff, V. 2008. The stepwise specification of embryonic stem cells to hematopoietic fate is driven by sequential exposure to Bmp4, activin A, bFGF and VEGF. *Development* **135**(8): 1525-1535.

Pietras, K., Pahler, J., Bergers, G., and Hanahan, D. 2008. Functions of paracrine PDGF signaling in the proangiogenic tumor stroma revealed by pharmacological targeting. *PLoS Med* **5**(1): e19.

Pipes, G.C., Creemers, E.E., and Olson, E.N. 2006. The myocardin family of transcriptional coactivators: versatile regulators of cell growth, migration, and myogenesis. *Genes Dev* **20**(12): 1545-1556.

Poschl, E., Schlotzer-Schrehardt, U., Brachvogel, B., Saito, K., Ninomiya, Y., and Mayer, U. 2004. Collagen IV is essential for basement membrane stability but dispensable for initiation of its assembly during early development. *Development* **131**(7): 1619-1628.

Reynolds, L.P. and Redmer, D.A. 1992. Growth and microvascular development of the uterus during early pregnancy in ewes. *Biol Reprod* **47**(5): 698-708.

Richarte, A.M., Mead, H.B., and Tallquist, M.D. 2007. Cooperation between the PDGF receptors in cardiac neural crest cell migration. *Dev Biol* **306**(2): 785-796.

Risau, W. and Lemmon, V. 1988. Changes in the vascular extracellular matrix during embryonic vasculogenesis and angiogenesis. *Dev Biol* **125**(2): 441-450.

Robbins, J.R., McGuire, P.G., Wehrle-Haller, B., and Rogers, S.L. 1999. Diminished matrix metalloproteinase 2 (MMP-2) in ectomesenchyme-derived tissues of the

Patch mutant mouse: regulation of MMP-2 by PDGF and effects on mesenchymal cell migration. *Dev Biol* **212**(2): 255-263.

Roche, S., Koegl, M., Barone, M.V., Roussel, M.F., and Courtneidge, S.A. 1995. DNA synthesis induced by some but not all growth factors requires Src family protein tyrosine kinases. *Mol Cell Biol* **15**(2): 1102-1109.

Rolny, C., Nilsson, I., Magnusson, P., Armulik, A., Jakobsson, L., Wentzel, P., Lindblom, P., Norlin, J., Betsholtz, C., Heuchel, R., Welsh, M., and Claesson-Welsh, L. 2006. Platelet-derived growth factor receptor-beta promotes early endothelial cell differentiation. *Blood* **108**(6): 1877-1886.

Sato, H., Takino, T., Okada, Y., Cao, J., Shinagawa, A., Yamamoto, E., and Seiki, M. 1994. A matrix metalloproteinase expressed on the surface of invasive tumour cells. *Nature* **370**(6484): 61-65.

Saunders, W.B., Bohnsack, B.L., Faske, J.B., Anthis, N.J., Bayless, K.J., Hirschi, K.K., and Davis, G.E. 2006. Coregulation of vascular tube stabilization by endothelial cell TIMP-2 and pericyte TIMP-3. *J Cell Biol* **175**(1): 179-191.

Savagner, P., Yamada, K.M., and Thiery, J.P. 1997. The zinc-finger protein slug causes desmosome dissociation, an initial and necessary step for growth factor-induced epithelial-mesenchymal transition. *J Cell Biol* **137**(6): 1403-1419.

Schatteman, G.C., Morrison-Graham, K., van Koppen, A., Weston, J.A., and Bowen-Pope, D.F. 1992. Regulation and role of PDGF receptor alpha-subunit expression during embryogenesis. *Development* **115**(1): 123-131.

Shen, Y., Li, N., Wu, S., Zhou, Y., Shan, Y., Zhang, Q., Ding, C., Yuan, Q., Zhao, F., Zeng, R., and Zhu, X. 2008. Nudel binds Cdc42GAP to modulate Cdc42 activity at the leading edge of migrating cells. *Dev Cell* **14**(3): 342-353.

Schlaeger, T.M., Bartunkova, S., Lawitts, J.A., Teichmann, G., Risau, W., Deutsch, U., and Sato, T.N. 1997. Uniform vascular-endothelial-cell-specific gene expression in both embryonic and adult transgenic mice. *Proc Natl Acad Sci U S A* **94**(7): 3058-3063.

Schneller, M., Vuori, K., and Ruoslahti, E. 1997. Alphavbeta3 integrin associates with activated insulin and PDGFbeta receptors and potentiates the biological activity of PDGF. *Embo J* **16**(18): 5600-5607.

Seifert, R.A., Alpers, C.E., and Bowen-Pope, D.F. 1998. Expression of platelet-derived growth factor and its receptors in the developing and adult mouse kidney. *Kidney Int* **54**(3): 731-746.

Shalaby, F., Ho, J., Stanford, W.L., Fischer, K.D., Schuh, A.C., Schwartz, L., Bernstein, A., and Rossant, J. 1997. A requirement for Flk1 in primitive and definitive hematopoiesis and vasculogenesis. *Cell* **89**(6): 981-990.

Shalaby, F., Rossant, J., Yamaguchi, T.P., Gertsenstein, M., Wu, X.F., Breitman, M.L., and Schuh, A.C. 1995. Failure of blood-island formation and vasculogenesis in Flk-1-deficient mice. *Nature* **376**(6535): 62-66.

Shih, S.C., Robinson, G.S., Perruzzi, C.A., Calvo, A., Desai, K., Green, J.E., Ali, I.U., Smith, L.E., and Senger, D.R. 2002. Molecular profiling of angiogenesis markers. *Am J Pathol* **161**(1): 35-41.

Soriano, P. 1994. Abnormal kidney development and hematological disorders in PDGF beta-receptor mutant mice. *Genes Dev* **8**(16): 1888-1896.

Soriano, P. 1997. The PDGF alpha receptor is required for neural crest cell development and for normal patterning of the somites. *Development* **124**(14): 2691-2700.

Soriano, P. 1999. Generalized lacZ expression with the ROSA26 Cre reporter strain. *Nat Genet* **21**(1): 70-71.

Stepanova, V., Jerke, U., Sagach, V., Lindschau, C., Dietz, R., Haller, H., and Dumler, I. 2002. Urokinase-dependent human vascular smooth muscle cell adhesion requires selective vitronectin phosphorylation by ectoprotein kinase CK2. *J Biol Chem* **277**(12): 10265-10272.

Strongin, A.Y., Collier, I., Bannikov, G., Marmer, B.L., Grant, G.A., and Goldberg, G.I. 1995. Mechanism of cell surface activation of 72-kDa type IV collagenase. Isolation of the activated form of the membrane metalloprotease. *J Biol Chem* **270**(10): 5331-5338.

Su, Z.Z., Gopalkrishnan, R.V., Narayan, G., Dent, P., and Fisher, P.B. 2002. Progression elevated gene-3, PEG-3, induces genomic instability in rodent and human tumor cells. *J Cell Physiol* **192**(1): 34-44.

Sugiyama, D. and Tsuji, K. 2006. Definitive hematopoiesis from endothelial cells in the mouse embryo; a simple guide. *Trends Cardiovasc Med* **16**(2): 45-49.

Suri, C., Jones, P.F., Patan, S., Bartunkova, S., Maisonpierre, P.C., Davis, S., Sato, T.N., and Yancopoulos, G.D. 1996. Requisite role of angiopoietin-1, a ligand for the TIE2 receptor, during embryonic angiogenesis. *Cell* **87**(7): 1171-1180.

Takakura, N., Yoshida, H., Ogura, Y., Kataoka, H., Nishikawa, S., and Nishikawa, S. 1997. PDGFR alpha expression during mouse embryogenesis: immunolocalization analyzed by whole-mount immunohistostaining using the monoclonal anti-mouse PDGFR alpha antibody APA5. *J Histochem Cytochem* **45**(6): 883-893.

Tallquist, M.D., Klinghoffer, R.A., Heuchel, R., Mueting-Nelsen, P.F., Corrin, P.D., Heldin, C.H., Johnson, R.J., and Soriano, P. 2000. Retention of PDGFR-beta function in mice in the absence of phosphatidylinositol 3'-kinase and phospholipase Cgamma signaling pathways. *Genes Dev* **14**(24): 3179-3190.

Tallquist, M.D. and Soriano, P. 2000. Epiblast-restricted Cre expression in MORE mice: a tool to distinguish embryonic vs. extra-embryonic gene function. *Genesis* **26**(2): 113-115.

Tallquist, M.D. and Soriano, P. 2003. Cell autonomous requirement for PDGFRalpha in populations of cranial and cardiac neural crest cells. *Development* **130**(3): 507-518.

Thyboll, J., Kortesmaa, J., Cao, R., Soininen, R., Wang, L., Iivanainen, A., Sorokin, L., Risling, M., Cao, Y., and Tryggvason, K. 2002. Deletion of the laminin alpha4 chain leads to impaired microvessel maturation. *Mol Cell Biol* **22**(4): 1194-1202.

Tidhar, A., Reichenstein, M., Cohen, D., Faerman, A., Copeland, N.G., Gilbert, D.J., Jenkins, N.A., and Shani, M. 2001. A novel transgenic marker for migrating limb muscle precursors and for vascular smooth muscle cells. *Dev Dyn* **220**(1): 60-73.

Twamley, G.M., Kypta, R.M., Hall, B., and Courtneidge, S.A. 1993. Src family tyrosine kinases and the response to platelet-derived growth factor. *Adv Second Messenger Phosphoprotein Res* **28**: 187-194.

Vaillancourt, R.R., Heasley, L.E., Zamarripa, J., Storey, B., Valius, M., Kazlauskas, A., and Johnson, G.L. 1995. Mitogen-activated protein kinase activation is insufficient for growth factor receptor-mediated PC12 cell differentiation. *Mol Cell Biol* **15**(7): 3644-3653.

Valius, M. and Kazlauskas, A. 1993. Phospholipase C-gamma 1 and phosphatidylinositol 3 kinase are the downstream mediators of the PDGF receptor's mitogenic signal. *Cell* **73**(2): 321-334.

Van den Akker, N.M., Winkel, L.C., Nisancioglu, M.H., Maas, S., Wisse, L.J., Armulik, A., Poelmann, R.E., Lie-Venema, H., Betsholtz, C., and Gittenberger-de Groot, A.C. 2008. PDGF-B signaling is important for murine cardiac development: Its role in developing atrioventricular valves, coronaries, and cardiac innervation. *Dev Dyn* **237**(2): 494-503.

Vignais, M.L., Sadowski, H.B., Watling, D., Rogers, N.C., and Gilman, M. 1996. Platelet-derived growth factor induces phosphorylation of multiple JAK family kinases and STAT proteins. *Mol Cell Biol* **16**(4): 1759-1769.

Vrancken Peeters, M.P., Gittenberger-de Groot, A.C., Mentink, M.M., and Poelmann, R.E. 1999. Smooth muscle cells and fibroblasts of the coronary arteries derive from epithelial-mesenchymal transformation of the epicardium. *Anat Embryol (Berl)* **199**(4): 367-378.

Wang, D., Chang, P.S., Wang, Z., Sutherland, L., Richardson, J.A., Small, E., Krieg, P.A., and Olson, E.N. 2001. Activation of cardiac gene expression by myocardin, a transcriptional cofactor for serum response factor. *Cell* **105**(7): 851-862.

Wang, Z., Wang, D.Z., Pipes, G.C., and Olson, E.N. 2003. Myocardin is a master regulator of smooth muscle gene expression. *Proc Natl Acad Sci U S A* **100**(12): 7129-7134.

Wei, K., Che, N., and Chen, F. 2007. Myocardin-related transcription factor B is required for normal mouse vascular development and smooth muscle gene expression. *Dev Dyn* **236**(2): 416-425.

Weiser, M.C., Grieshaber, N.A., Schwartz, P.E., and Majack, R.A. 1997. Perlecan regulates Oct-1 gene expression in vascular smooth muscle cells. *Mol Biol Cell* **8**(6): 999-1011.

Wennstrom, S., Hawkins, P., Cooke, F., Hara, K., Yonezawa, K., Kasuga, M., Jackson, T., Claesson-Welsh, L., and Stephens, L. 1994a. Activation of phosphoinositide 3-kinase is required for PDGF-stimulated membrane ruffling. *Curr Biol* **4**(5): 385-393.

Wennstrom, S., Siegbahn, A., Yokote, K., Arvidsson, A.K., Heldin, C.H., Mori, S., and Claesson-Welsh, L. 1994b. Membrane ruffling and chemotaxis transduced by the PDGF beta-receptor require the binding site for phosphatidylinositol 3' kinase. *Oncogene* **9**(2): 651-660.

Wildeboer, D., Naus, S., Amy Sang, Q.X., Bartsch, J.W., and Pagenstecher, A. 2006. Metalloproteinase disintegrins ADAM8 and ADAM19 are highly regulated in human primary brain tumors and their expression levels and activities are associated with invasiveness. *J Neuropathol Exp Neurol* **65**(5): 516-527.

Wilm, B., Ipenberg, A., Hastie, N.D., Burch, J.B., and Bader, D.M. 2005. The serosal mesothelium is a major source of smooth muscle cells of the gut vasculature. *Development* **132**(23): 5317-5328.

Winnier, G., Blessing, M., Labosky, P.A., and Hogan, B.L. 1995. Bone morphogenetic protein-4 is required for mesoderm formation and patterning in the mouse. *Genes Dev* **9**(17): 2105-2116.

Woodard, A.S., Garcia-Cardena, G., Leong, M., Madri, J.A., Sessa, W.C., and Languino, L.R. 1998. The synergistic activity of alphavbeta3 integrin and PDGF receptor increases cell migration. *J Cell Sci* **111 (Pt 4)**: 469-478.

Xu, C., Kauffmann, R.C., Zhang, J., Kladny, S., and Carthew, R.W. 2000. Overlapping activators and repressors delimit transcriptional response to receptor tyrosine kinase signals in the Drosophila eye. *Cell* **103**(1): 87-97.

Xu, R.H., Ault, K.T., Kim, J., Park, M.J., Hwang, Y.S., Peng, Y., Sredni, D., and Kung, H. 1999. Opposite effects of FGF and BMP-4 on embryonic blood formation: roles of PV.1 and GATA-2. *Dev Biol* **208**(2): 352-361.

Yae, K., Keng, V.W., Koike, M., Yusa, K., Kouno, M., Uno, Y., Kondoh, G., Gotow, T., Uchiyama, Y., Horie, K., and Takeda, J. 2006. Sleeping beauty transposon-based phenotypic analysis of mice: lack of Arpc3 results in defective trophoblast outgrowth. *Mol Cell Biol* **26**(16): 6185-6196.

Yang, X., Castilla, L.H., Xu, X., Li, C., Gotay, J., Weinstein, M., Liu, P.P., and Deng, C.X. 1999. Angiogenesis defects and mesenchymal apoptosis in mice lacking SMAD5. *Development* **126**(8): 1571-1580.

Yoder, M.C. 2001. Introduction: spatial origin of murine hematopoietic stem cells. *Blood* **98**(1): 3-5.

Yoder, M.C., Papaioannou, V.E., Breitfeld, P.P., and Williams, D.A. 1994. Murine yolk sac endoderm- and mesoderm-derived cell lines support in vitro growth and differentiation of hematopoietic cells. *Blood* **83**(9): 2436-2443.

Yokote, K., Margolis, B., Heldin, C.H., and Claesson-Welsh, L. 1996. Grb7 is a downstream signaling component of platelet-derived growth factor alpha- and beta-receptors. *J Biol Chem* **271**(48): 30942-30949.

Yokote, K., Mori, S., Hansen, K., McGlade, J., Pawson, T., Heldin, C.H., and Claesson-Welsh, L. 1994. Direct interaction between Shc and the platelet-derived growth factor beta-receptor. *J Biol Chem* **269**(21): 15337-15343.

Yu, Y., Gao, Y., Wang, H., Huang, L., Qin, J., Guo, R., Song, M., Yu, S., Chen, J., Cui, B., and Gao, P. 2008. The matrix protein CCN1 (CYR61) promotes proliferation, migration and tube formation of endothelial progenitor cells. *Exp Cell Res* **314**(17): 3198-3208.

Zecca, M., Basler, K., and Struhl, G. 1996. Direct and long-range action of a wingless morphogen gradient. *Cell* **87**(5): 833-844.

Zhang, H., Liu, C.Y., Zha, Z.Y., Zhao, B., Yao, J., Zhao, S., Xiong, Y., Lei, Q.Y., and Guan, K.L. 2009. TEAD transcription factors mediate the function of TAZ in cell growth and epithelial-mesenchymal transition. *J Biol Chem*.

Zhang, J.C., Kim, S., Helmke, B.P., Yu, W.W., Du, K.L., Lu, M.M., Strobeck, M., Yu, Q., and Parmacek, M.S. 2001. Analysis of SM22alpha-deficient mice reveals

unanticipated insights into smooth muscle cell differentiation and function. *Mol Cell Biol* **21**(4): 1336-1344.

Zhang, X.Q., Afink, G.B., Svensson, K., Jacobs, J.J., Gunther, T., Forsberg-Nilsson, K., van Zoelen, E.J., Westermark, B., and Nister, M. 1998. Specific expression in mouse mesoderm- and neural crest-derived tissues of a human PDGFRA promoter/lacZ transgene. *Mech Dev* **70**(1-2): 167-180.

Zhong, J., Gencay, M.M., Bubendorf, L., Burgess, J.K., Parson, H., Robinson, B.W., Tamm, M., Black, J.L., and Roth, M. 2006. ERK1/2 and p38 MAP kinase control MMP-2, MT1-MMP, and TIMP action and affect cell migration: a comparison between mesothelioma and mesothelial cells. *J Cell Physiol* **207**(2): 540-552.

Zhu, Y., Lee, C., Shen, F., Du, R., Young, W.L., and Yang, G.Y. 2005. Angiopoietin-2 facilitates vascular endothelial growth factor-induced angiogenesis in the mature mouse brain. *Stroke* **36**(7): 1533-153.